WELL TEST ANALYSIS OF A MULTILAYERED RESERVOIR WITH FORMATION CROSSFLOW

A DISSERTATION
SUBMITTED TO THE DEPARTMENT OF PETROLEUM ENGINEERING
AND THE COMMITTEE ON GRADUATE STUDIES
OF STANFORD UNIVERSITY
IN PARTIAL FULFILLMENT OF THE REQUIREMENTS
FOR THE DEGREE OF
DOCTOR OF PHILOSOPHY

By
Heungjun Park
June, 1989

I certify that I have read this thesis and that in my opinion it is fully adequate, in scope and in quality, as a dissertation for the degree of Doctor of Philosophy.

Dr. Roland N. Horne
(Principal Advisor)

I certify that I have read this thesis and that in my opinion it is fully adequate, in scope and in quality, as a dissertation for the degree of Doctor of Philosophy.

Dr. Henry J. Ramey Jr.
Petroleum Engineering

I certify that I have read this thesis and that in my opinion it is fully adequate, in scope and in quality, as a dissertation for the degree of Doctor of Philosophy.

Dr. Younes Jalali-Yazdi
Petroleum Engineering

Approved for the University Committee on Graduate Studies:

Abstract

The purpose of well test analysis is to identify the type of a reservoir and to determine the parameters of the reservoir quantitatively. This work is about the well test analysis of a multilayered reservoir with formation crossflow. The results are described in two parts.

In the first part, the effects of the reservoir parameters such as permeability, vertical permeability, skin, storage coefficient, and others such as outer boundary conditions and layering on the wellbore response, pressure and layer production rate, were investigated. Some important discoveries are:

- The wellbore response is observed in three different stages; it is identical to that of the commingled system at early time and and to that of the homogeneous system at late time. Transition occurs at intermediate time.
- The vertical permeability is the only parameter governing the initiation and termination of the transition from the early time commingled system response to the late time homogeneous system response.
- The direction of the formation crossflow is determined first by the layer permeabilities and later by the skin factors.
- The influence of the wellbore storage effect can be minimized by using sandface flow rate from each layer.
- The outer boundary conditions have only small effect on the wellbore response as long as the transition terminates before the system feels the boundary.

In addition, the early time and the late time limiting forms of the wellbore response were derived and some approximations for the late time layer production rate were suggested.

In the second part, the nonlinear parameter estimation method was applied as a means to determine the layer parameters. Here, two new methods for the initial estimation of the parameter values were suggested and tested, where the early time and the late time limiting values of the layer production rate were used with the conventional pressure analysis for the average permeability and skin of the total system. Several examples including a real well test analysis were given.

Acknowledgements

The author would like to express sincere gratitude to Dr. Roland. N. Horne, Department of Petroleum Engineering, for his valuable guidance and counsel as principal advisor during this study.

I would also like to thank my colleagues, Ramagopal Nutakki, Terry Wong, Ronald Gajdica, Michael Riley, and Jitendra Kikani. Through academic and personal discussions, many things were obtained.

Financial support from the Korean Government in the form of scholarship and from Stanford University in the form of research assistantship made this work possible.

Real well test data were supplied by Flopetrol Johnston Schlumberger, which is appreciated.

Grateful encouragement and love by my wife, Youngran and my daughter, Saeram will always be cherished in this dissertation.

Contents

List of Tables

List of Figures

Chapter 1

Introduction

This study concerns the computer-aided well test analysis of multilayered reservoirs with formation crossflow. In this chapter, we will consider the recent literature on this subject and introduce the study problem.

1.1 Multilayered System

Well test data has often been interpreted based on an assumption that the reservoir is a homogeneous single layer. However, many reservoirs are found to be composed of a number of layers whose characteristics are different from each other. Wells in such reservoirs may produce from more than one layer. Pressure behavior in this kind of vertically heterogeneous system is not necessarily like that of a single layered system, and seldom reveals more than the average properties of the entire system. To identify the characteristics of the individual layers is important, especially if the reservoir fluid is produced by a waterflooding or an enhanced recovery scheme. Detailed layer information may enable us to prevent the early breakthrough and to obtain maximum oil recovery.

Since the early 1960's, there have been many studies of the behavior of multilayered systems. In the 1980's, substantial efforts have been made to interpret multilayered systems quantitatively with the introduction of production logging tools that measure the bottom hole pressure and flow rate simultaneously.

Two different multilayered reservoir models have been proposed, depending on the presence or absence of interlayer crossflow. A multilayered reservoir is called a crossflow system if fluid can move between layers, and a commingled system if layers communicate only through the wellbore. A commingled system may be regarded as a limiting case of a crossflow system where the vertical permeabilities of all the layers are zero.

Lefkovits, *et al.* (1961) presented a rigorous study of multilayered systems without crossflow. They derived analytical solutions for wellbore pressure and layer production rates in a bounded multilayered reservoir, where each layer had different reservoir parameters. They also presented the practical implications of the mathematical results for a two layered commingled system. Tempelaar-Lietz (1961) had already studied the performance of a two layered depletion-type reservoir without crossflow. However, his treatment was simplified and the study did not cover the entire history of the wellbore pressure.

The first studies concerning multilayered system with crossflow were done by Russell and Prats (1962 a) and Katz and Tek (1962). Both papers solved the problem with a constant pressure inner boundary condition at the wellbore. Many interesting facts were discovered, for example, the behavior of a crossflow system is bounded by that of a commingled system and that of a homogeneous system. Russell and Prats (1962 b) published a separate paper about practical aspects of crossflow, in which they concluded that crossflow between communicating adjacent layers was of great economic significance, and was beneficial by shortening the operating life of a reservoir and by raising primary ultimate recovery.

Pendergrass and Berry (1962) also solved the same problem, concentrating on the effect of permeability distribution between the layers. They concluded that it was not possible to diagnose stratification from wellbore pressure data except at early time. Their conclusion may be due to the negligence of the vertical permeabilities of the layers.

Kazemi and Seth (1969) used a more realistic inner boundary condition by restricting the flow entry into the wellbore. One of their major discoveries was the presence of two semilog straight lines in the pressure response; the early one yielded

the flow capacity of the perforated interval and the later one gave the flow capacity of the entire formation. This fact was utilized later by Gao (1983 b) in an attempt to determine individual layer parameters.

Kazemi (1970) also studied the use of a pressure buildup test to determine the reservoir limit. As might be expected, conventional methods worked well for crossflow systems because crossflow systems behaved like a single homogeneous layer at late time. For a commingled system, however, conventional methods could not be applied, or could only be used with caution, at best.

Cobb, *et al.* (1972) examined the wellbore pressure response of a two layered reservoir for various production and shut-in conditions, in an unsuccessful attempt to identify individual reservoir parameters for each layer. Later, Raghavan, *et al.* (1974) approached a similar problem with unequal formation thickness. By displaying the data in various ways, they were able to estimate the individual layer properties in some favorable cases.

Earlougher, *et al.* (1974) studied the characteristics of pressure behavior in buildup tests for a multilayered commingled system. They presented many unique observations, especially in cases when there were more than a single well in the system and when the reservoir boundaries were not circular.

Tariq and Ramey (1978) extended the study of a commingled system by considering the effect of wellbore storage and skin. A major contribution of their research was the introduction of the Stehfest algorithm (1970), which was used to invert the solution in Laplace space into real space numerically. Since the method is easier than the method of direct inversion by complex analysis, this algorithm has since been used in many studies concerning well test analysis.

Deans and Gao (1983) developed a very useful idea to reduce the dimension of the governing equation by one. The terms for vertical movement were represented by the pseudo-steady state approximation in their semi-permeable wall model, which is explained in Chapter 2. They derived approximate analytical solutions for wellbore pressure and formation crossflow. They did not consider the effect of skin factors and wellbore storage.

Bourdet (1985) solved the pressure response for a two layered reservoir with crossflow with consideration of wellbore storage and skin. He showed that his solution could be placed in the general form of many other reservoir model solutions by showing that the solution was identical to the solutions of other problems when some reservoir parameters took limiting values.

Kucuk, *et al.* (1984) suggested a new testing method for a two layered commingled reservoir. They used the technique of nonlinear parameter estimation by coupling sandface production rate of each layer with wellbore pressure. The coupling of layer production rate is very significant for multilayered reservoirs because rate transient of each layer reveals information about the layer, while wellbore pressure is determined more by average reservoir parameters.

Raghavan, *et al.* (1985) investigated the pressure response of a two layered reservoir with formation crossflow. The effects of various heterogeneities were considered. Unlike most other authors, they applied the concept of the thick skin. However, the overall effects on the wellbore pressure were not different from the results of other authors who had considered a thin skin. One special contribution of their work was demonstration that the skin factors of individual layers could be determined uniquely with production rate data when other parameters, including average skin factor of the total system, were known.

Ehlig-Economides and Joseph (1985) made a major advance in this problem in their study of well test analysis for a multilayered system with formation crossflow. They gave an excellent literature survey up to 1985, developed a complete analytical solution for the N-layered crossflow system with wellbore storage and skin, and investigated early time and late time behavior of the production rate for each layer.

Larsen (1982) proposed a method to determine flow capacities and skin factors of individual layers in two layered commingled systems, by using an approximate equation for the wellbore pressure. To apply his method, the values of several dimensionless parameters must be determined, which could be difficult and would sometimes require a trial-and-error solution. His method worked under favorable conditions where the data set fall on a smooth curve and exhibit a definite curvature in the infinite-acting period.

Larsen (1988) investigated the similarities and differences of mathematical methods for various multilayered models. This is a good summary of the many papers concerning multilayered reservoirs. One important conclusion was that the pressure response could be varied by a change in reservoir modeling, such as the numbers of sublayers into which a single layer was discretized to simulate a real reservoir under crossflow conditions.

Some authors investigated the response of a multilayered reservoir for other than single well tests. Woods (1970) studied the characteristics of two layered reservoirs either with or without formation crossflow. One of his conclusions was that the apparent transmissivity in a commingled system obtained by pulse testing was always equal to or greater than the total transmissivity of the entire system, which was later verified by Larsen (1982). He also proposed the use of flowmeters to obtain flow rate data to determine individual layer properties from pulse tests between wells. Chu and Raghavan (1981) studied interference testing for a multilayered reservoir. One of the important observations was that the skin factors of the active well play an important role in the pressure response of the observation well, unlike the behavior of a single layered system. More recent works on interference testing can be found in Streltsova (1984) and Prats (1983).

The fractured reservoir model is another model used in well test analysis. Some authors studied the behavior of a combination of multilayered systems and fractured reservoirs. Recent similar works can be found in Camacho-V., *et al.* (1984) and Bennet, *et al.* (1986).

Some authors studied the three layer problem in which a tight layer is present between two permeable layers. These were Lee, *et al.* (1984), Ehlig-Economides and Ayoub (1984) and Bremer, *et al.* (1985).

1.2 Computer Aided Well Test Analysis

With recent developments in computers, especially combined with graphic features, automated well test analysis has become popular. Automated well test analysis has several definite advantages over personal interpretation. Since the computer is doing

the chores of calculation, a lot of human labor and time is saved. Automated analysis avoids subjectivity in determining the proper semilog straight line which is involved when conventional methods are applied manually. Besides, automated analysis is numerically error free. Most important, an automated matching procedure is capable of matching subtleties of the response that are not perceptible to the human eye, thus allowing an algorithmic interpretation of some data that are impossible to interpret by conventional techniques. Because of definite advantages, the method has become a powerful tool in analyzing well test data.

The first use of computer aided well test analysis dates back to the 1960's. Most of the early works aimed at determining areal distributions of permeability were based on performance data from several wells in a reservoir. Jacquard and Jain (1965) divided a single layered reservoir into a number of homogeneous blocks of constant reservoir properties to interpret interference tests, and used regression analysis techniques to estimate the permeabilities of the blocks. Jahns (1966) applied a similar principle to solve a five spot interference test problem. Coats, *et al.* (1970) developed a linear programming method. Some of their examples covered two-phase flow problems.

Important contributions to computer-aided single well test analysis were made by Rosa and Horne (1983). Many previous studies concerned various regression techniques, but they used only approximate solutions such as numerical solutions or tabular data. However, Rosa and Horne developed a method to compute the parameter gradients by differentiating the pressure solution in Laplace space and then inverting using the Stehfest (1970) algorithm. This made it possible to use the exact solution without having the trouble usually required to solve complex problems. In their paper, they compared several regression methods and found the Gauss-Marquardt method the best for most problems. They also introduced the confidence interval which showed the quality of the estimated parameter values.

Barua, *et al.* (1988) considered practical problems that could be encountered in application of automated well test analysis due to poor initial estimates or from inherently ill-defined parameters. Their major objective was to find an alternative regression algorithm when the popular Gauss-Marquardt method fails, and they succeeded in developing a variant of the Newton-Greenstadt method that was more

powerful but required additional work in calculating second derivatives.

1.3 The Purpose of the Study

The purpose of well test analysis is a quantification of reservoir parameters. The purpose of this study is to find a method to analyze well test data to determine the reservoir parameters for each layer of a multilayered reservoir with formation crossflow. The analysis technique will be automated and use nonlinear parameter estimation method.

Automated well test analysis may be performed in two steps. The first step is to estimate the parameter values and the second step is to develop a systematic regression method to determine reliable values for the unknown reservoir parameters. To have a powerful regression method that guarantees quick convergence is important. However, if the initial estimate is poor, the optimization process may lead to wrong answers, or may not converge at all. A lot of effort has been made to improve the second step, the regression method. However, most authors have not described how they had selected initial estimates for the unknown parameters. An objective of this work is to establish a methodology for determining initial estimates of parameters.

A thorough study of useful characteristics of multilayered systems with crossflow must precede development of systematic methods to determine initial estimates of system parameters for automated data matching. The effect of every reservoir parameter on wellbore pressure and layer production rate was examined, including radial permeability, skin factor, vertical permeability, outer boundary conditions, and order of layering.

In particular, considerable effort has been spent in describing early time and late time wellbore response. Crossflow systems behave like commingled systems at early time, and like equivalent homogeneous systems at late time. Besides this general behavior, crossflow systems show unique characteristics in both limiting cases. The new methods found in this study for the initial parameter estimation are based on the characteristics of early and late time response of multilayered crossflow systems, because the layer production rates become constant in both limiting cases.

The main objectives of this study of multilayered reservoirs with formation cross-flow may be described as follows:

1. Examination of the effects of reservoir parameters on wellbore pressure and flow rate response.

2. Investigation of limiting behavior at early time and at late time.

3. Establishment of new methods by which initial estimates of reservoir parameters may be determined in a systematic way to aid automatic nonlinear regression analysis of well test data for layered systems.

Chapter 2

Model Description

The reservoir model considered in this study is shown schematically in Fig. 2.1. The reservoir consists of an arbitrary number of horizontal layers each of which are homogeneous, but different from each other. The reservoir parameters permitted to vary are radial permeability, vertical permeability, and skin factor. At the center of the reservoir, a single well penetrates all layers, which are initially in hydraulic pressure equilibrium. The reservoir fluid, produced at a constant rate from the well head, is a slightly compressible, single-phase fluid of constant viscosity. The top and the bottom of the reservoir are sealed by impermeable layers. At the outer boundary, three typical conditions are considered; infinitely large reservoir, and either a no-flow, or constant-pressure outer boundary condition. Isothermal expansion and a constant wellbore storage coefficient are assumed, and gravity effects are not considered.

If the number of layers is reduced to two, the model is identical to that of Bourdet (1985), and if crossflow between formation is neglected, it is the same as that of Lefkovits, *et al.* (1961).

In describing formation crossflow between adjacent layers, the semi-permeable wall model of Gao and Dean (1983) was used. Each layer has a finite radial permeability, and a finite vertical permeability. However, all vertical permeabilities are assumed to be associated only with the interface between layers. Inside any layer, there is no vertical pressure gradient and the flow direction is essentially radial. The magnitude of the vertical resistance at the interface $j+\frac{1}{2}$ is determined by the vertical permeabilities

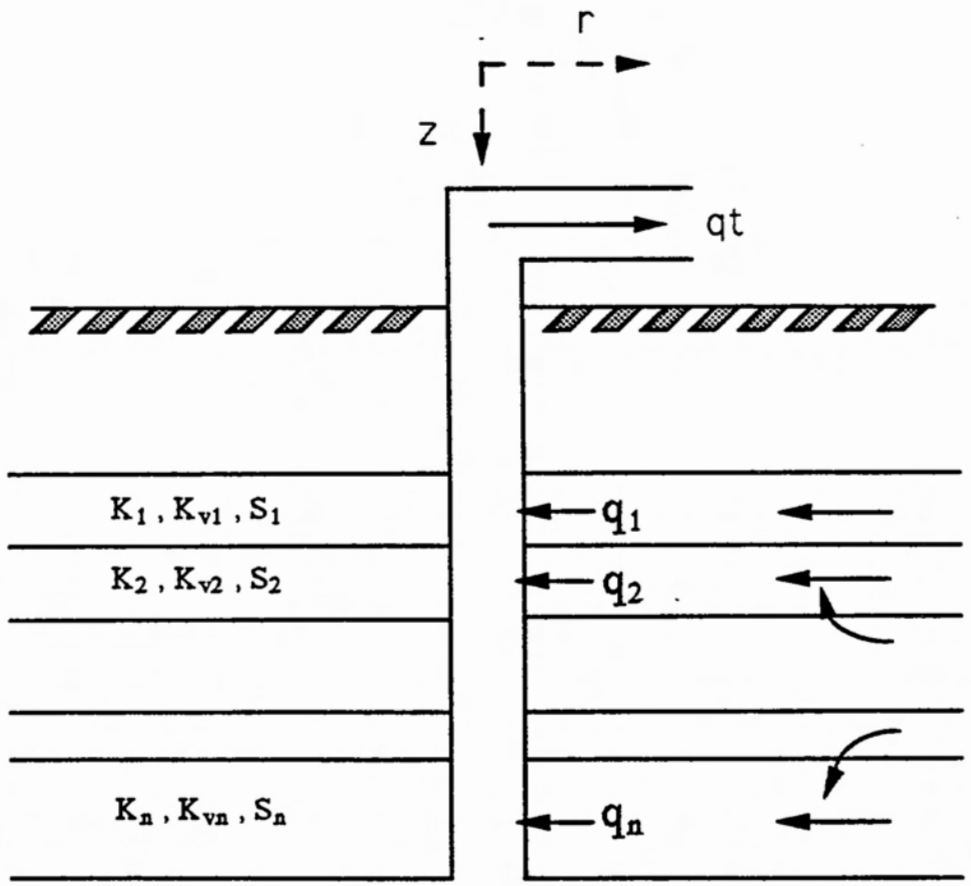

Figure 2.1: A Schematic Diagram of a Multilayered System with Formation Crossflow

of the two adjacent layers, j and $j+1$, as follows:

$$k_{v_{j+\frac{1}{2}}} = \frac{h_j + h_{j+1}}{\frac{h_j}{k_{v_j}} + \frac{h_{j+1}}{k_{v_{j+1}}}} \tag{2.1}$$

The governing partial differential equation which describes the flow in layer j in cylindrical coordinates is given by:

$$\frac{1}{r}\frac{\partial}{\partial r}(rk_j\frac{\partial p_j}{\partial r}) + \frac{\partial}{\partial z}(k_{v_j}\frac{\partial p_j}{\partial z}) = (\phi\mu c_t)_j\frac{\partial p_j}{\partial t} \tag{2.2}$$

Integrating Eq. 2.2 with respect to z from the top to the bottom of layer j yields:

$$(kh)_j\nabla^2 p_j + k_v\frac{\partial p_j}{\partial z}|_{z=z_{j+\frac{1}{2}}} - k_v\frac{\partial p_j}{\partial z}|_{z=z_{j-\frac{1}{2}}} = (\phi\mu c_t h)_j\frac{\partial p_j}{\partial t} \tag{2.3}$$

We can modify the second and the third term in the left hand side of Eq. 2.3 by applying finite difference methods:

$$\begin{aligned}\frac{\partial p_j}{\partial z}|_{z=z_{j+\frac{1}{2}}} &= \frac{p_{j+1}-p_j}{z_{j+1}-z_{j-1}} \\ &= \frac{p_{j+1}-p_j}{\frac{1}{2}(h_{j+1}+h_{j-1})} \\ &= \frac{p_{j+1}-p_j}{h_{j+\frac{1}{2}}}\end{aligned} \tag{2.4}$$

Then Eq. 2.3 becomes:

$$(kh)_j\nabla^2 p_j + \frac{k_{v_{j+\frac{1}{2}}}}{h_{j+\frac{1}{2}}}(p_{j+1}-p_j) + \frac{k_{v_{j-\frac{1}{2}}}}{h_{j-\frac{1}{2}}}(p_{j-1}-p_j) = (\phi\mu c_t h)_j\frac{\partial p_j}{\partial t} \tag{2.5}$$

For the inner boundary conditions, both hydraulic pressure equilibrium and constant production rate at the well head are assumed, with the presence of skin factors and constant wellbore storage coefficient considered. These conditions may be expressed as:

$$p_{wf} = p_j - s_j(r\frac{\partial p_j}{\partial r})_{r=r_w} \tag{2.6}$$

$$q_t = -C\frac{dp_{wf}}{dt} + \sum_{j=1}^{n} \frac{2\pi(kh)_j}{\mu}(r\frac{\partial p_j}{\partial r})_{r=r_w} \tag{2.7}$$

The three outer boundary conditions are:

$$\lim_{r\to\infty} p_j(r,t) = p_i, \qquad \text{for an infinite system,} \tag{2.8}$$

$$\frac{\partial p_j}{\partial r}|_{r=r_e} = 0, \qquad \text{for the no-flow condition, and} \tag{2.9}$$

$$p_j(r_e,t) = p_i, \quad \text{for the constant-pressure condition.} \tag{2.10}$$

The initial condition is:

$$p_j(r,0) = p_i \tag{2.11}$$

The sand face flow rate from each layer is:

$$q_j = \frac{2\pi(kh)_j}{\mu}(r\frac{\partial p_j}{\partial r})_{r=r_w} \tag{2.12}$$

All conditions can be non-dimensionalized for analysis with the introduction of the following dimensionless variables and parameters:

$$p_{jD} = \frac{2\pi(kh)_t}{q\mu}(p_i - p_j) \tag{2.13}$$

$$t_D = \frac{(kh)_t t}{(\phi h)_t \mu c_t r_w^2} \tag{2.14}$$

$$r_D = \frac{r}{r_w} \tag{2.15}$$

$$r_{eD} = \frac{r_e}{r_w} \tag{2.16}$$

$$\kappa_j = \frac{(kh)_j}{(kh)_t} \tag{2.17}$$

$$\omega_j = \frac{(\phi h)_j}{(\phi h)_t} \tag{2.18}$$

$$\lambda_{j+\frac{1}{2}} = (\frac{k_v}{h})_{j+\frac{1}{2}}\frac{r_w^2}{(kh)_t} \tag{2.19}$$

$$C_D = \frac{C}{2\pi(\phi h)_t c_t r_w^2} \tag{2.20}$$

where

$$(kh)_t = \sum_{j=1}^{n} (kh)_j \tag{2.21}$$

$$(\phi h)_t = \sum_{j=1}^{n} (\phi h)_j \tag{2.22}$$

The non-dimensionalized equations and conditions are:

$$\kappa_j \nabla^2 p_{jD} + \lambda_{j+\frac{1}{2}}(p_{j+1D} - p_{jD}) + \lambda_{j-\frac{1}{2}}(p_{j-1D} - p_{jD}) = \omega_j \frac{\partial p_{jD}}{\partial t_D} \tag{2.23}$$

Inner boundary conditions:

$$p_{wD} = p_{jD} - s_j \frac{\partial p_{jD}}{\partial r_D}|_{r_D=1} \tag{2.24}$$

$$1 = C_D \frac{dp_{wD}}{dt_D} - \sum_{j=1}^{n} \kappa_j \frac{\partial p_{j_D}}{\partial r_D}|_{r_D=1} \tag{2.25}$$

Outer boundary conditions:

$$\lim_{r_D \to \infty} p_{jD}(r_D, t_D) = 0, \qquad \text{for an infinite system} \tag{2.26}$$

$$\frac{\partial p_{jD}}{\partial r_D}|_{r_{eD}} = 0, \qquad \text{for the no-flow condition} \tag{2.27}$$

$$p_{jD}(r_{eD}, t_D) = 0, \quad \text{for constant-pressure condition} \tag{2.28}$$

Initial condition:

$$p_{jD}(r_D, 0) = 0 \tag{2.29}$$

Sandface flow rate:

$$q_{jD} = \frac{q_j}{q_t} = -\kappa_j \frac{\partial p_{jD}}{\partial r_D}|_{r_D=1} \tag{2.30}$$

The non-dimensionalized equations solved in Laplace domain are presented in Appendix A. The non-dimensionalized solution will be used in Chapter 3 to describe the behavior of crossflow systems.

Chapter 3

Multilayered Crossflow System

Whenever there is a pressure difference between two layers, crossflow will occur if there is communication between layers. Generally, differences in radial permeability and skin factor are the most important reasons for causing the formation crossflow. A more permeable layer produces rapidly, which causes bigger pressure drop. Thus at the same distance from the wellbore, the formation pressure becomes higher in the less permeable layer than that in the more permeable layer, and the reservoir fluid starts flowing from the less to the more permeable layer. This crossflow phenomenon has many characteristic effects both on the response of the wellbore pressure and on the production rate from each layer. In this chapter, many interesting characteristics of a multilayered reservoir with formation crossflow are discussed.

3.1 General Behavior of Crossflow Systems

The typical wellbore responses in a multilayered reservoir with formation crossflow are shown in Figs. 3.1- 3.3, compared to those of a commingled system for reservoir parameters listed in Table 3.1.

Shown in Fig. 3.1 are two cases, A and B. In case A, wellbore pressure responds to production at a constant rate in three progressive stages. At early time ($t_D < t_{D1}$), pressure response of a crossflow system is identical to that of a commingled system with same reservoir parameters. This suggests that it takes time for the formation

Table 3.1: Reservoir Parameters for Studies of Wellbore Response of Multilayered Crossflow Systems

Layer	k (md)	s		
		case A	case B	case C
1	1000	0	5	4
2	100	5	0	1

crossflow to be initiated.

At late time ($t_D > t_{D2}$), wellbore pressure response reaches a semilog straight line behavior similar to that of a homogeneous single layered system whose reservoir parameters are the arithmetic average of the parameters of each layer, such that:

$$\overline{k} = \frac{k_1 h_1 + k_2 h_2 + \cdots + k_n h_n}{h_1 + h_2 + \cdots + h_n} \tag{3.1}$$

$$\overline{s} = \frac{q_1 s_1 + q_2 s_2 + \cdots + q_n s_n}{q_t} \tag{3.2}$$

At this stage, the pressure may be expressed as:

$$p_D = \frac{1}{2} \ln t_D + 0.404535 + \overline{s} \tag{3.3}$$

During intermediate time ($t_{D1} < t_D < t_{D2}$), the pressure curve deviates from that of the commingled system and approaches that of the homogeneous system. The dividing times, t_{D1} and t_{D2}, are governed by the vertical permeability.

The three stage response is better seen in Fig. 3.2, dimensionless wellbore pressure derivative vs. the logarithm of dimensionless time. The pressure derivative curves for a crossflow system are identical to the behavior of a commingled system at early time, and reach a constant value of 0.5 at late time, corresponding to the semilog straight line behavior of a homogeneous, single layered system. The two parts are connected by a transitional stage.

When the less permeable layer has smaller skin factor, as in case B of Fig. 3.1, the transitional phenomenon during the intermediate period appears to happen quickly,

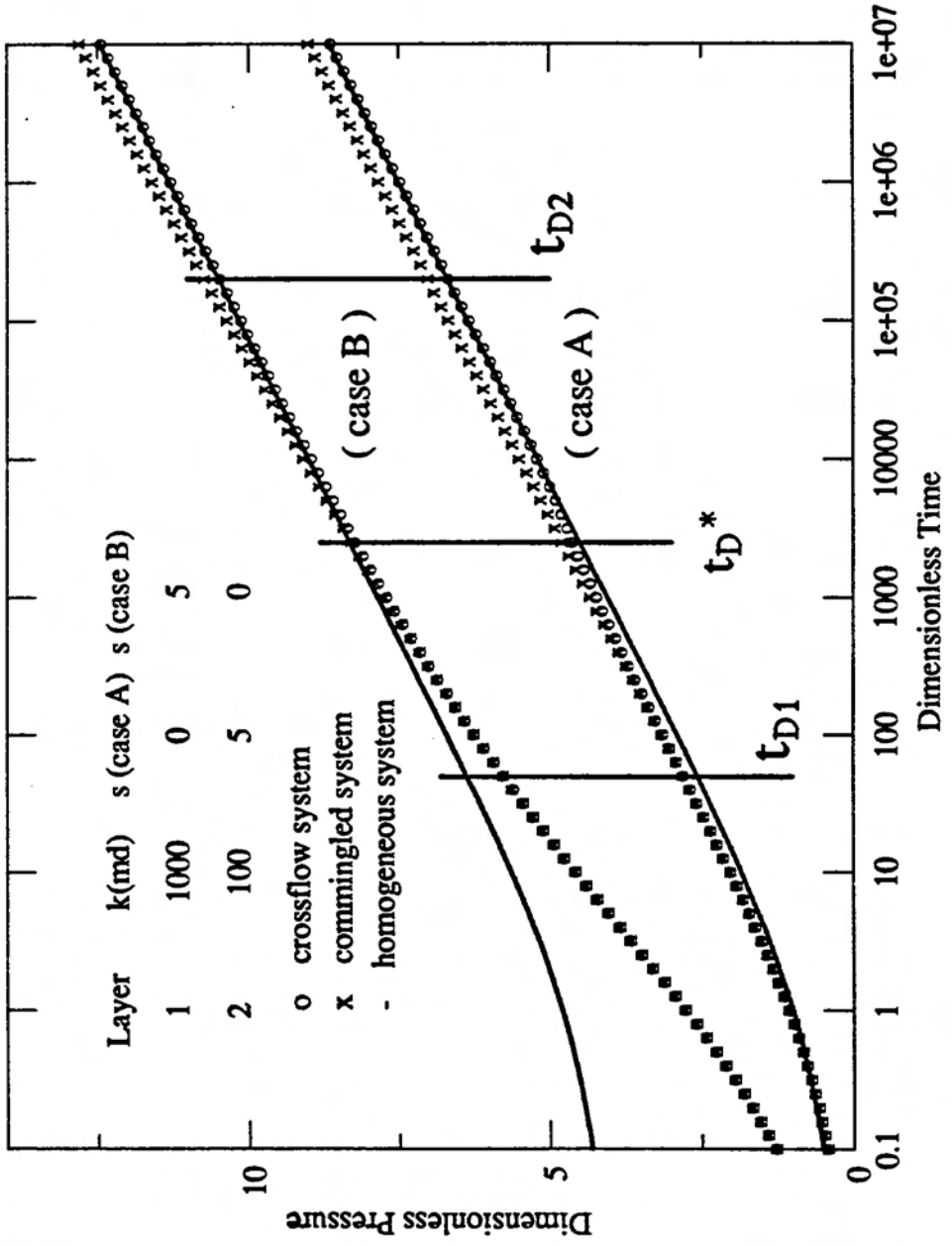

Figure 3.1: Wellbore Pressure Curves for Infinitely Large Layered Systems

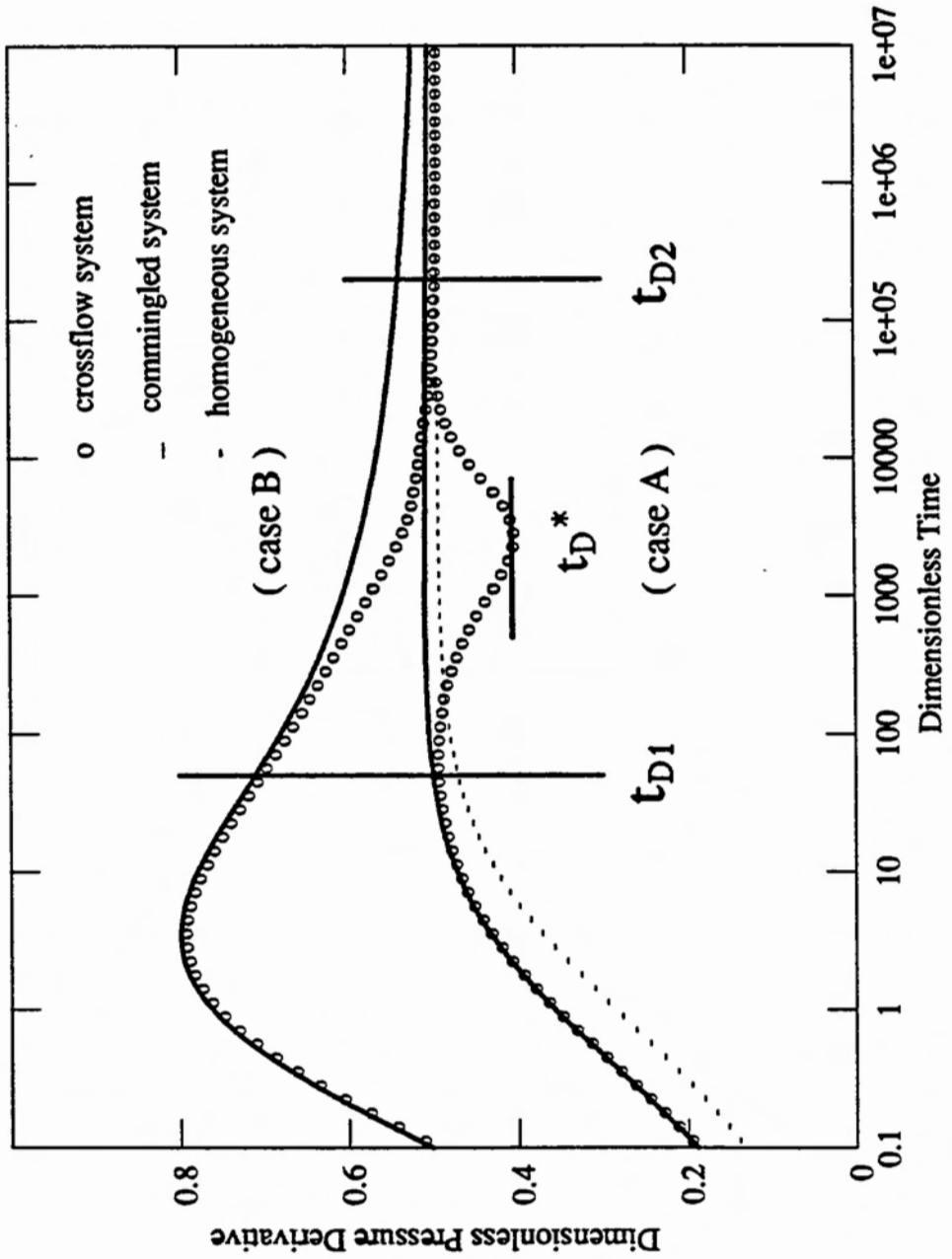

Figure 3.2: Wellbore Pressure Derivative Curves for Infinitely Large Layered Systems

but this is not so. From the pressure derivative curves in Fig. 3.2, we can see that the duration of the intermediate period in case B is as long as in case A.

In case A, where the more permeable layer has the smaller skin factor, a minimum develops in the derivative curve during the transitional stage. The location of the minimum may be important in determining the reservoir parameters, as will be discussed in Chapter 4.

The production rate history for layer 1, the more permeable layer, is shown in Fig. 3.3 for both crossflow as well as commingled systems, for cases A, B and C. There are two important features in Fig. 3.3. One is that the layer production rates for crossflow system become constant at late time, whereas those for the commingled system do not. This is an important factor in the determination of the reservoir parameters for each layer, and shall be discussed in detail in Section 3.9. The early time limiting production rate from each layer is also constant, as can be seen in case C. A and B are two extreme cases in that the layers produce all or nothing.

The second key observation is that the more permeable layer produces more in case A, and less in case B, than the commingled system. This means that both the permeabilities and the skin factors play a determining role in deciding the direction and the magnitude of the crossflow. This too will be discussed more in Section 3.9.

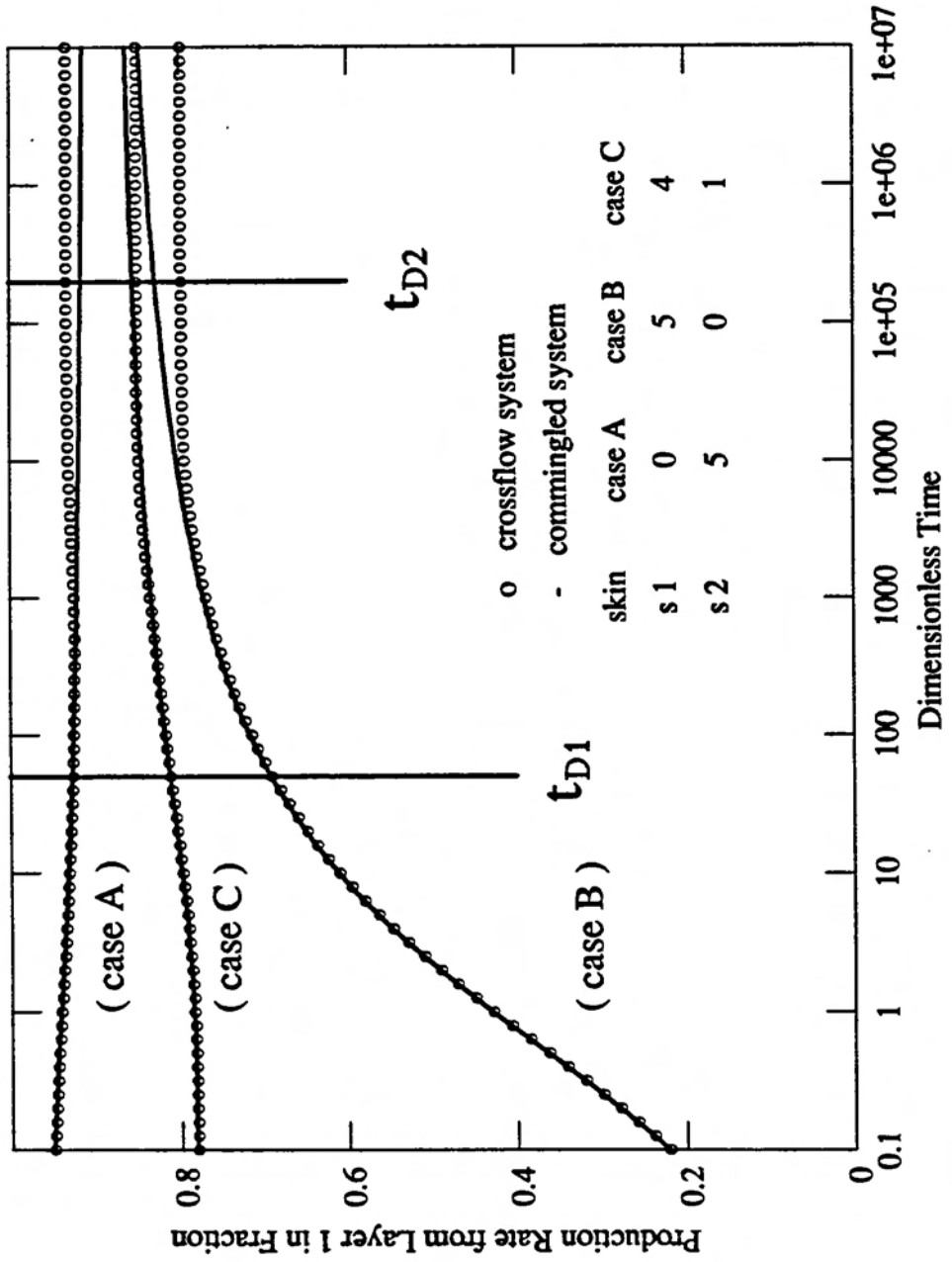

Figure 3.3: Rate Transients for Infinitely Large Layered Systems

3.2 Effect of Permeability

The effect of the layer permeability ratio on the wellbore pressure response is shown in Fig. 3.4. The examples are for a two layered reservoir with the parameters shown in Table 3.2.

Table 3.2: Reservoir Parameters for Studies of the Effect of Permeability

	case A	case B	case C	case D
k_1(md)	10	100	1000	10000
k_2(md)	10	10	10	10
k_1/k_2	1	10	100	1000
$k_{v1} = k_{v2} = 100$ md $s_1 = s_2 = 0$				

As the ratio k_1/k_2 increases, the dimensionless pressure drop at early time increases compared to that of the homogeneous system ($k_1/k_2 = 1$). Transition to the response of the homogeneous system follows immediately.

The transitional stage is interesting. Fig. 3.5 shows the pressure derivative curves for four cases. The small minimum advances approximately one log cycle as the ratio k_1/k_2 increases ten fold. However, the definition of t_D is:

$$t_D = \frac{2\pi(kh)_t t}{(\phi h)_t \mu c_t r_w^2} \tag{3.4}$$

The advance of the transitional period is caused by the increase of $(kh)_t$ rather than a change in real time t. The pressure derivative vs. real time is presented in Fig. 3.6. The minimum in the pressure derivative happens at the same actual time, which means that the permeability ratio does not affect the transition period time.

The size of the minimum increases with an increase in the permeability ratio between the layers. However there seems to be a limiting value, beyond which the minimum does not increase, no matter how large the permeability ratio is.

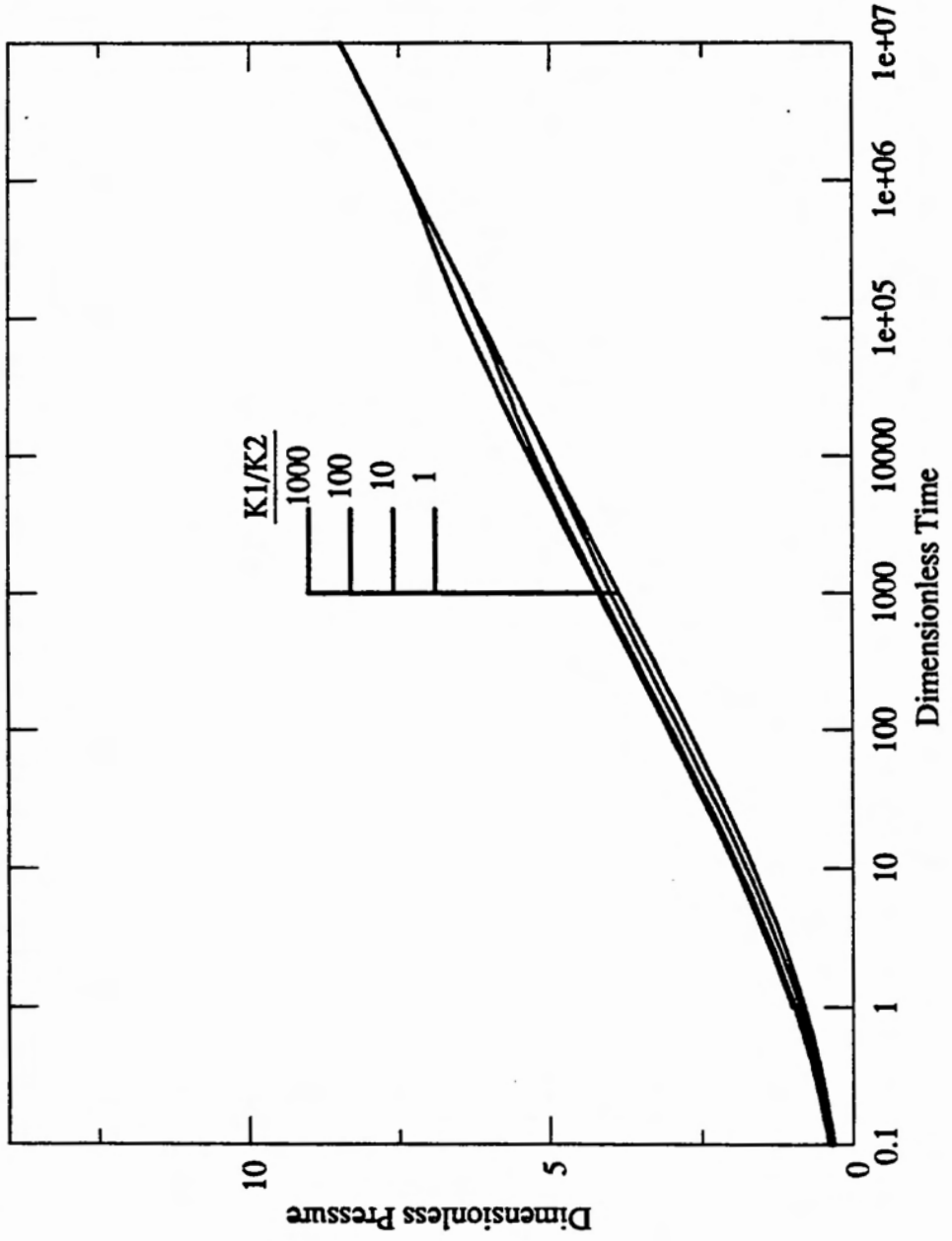

Figure 3.4: Wellbore Pressure Response for Various Permeability Distribution

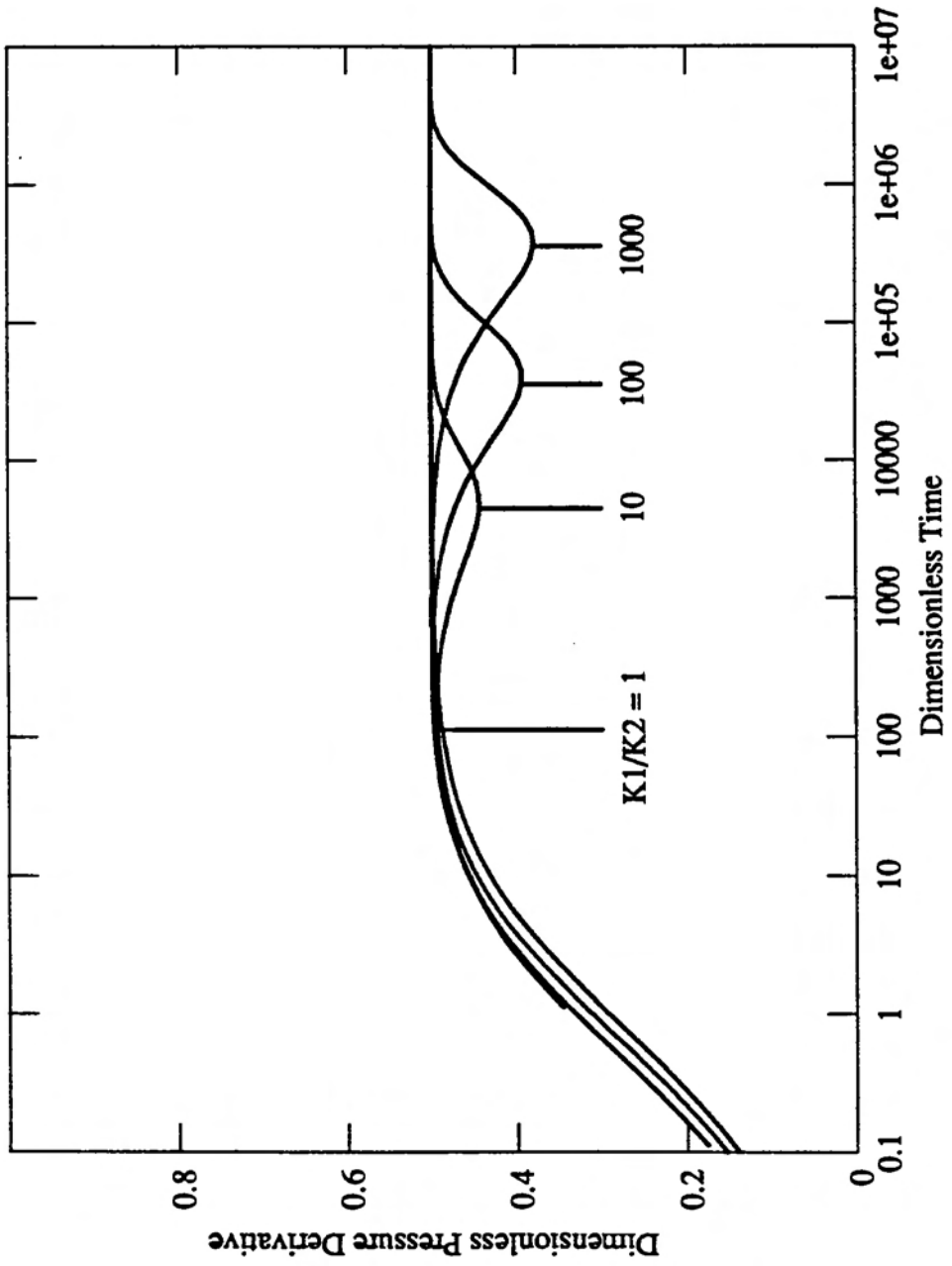

Figure 3.5: Wellbore Pressure Derivative Curves for Various Permeability Distribution (Dimensionless Time)

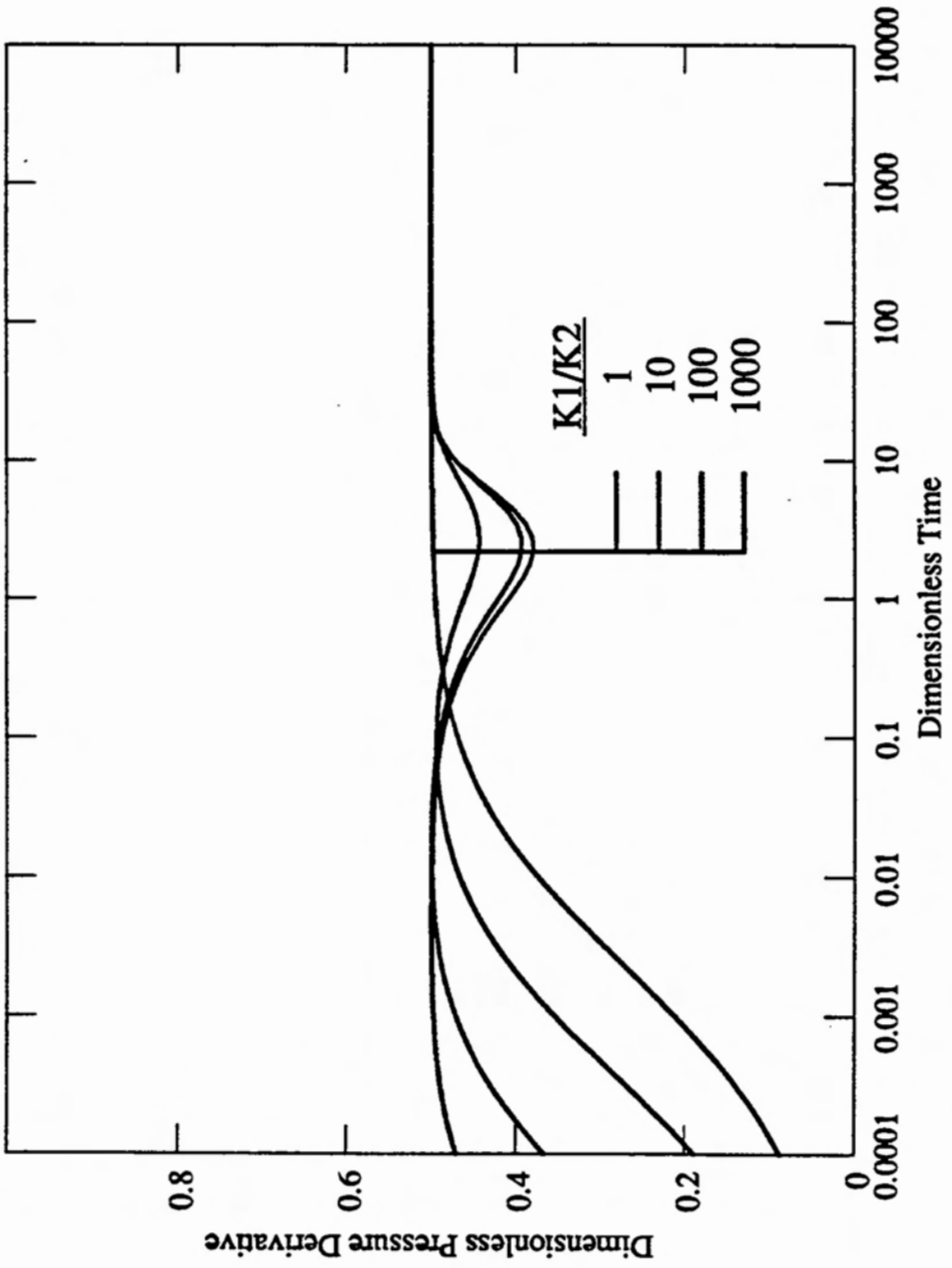

Figure 3.6: Wellbore Pressure Derivative Curves for Various Permeability Distribution (Real Time)

3.3 Effect of Skin Factor

Skin factors also play an important role in the behavior of wellbore pressure and layer production rates. The effect of skin factors on the wellbore response are shown in Figs. 3.7- 3.9, for a two layered reservoir with the parameters as shown in Table 3.3.

Table 3.3: Reservoir Parameters for Studies of the Effect of Skin

Layer	case A	case B	case C	case D	case E
s_1	10	5	0	5	10
s_2	0	0	5	10	5
$k_1 = k_{v1} = 100$ md $k_2 = k_{v2} = 10$ md					

Fig. 3.7 shows the wellbore pressure response, and Fig. 3.8 shows the wellbore pressure derivative curves for various combinations of skin factors for two layered systems. As mentioned in Section 3.1, wellbore pressure drops suddenly at early time (p_D increases) when the more permeable layer has a larger skin. Throughout the transition at intermediate time, the pressure curve becomes a semilog straight line which is characteristic of a homogeneous system. At this stage, the straight line can be approximated by:

$$p_D = \frac{1}{2}\ln t_D + 0.404535 + \overline{s} \tag{3.5}$$

$$\overline{s} = q_{1D}s_1 + \ldots + q_{nD}s_n \tag{3.6}$$

This is the basis for conventional well test analysis by which the average properties, $(kh)_t$ and $\overline{s}$ can be obtained.

$$(kh)_t = -\frac{162.6 q_t B \mu}{m} \tag{3.7}$$

$$\overline{s} = 1.1513[\frac{p_{1hr} - p_i}{m} - \log\frac{(kh)_t}{(\phi h)_t \mu c_t r_w^2} + 3.2275] \tag{3.8}$$

where all the variables and parameters are given in oil field units and m is the slope of the semilog straight line.

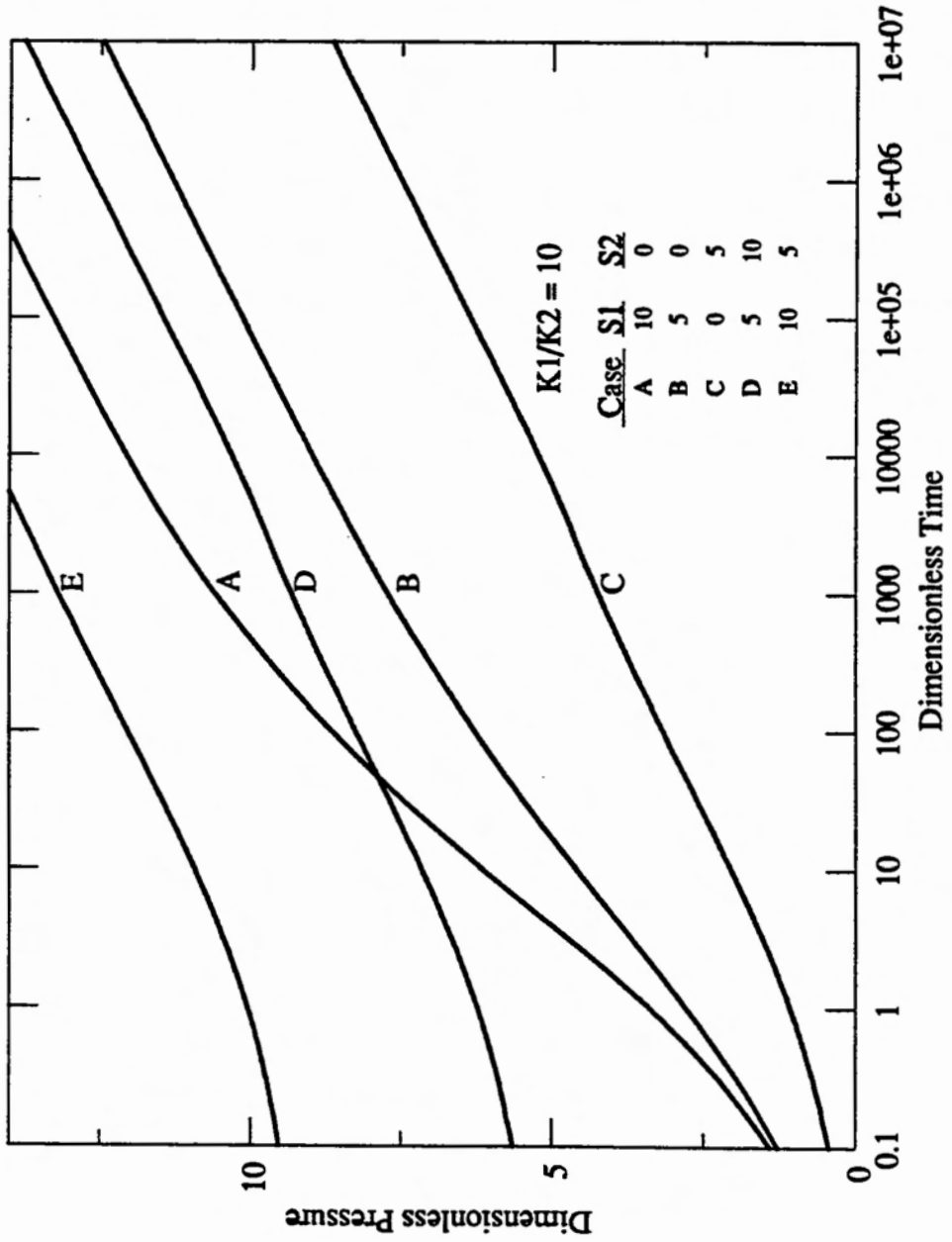

Figure 3.7: Wellbore Pressure Response for Various Skin

However, the skin factors do not affect the start and the end of the transition period, as shown in Fig. 3.8 . The point of divergence from the response of a commingled system and the point of convergence to the response of a homogeneous system change very little with various combinations of skin factors for each layer.

Another point is that the initial and the final layer production rates are constant and are determined by the permeabilities, vertical permeabilities and skin factors only, as shall be shown later in Section 3.9.

The most important role of skin factors in a multilayered crossflow system is determination of the direction of the formation crossflow at late time. As mentioned briefly in Section 3.1, the late time production rate of layer 1 in case A, where the more permeable layer has the smaller skin, is higher than that for a commingled system. This means that the direction of the formation crossflow is from the less permeable layer to the more permeable layer. However in case B of the same figure, the formation crossflow is from the more permeable layer to the less permeable layer. Even if the difference in the skin factors of the two layers is very small, the direction of the formation crossflow is always from the layer with larger skin to the layer with smaller skin, not from the less permeable layer to the more permeable layer.

Fig. 3.10 shows the effect of skin factors on formation crossflow schematically. Consider two points located at the same radial distance from the wellbore ($r_D = 20$ or $r_D = 40$) in a two layered reservoir where k_1 is higher than k_2, and define Δp_D as the difference of the dimensionless presure at the two points:

$$\begin{aligned} \Delta p_D &\equiv p_{D1} - p_{D2} \\ &= \frac{2\pi (kh)_t}{q_t \mu} (p_2 - p_1) \end{aligned} \tag{3.9}$$

Positive Δp_D means that reservoir pressure is higher in layer 2 than in layer 1, and the crossflow will be from layer 2 to layer 1.

Firstly, consider the case when $s_1 = s_2$. For some time after the start of production, the two points do not feel a pressure gradient, neither radial nor vertical. Soon the reservoir fluid at the points will begin to move toward the wellbore, but not vertically. That is because there is no vertical pressure difference inside either layer by the assumption of the semi-permeable wall model stated in Chapter 2 and because

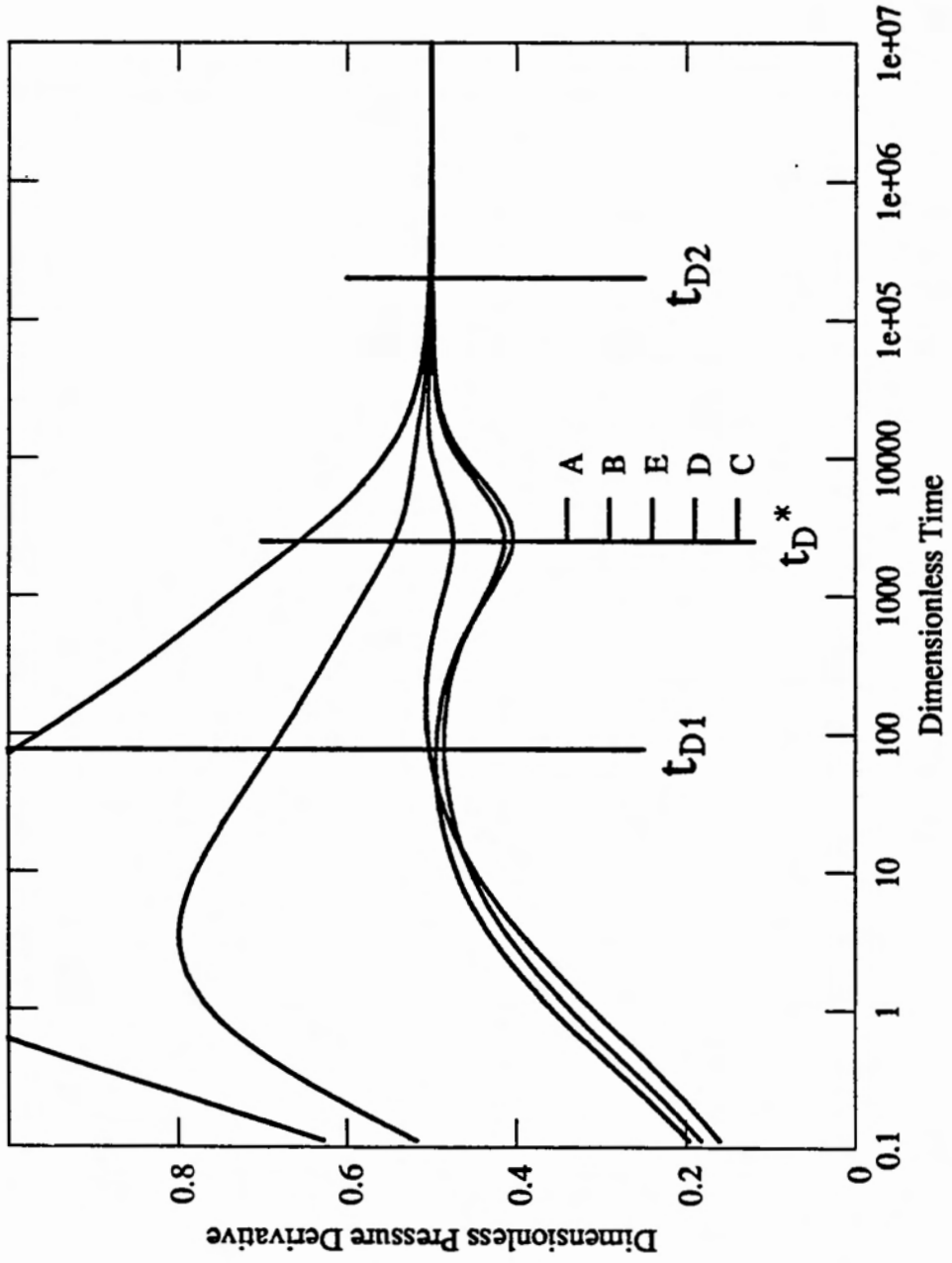

Figure 3.8: Wellbore Pressure Derivative Curves for Various Skin

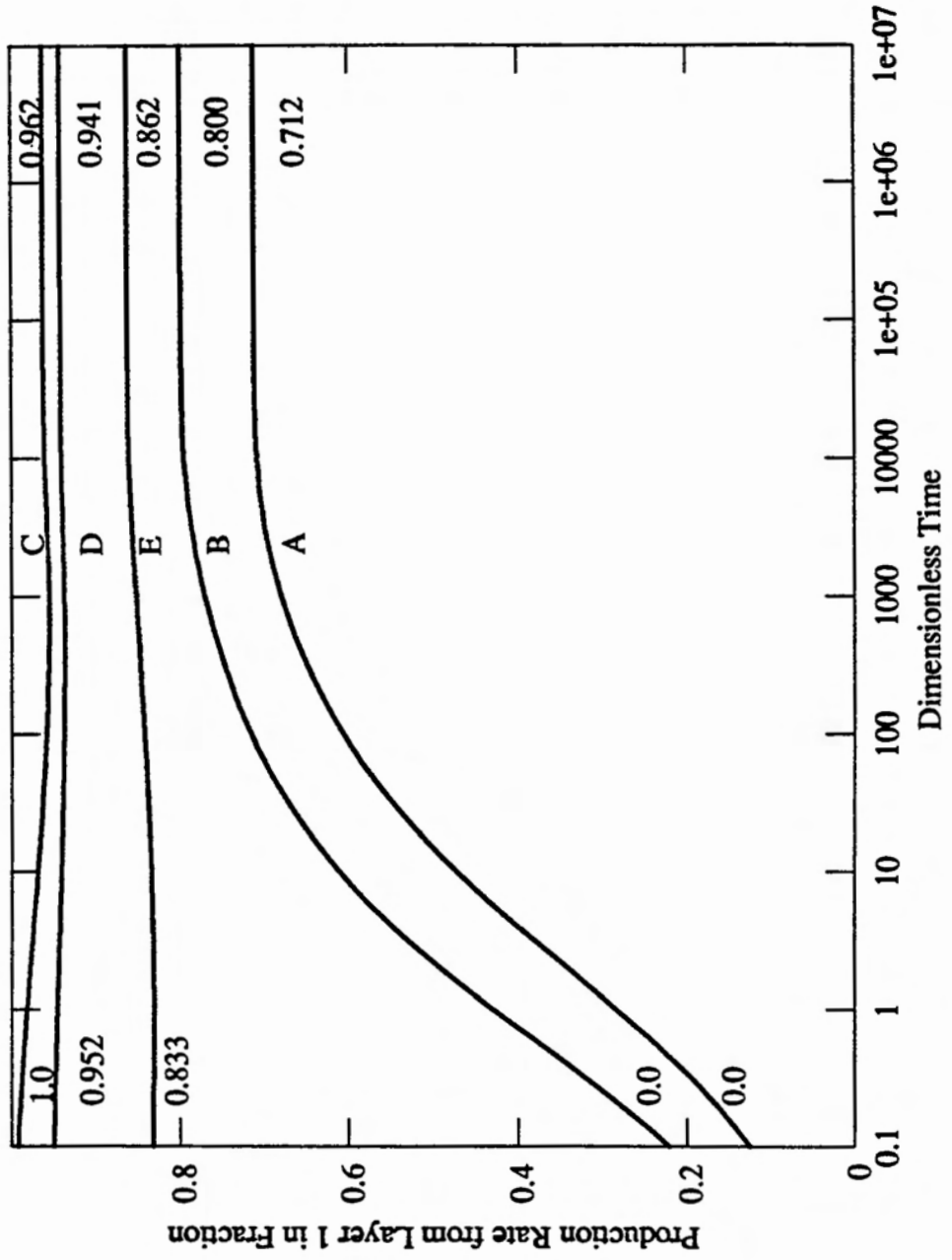

Figure 3.9: Rate Transients for Various Skin

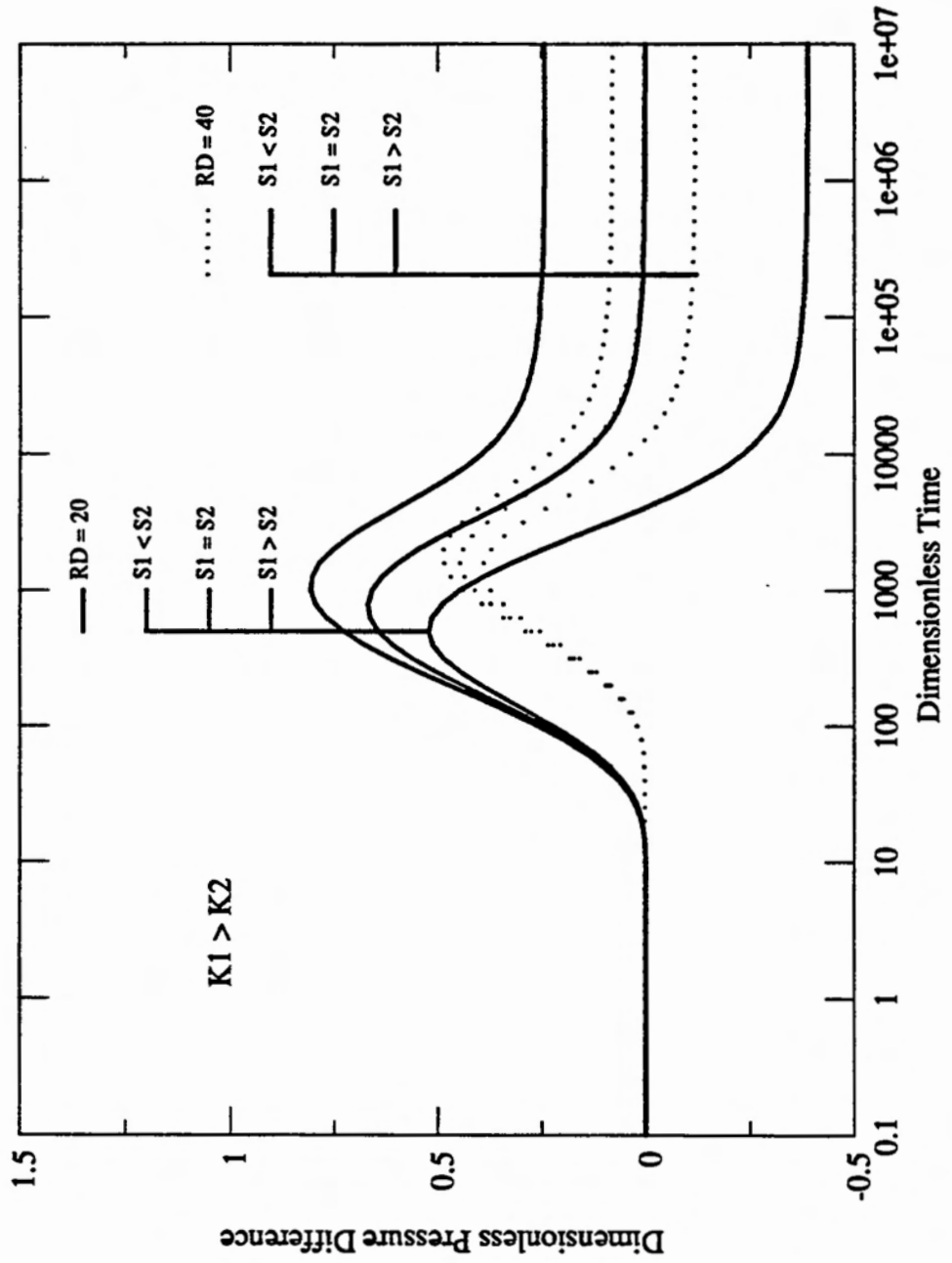

Figure 3.10: Effect of Skin on Vertical Pressure Difference Between Two Layers

even the wellbore takes some time to feel the effect of vertical permeability. Thus the Δp_D curve remains zero up to this time.

Next, vertical permeability begins to take effect and causes a vertical pressure difference between the two points. Now the Δp_D curve begins to increase, since the permeability is greater in layer 1 than in layer 2. The more permeable layer produces faster than the less permeable layer and the pressure drop is bigger in the more permeable layer. Later Δp_D reaches a maximum, begins to decrease and eventually becomes zero at late time.

If $s_1 \neq s_2$, then an interesting phenomenon happens. The general shape looks like that of the case where $s_1 = s_2$ until Δp_D reaches the maximum. The difference is found at late time when the transition ends. Δp_D stays positively constant in the case where $s_2 > s_1$, and negatively constant in the case where $s_1 > s_2$.

Thus two facts can be deduced about the crossflow at late time when the system response converges to that of the homogeneous system:

1. The magnitude of Δp_D at late time remains constant.

2. The crossflow is from the layer with larger skin to the layer with smaller skin. Surprisingly, the effect of permeability is present only for the transition period and when the transition is over, the permeability does not affect the direction of crossflow.

The late time behavior in the crossflow system is due to the late time limiting form for Δp_D, which will be discussed later in Section 3.9.

3.4 Effect of Vertical Permeability

As mentioned in the previous section, the wellbore response of a multilayered crossflow system shows a three stage pattern. The response is identical to that of a commingled system at early time, and to that of a homogeneous system at late time. Consequently, a transition from a commingled system behavior to homogeneous system behavior must occur. The time period when this transition phenomenon starts and stops is dependent on vertical permeability. Radial permeability and skin factor have little effect on the transition times as shown in Section 3.2 and Section 3.3 .

Figs. 3.11- 3.13 show the effect of vertical permeability on wellbore pressure, on the derivative of wellbore pressure and on the fractional production rate of the more permeable layer for a two layered crossflow system with the reservoir parameters as shown in Table 3.4.

Table 3.4: Reservoir Parameters for Studies of the Effect of Vertical Permeability

	case A	case B	case C	case D	case E
k_{vj}/k_j	1	0.1	0.01	0.001	0
case A : Isotropic System case E : Commingled System $k_1 = 1000$ md; $k_2 = 100$ md $s_1 = s_2 = 0$					

All figures show that the smaller the vertical permeabilities are, the later the transition to homogeneous system behavior occurs. In Fig. 3.11, it can be seen that a ten-fold reduction in vertical permeability causes a ten-fold increase in the start of the transition zone. As can be seen in Fig. 3.12, the transition causes a small minimum in the pressure derivative which advances exactly one log cycle as the vertical permeability is decreased by one tenth of the previous value. In Fig. 3.13, the fractional production rate from layer 1 becomes the same constant rate at late time for all cases. The production rate from layer 1 of the commingled system ($k_v = 0$) approaches the same constant rate at very long time.

Thus, it appears that the effect of vertical permeability is to determine when

wellbore pressure reaches a semilog straight line, and when the layer production rates stabilize. Both factors depend on vertical permeability.

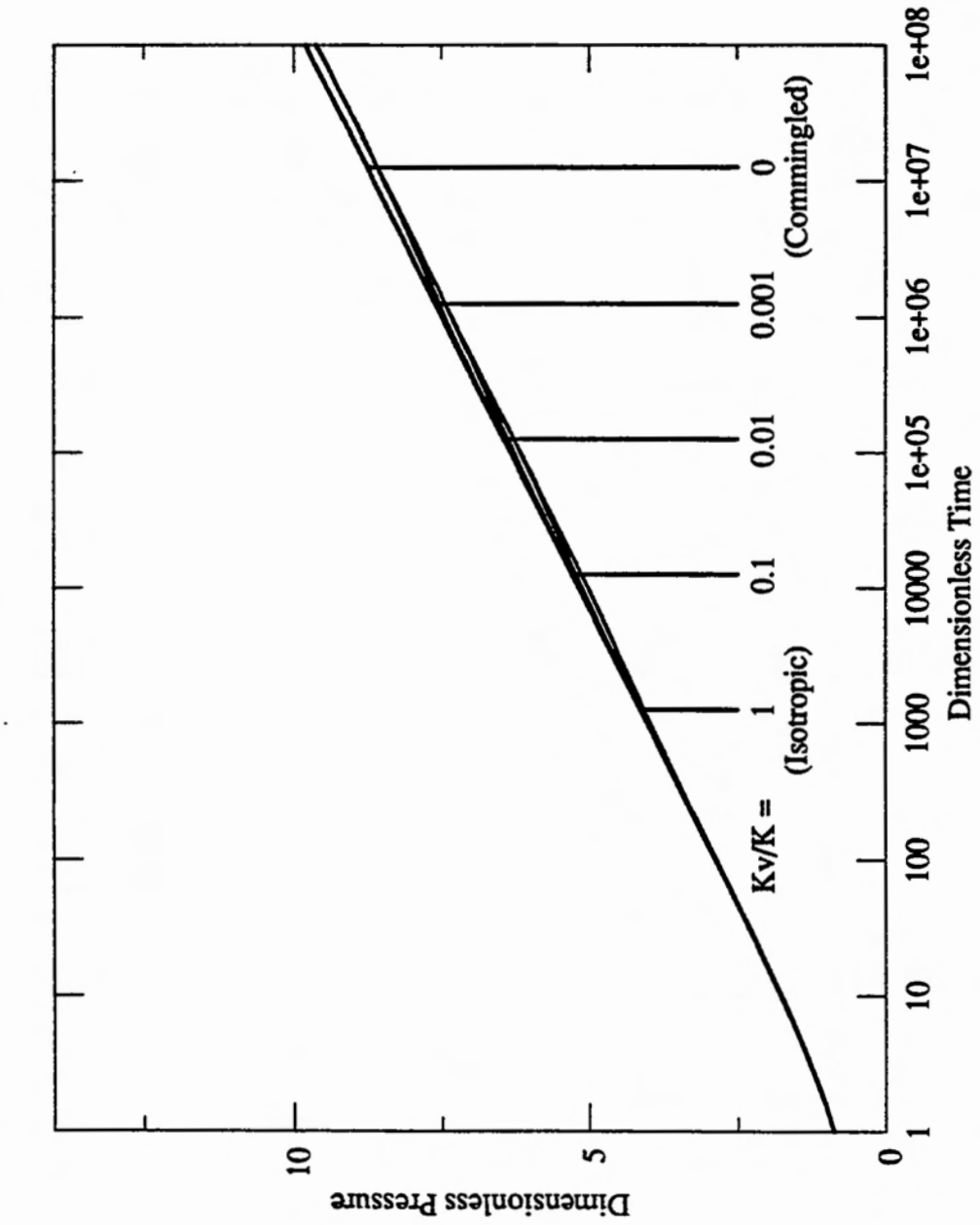

Figure 3.11: Wellbore Pressure Response for Various Vertical Permeabilities

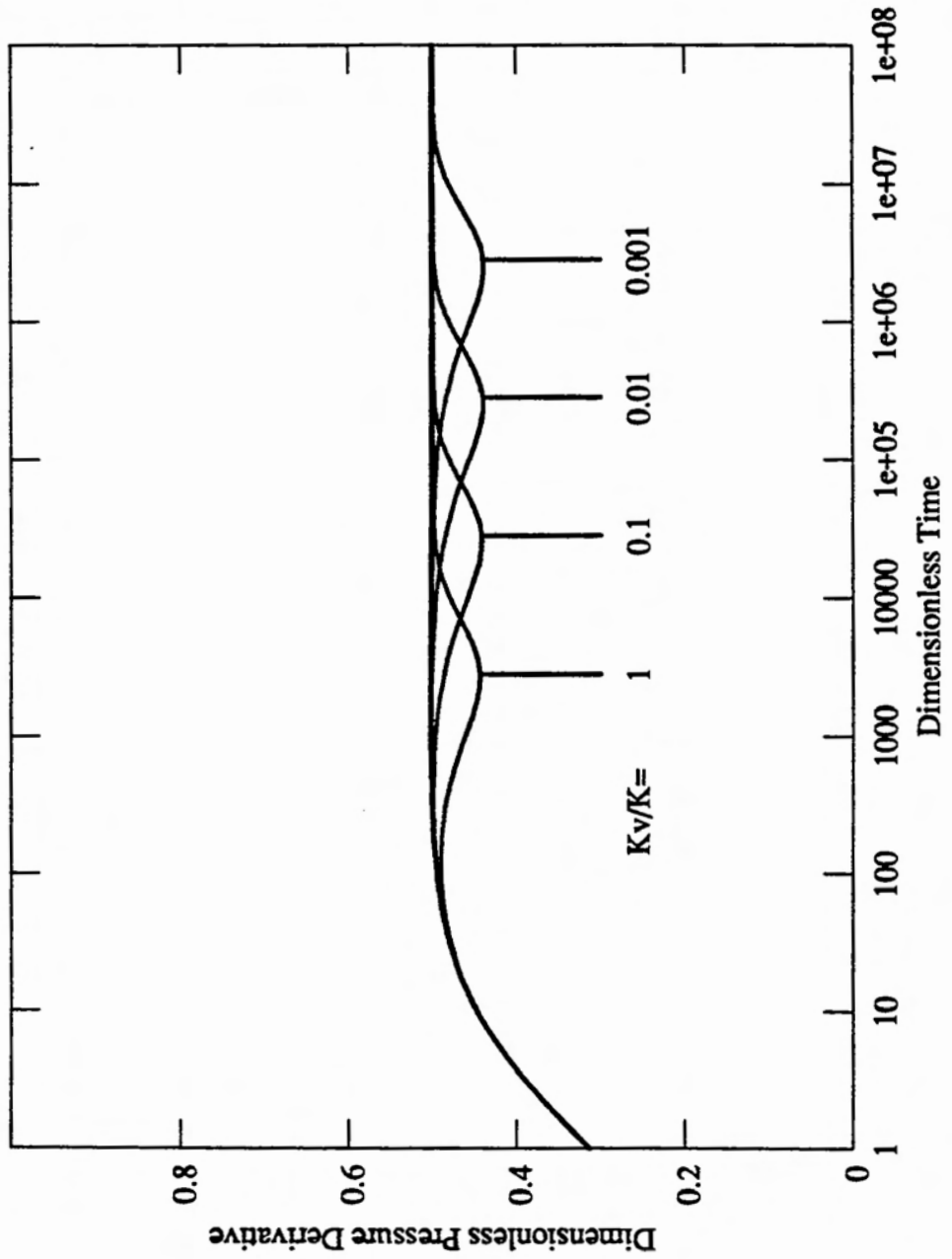

Figure 3.12: Wellbore Pressure Derivative Curves for Various Vertical Permeabilities

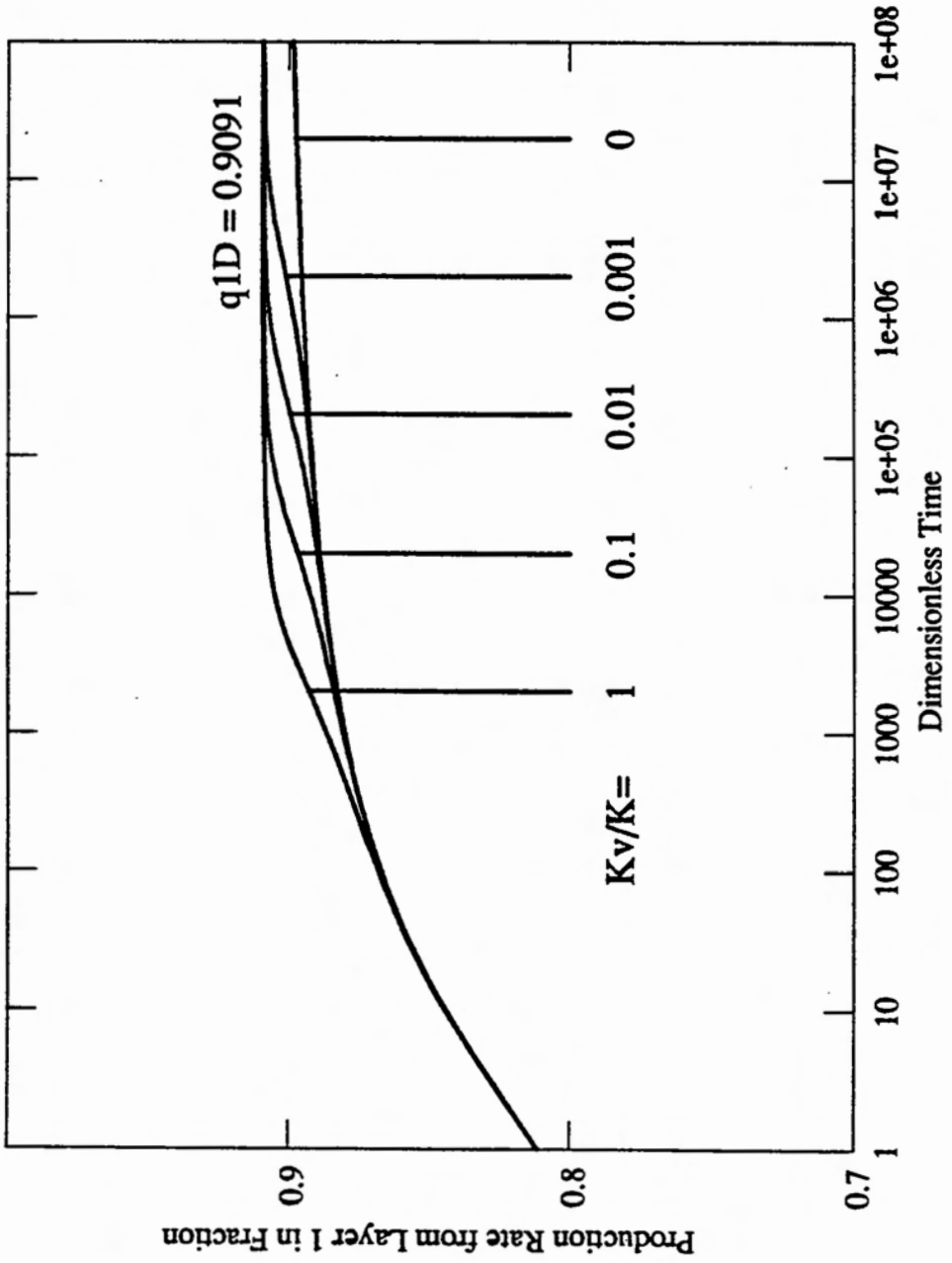

Figure 3.13: Rate Transients for Various Vertical Permeabilities

3.5 Effect of Outer Boundary Conditions

To have a semilog straight line is extremely important in conventional well test analysis for a single layered system because we can determine the permeability and the skin factor directly from the expression of the line. Fortunately, in all crossflow systems, the wellbore pressure reaches to a semilog straight line at late time, as mentioned in Section 3.1, no matter what permeability and skin factor each layer has. However, all we can get from the straight line is just the average values of permeability and skin for the total system, not for the individual layers.

$$(kh)_t = k_1 h_1 + \ldots + k_n h_n \tag{3.10}$$

$$q_t \overline{s} = q_1 s_1 + \ldots + q_n s_n \tag{3.11}$$

One thing to be emphasized here is that in order to have the proper semilog straight line, the transition phenomenon should terminate before the system feels the outer boundary conditions for a reservoir of finite size. As discussed in Section 3.4, the duration of the transition period is entirely determined by the vertical permeabilities of each layer. Thus, the factors that decide if the system will reach to the homogeneous system, are magnitude of the vertical permeabilities and the reservoir size. If the reservoir size is larger and the vertical permeability of each layer is larger, then we may expect to have the semilog straight line, because the multilayered crossflow system feels the outer boundary condition later and the transition period terminates earlier.

Fig. 3.14 and 3.15 shows the effect of outer boundary condition and the vertical permeability on wellbore pressure for a two layered system with the reservoir parameters in Table 3.5.

Table 3.5: Reservoir Parameters for Studies of the Effect of the Outer Boundary Conditions and Vertical Permeabilities on Wellbore Response

Layer	k (md)	k_v (md)	s
1	100	10	0
2	10	10	0

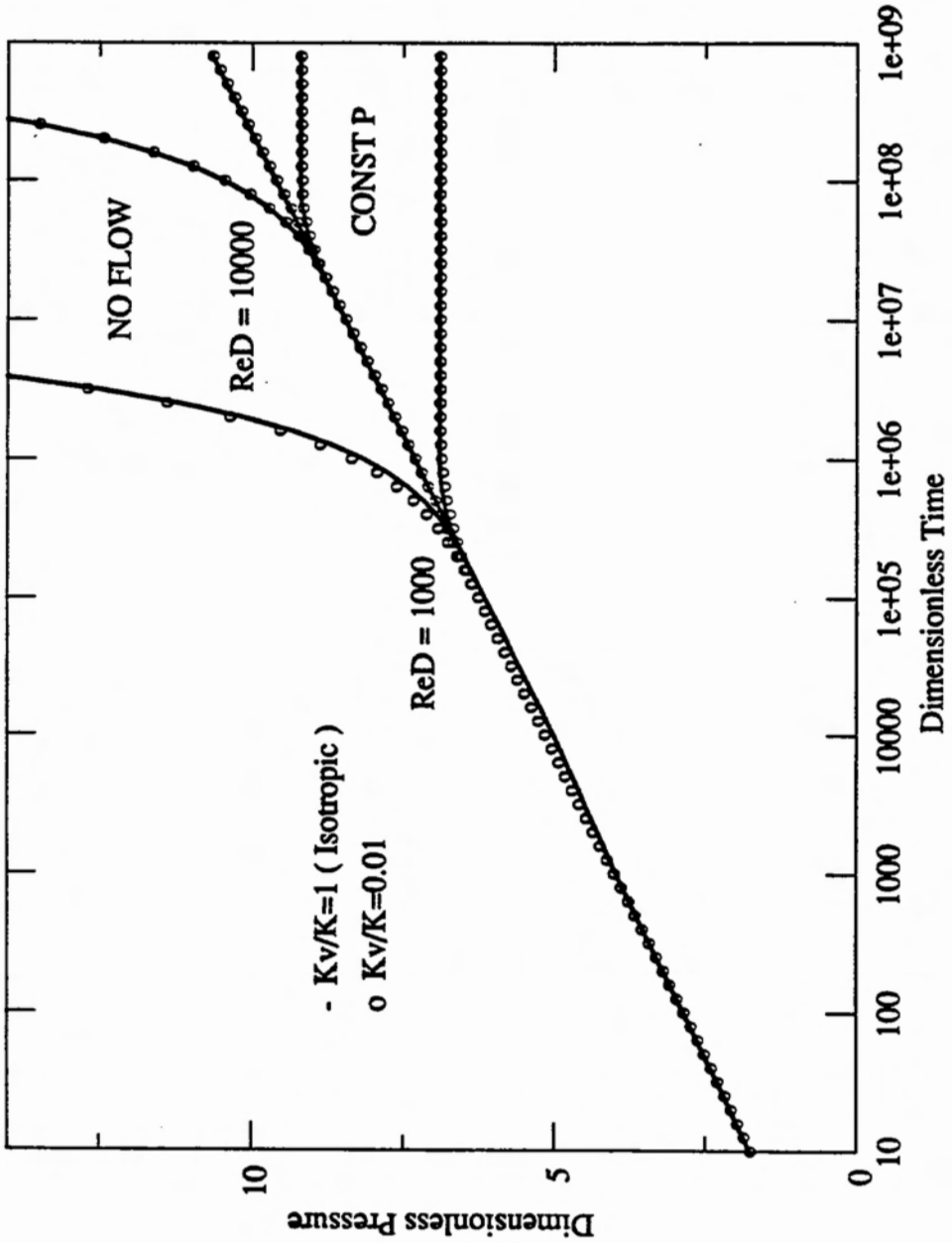

Figure 3.14: Wellbore Pressure Response for Three Typical Outer Boundary Conditions

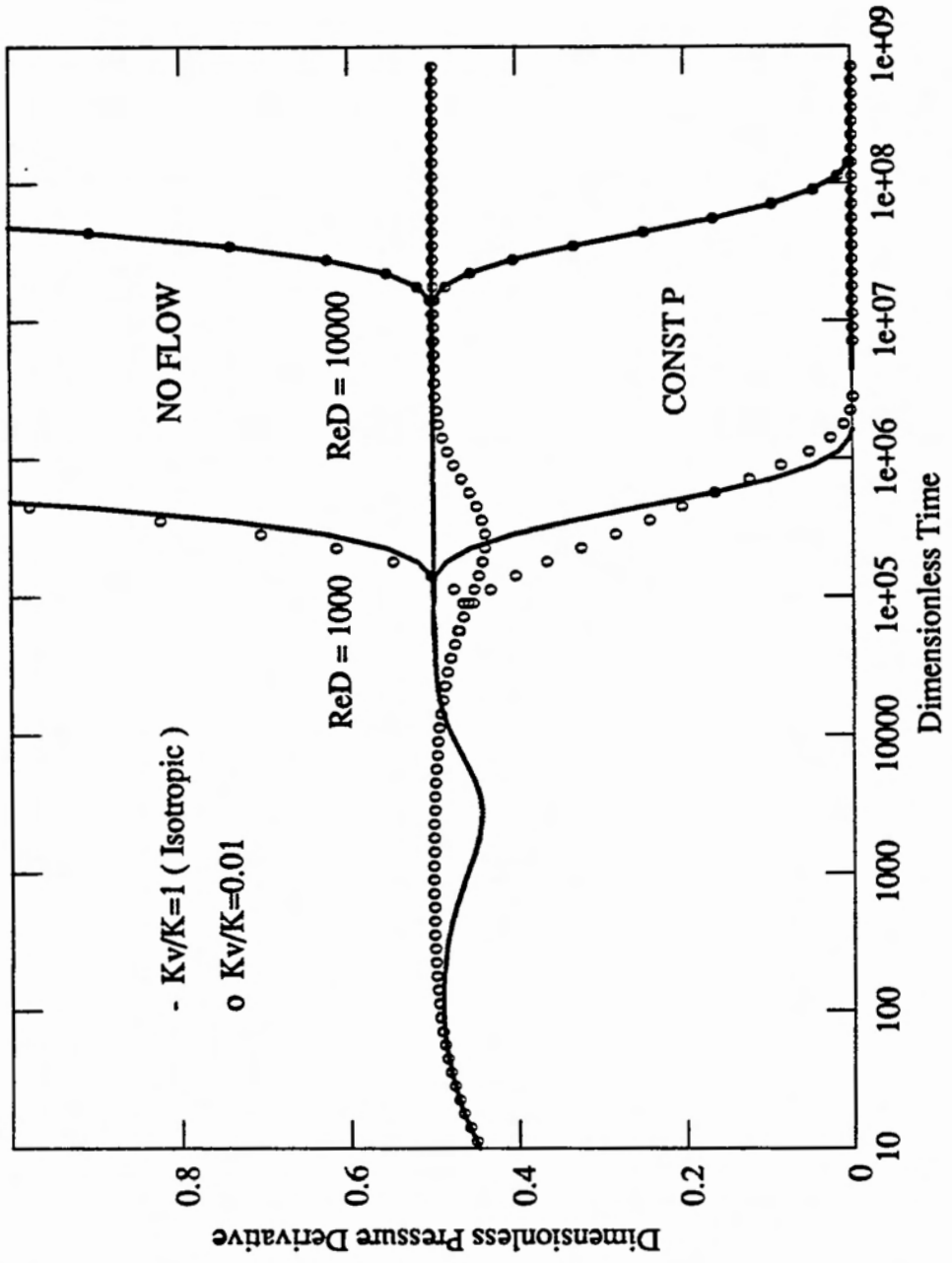

Figure 3.15: Wellbore Pressure Derivative Curves for Three Typical Outer Boundary Conditions

Judging from Fig. 3.14 and Fig. 3.15, the cases of larger reservoir size and larger vertical permeability ($r_{eD} = 10000, k_v/k = 1.0$) reach the proper semilog straight line before the system detects the outer boundary conditions. But the cases of smaller reservoir size and smaller vertical permeability ($r_{eD} = 1000, k_v/k = 0.01$) do not. Although these cases look likely to have some semilog straight line interval in Fig. 3.14, they do not in reality as can be seen in Fig. 3.15 and we may not obtain the correct $(kh)_t$ and $\overline{s}$ accordingly.

Fig. 3.16 shows the production rate from layer 1 in a two layered reservoir for three different outer boundary conditions. In the cases of infinite acting boundary condition, the terminal production rate is just equivalent to $\kappa_1 (= k_1 h_1/(kh)_t)$, since the skin factors are zero as shall be discussed in Section 3.9. A more interesting fact is that the terminal production rate from each layer is same, regardless of the outer boundary conditions as long as the multilayered crossflow system reaches to the homogeneous system response before detecting outer boundary conditions ($k_v/k = 1.0$). However, if the outer boundary condition is felt significantly before the system reaches to the homogeneous system response, then the terminal layer production rate is affected also by outer boundary condition and we see some divergence as in cases of $k_v/k = 0.01$. The terminal production rate of the case of constant pressure outer boundary condition reaches a value of κ_1 much earlier than the case of the infinite reservoir. The value of the terminal production rate in the case of no flow outer boundary condition is significantly different from κ_1.

Concerning the wellbore pressure, it can be easily noticed that vertical permeability does not affect the pressure response much, no matter how big or small vertical permeability is, once the system reaches to the homogeneous system response. This holds regardless of the outer boundary conditions. Thus at late time, the usual expression can be applied:

$$p_D = \frac{1}{2}\ln t_D + 0.4045 + \overline{s} \qquad \text{infinite reservoir,} \tag{3.12}$$

$$p_D = \ln r_{eD} + \overline{s} \quad \text{constant pressure condition, and} \tag{3.13}$$

$$p_D = \frac{2t_D}{r_{eD}^2 - 1} \qquad \text{no-flow boundary condition} \tag{3.14}$$

All the behaviors described above still hold for the cases when skin factors are

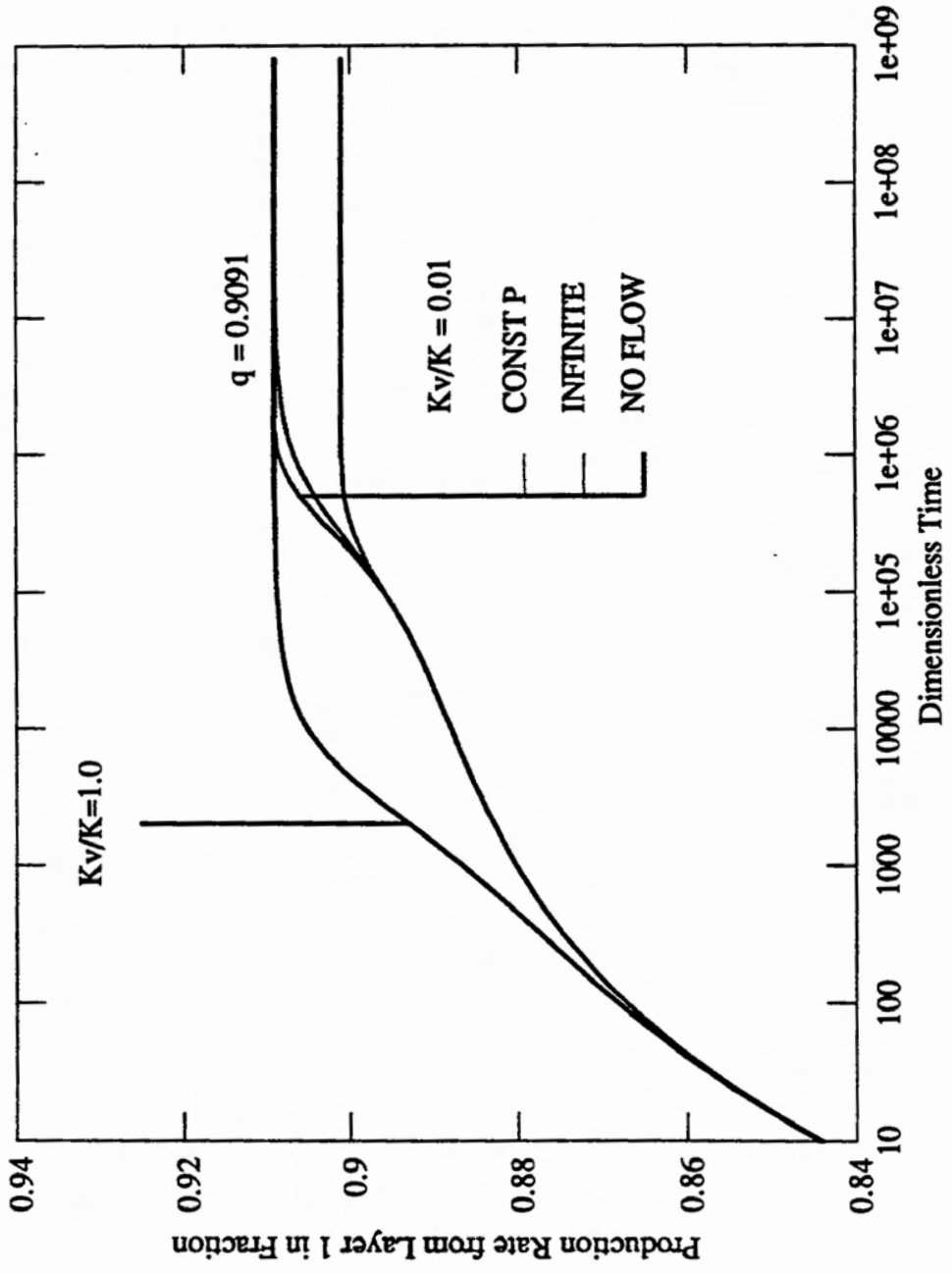

Figure 3.16: Rate Transients for Three Typical Outer Boundary Conditions

involved. However, the terminal production rate from each layer is also affected by λ, if the skin factor of each layer is different. For example, in a two layered system:

$$q_{1D}{}^{LT} = \kappa_1(1 + \frac{\kappa_2(s_2 - s_1)}{K_1^0(\sigma_1) + \kappa_1 s_2 + \kappa_2 s_1}) \tag{3.15}$$

$$q_{2D}{}^{LT} = \kappa_2(1 + \frac{\kappa_1(s_1 - s_2)}{K_1^0(\sigma_1) + \kappa_1 s_2 + \kappa_2 s_1}) \tag{3.16}$$

where

$$K_1^0(\sigma_1) = \frac{K_0(\sigma_1)}{\sigma_1 K_1(\sigma_1)} \tag{3.17}$$

$$\sigma_1 = \sqrt{\frac{\lambda}{\kappa_1} + \frac{\lambda}{\kappa_2}} \tag{3.18}$$

By definition, the average skin value is also affected by λ, since the terminal production rate from each layer is a function of λ.

$$\overline{s} = s_1 q_{1D} + \ldots + s_n q_{nD} \tag{3.19}$$

Thus, even the simplest cases when the outer boundary condition is infinite acting, each case reaches to the proper semilog straight line, but not the same line because of the small variation in the average skin of the system.

3.6 Effect of Wellbore Storage

As the pressure drops, reservoir fluid expands. The fluid of expanded volume cannot stay inside the original pore space and flows toward the lower pressure zone. This expansion happens not only in the reservoir but also in the wellbore. Thus when we say that we produce the reservoir fluid at a constant rate at the wellhead, some portion of the production comes from the expanded volume of the fluid that fills the wellbore while the rest comes from the reservoir pore space. The contribution of the expansion of the reservoir fluid in the wellbore to the pressure or the layer production rate is called wellbore storage effect. This wellbore storage effect is taken into consideration as an inner boundary condition:

$$q_t = -C\frac{dp_{wf}}{dt} + \sum_{j=1}^{n} \frac{2\pi(kh)_t}{\mu}\frac{\partial p_j}{\partial r}|_{r=r_w} \tag{3.20}$$

or in a dimensionless form:

$$1 = C_D\frac{dp_{wD}}{dt_D} - \sum_{j=1}^{n} \kappa_j \frac{\partial p_{jD}}{\partial r_D}|_{r_D=1} \tag{3.21}$$

where

$$C_D = \frac{C}{2\pi(\phi h)c_t r_w^2}$$

As mentioned in Section 3.1, early time behavior of the crossflow system is identical to that of the commingled system. Thus, as can be seen in Appendix B, wellbore pressure at early time for the multilayered crossflow system with wellbore storage effect is:

$$\overline{p_{wD}} = \frac{1}{z[C_D z + \sum_{k=1}^{n} \frac{\kappa_k \sigma_k K_1(\sigma_k)}{K_0(\sigma_k)+s_k\sigma_k K_1(\sigma_k)}]} \tag{3.22}$$

Since z becomes very large at early time, the first term in the denominator, $C_D z$, is large enough to dominate over the summation terms, and the $\overline{p_{wD}}$ can be approximated as:

$$\overline{p_{wD}} \simeq \frac{1}{C_D z^2} \tag{3.23}$$

or in an inversely transformed dimensionless time domain:

$$p_{wD} \simeq \frac{t_D}{C_D} \tag{3.24}$$

This is just a unit slope straight line in a log-log scale plot as can be seen in Fig. 3.17 and none of the reservoir information can be obtained while wellbore storage effect dominates the well test data. Fortunately, z gets smaller as time increases and the wellbore storage effect ($C_D z$) becomes negligible. Thus it may be said that the effect of wellbore storage in a multilayered crossflow system is just to mask the valuable reservoir information at early time, as in many other reservoir models.

Early time data is as important as late time data, since the former shows diverse pattern according to the individual layer parameters while the latter shows only the average values of the total system such as $(kh)_t$ or $\overline{s}$. Ehlig-Economides and Joseph (1985), however, discovered a useful way to minimize the effect of wellbore storage on the wellbore pressure and the layer production rate.

From Eq. 3.22, wellbore pressure without storage effect can be written as:

$$\overline{p_{wD,C_D=0}} = \frac{1}{z[\sum_{k=1}^{n} \frac{\kappa_k \sigma_k K_1(\sigma_k)}{K_0(\sigma_k)+s_k \sigma_k K_1(\sigma_k)}]} \tag{3.25}$$

where $\overline{p_{wD,C_D=0}}$ means wellbore pressure without storage effect.

From Eq. 3.22 and Eq. 3.25, we can find a relationship between the wellbore pressure with and without storage effect, which is:

$$\frac{1}{\overline{p_{wD}}} = C_D z^2 + \frac{1}{\overline{p_{wD,C_D=0}}} \tag{3.26}$$

By rearranging for $\overline{p_{wD,C_D=0}}$,

$$\overline{p_{wD,C_D=0}} = \frac{1}{\frac{1}{\overline{p_{wD}}} - C_D z^2} = \frac{\overline{p_{wD}}}{1 - C_D z^2 \overline{p_{wD}}} \tag{3.27}$$

Examples of eliminating the storage effect from wellbore pressure using Eq. 3.27 for various storage coefficient are shown in Fig. 3.17.

Analogy is found in the equation for the layer production rate. From Appendix B, the production rate from layer j with storage effect is:

$$\overline{q_{jD}} = \frac{\kappa_j \sigma_j K_1(\sigma_j)}{K_0(\sigma_j) + s_j \sigma_j K_1(\sigma_j)} \overline{p_{wD}} \tag{3.28}$$

where

$$\sigma_j = \sqrt{\frac{\omega_j z}{\kappa_j}} \tag{3.29}$$

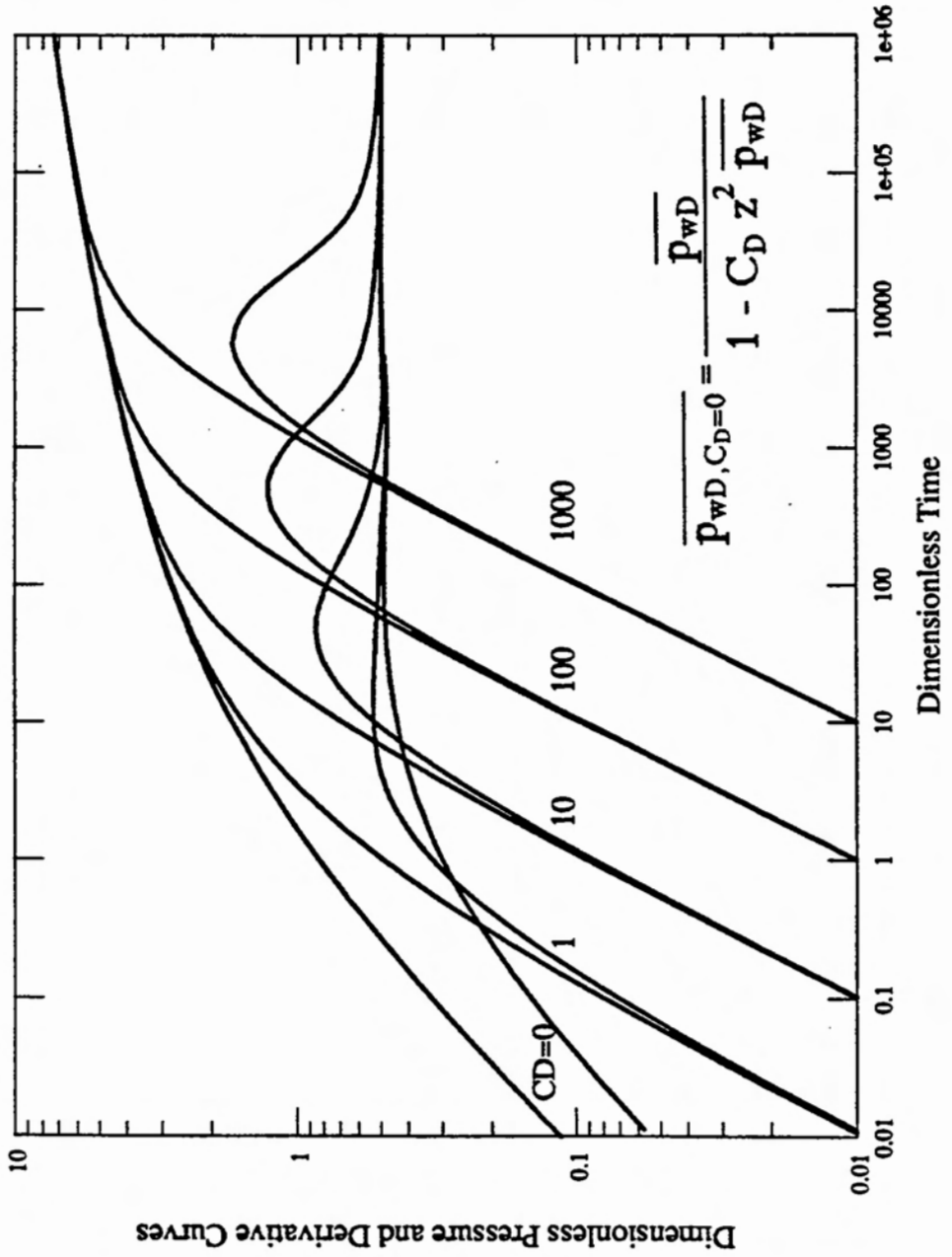

Figure 3.17: Wellbore Pressure Curves and Their Derivatives for Various Storage Coefficients

From Eq. 3.26,

$$\begin{aligned} \overline{p_{wD}} &= \frac{1}{C_D z^2 + \frac{1}{\overline{p_{wD,C_D=0}}}} \\ &= \frac{\overline{p_{wD,C_D=0}}}{C_D z^2 \overline{p_{wD,C_D=0}} + 1} \end{aligned} \tag{3.30}$$

Substituting Eq. 3.30 into Eq. 3.28 yields:

$$\begin{aligned} \overline{q_{jD}} &= \frac{\kappa_j \sigma_j K_1(\sigma_j)}{K_0(\sigma_j) + s_j \sigma_j K_1(\sigma_j)} \overline{p_{wD}} \\ &= \frac{\kappa_j \sigma_j K_1(\sigma_j)}{K_0(\sigma_j) + s_j \sigma_j K_1(\sigma_j)} \frac{\overline{p_{wD,C_D=0}}}{C_D z^2 \overline{p_{wD,C_D=0}} + 1} \\ &= \frac{\overline{q_{jD,C_D=0}}}{C_D z^2 \overline{p_{wD,C_D=0}} + 1} \end{aligned} \tag{3.31}$$

where $\overline{q_{jD,C_D=0}}$ means the production rate from layer j without wellbore storage effect.

By simple rearrangement, Eq. 3.31 can be written as:

$$\overline{q_{jD}} = (1 - C_D z^2 \overline{p_{wD}}) \overline{q_{jD,C_D=0}} \tag{3.32}$$

By taking the summation for the production rate from each layer:

$$\begin{aligned} \sum_{j=1}^{n} q_{jD} &= (1 - C_D z^2 \overline{p_{wD}}) \sum_{j=1}^{n} q_{jD,C_D=0} \\ &= (1 - C_D z^2 \overline{p_{wD}}) \end{aligned} \tag{3.33}$$

There is a relationship between Eq. 3.32 and Eq. 3.33 such that:

$$\frac{q_{jD}}{\sum_{j=1}^{n} q_{jD}} = \frac{(1 - C_D \overline{p_{wD}} z^2)}{(1 - C_D \overline{p_{wD}} z^2)} q_{jD,C_D=0} \tag{3.34}$$

Finally, the layer production rate with the wellbore storage effect eliminated is:

$$q_{jD,C_D=0} = \frac{q_{jD}}{\sum_{j=1}^{n} q_{jD}} \tag{3.35}$$

which means the ratio of the layer production rate and the sum of the production rate from the reservoir is equivalent to the layer production rate with no wellbore storage effect. Examples of eliminating the storage effect using Eq. 3.35 can be found in Fig. 3.18 for various wellbore storage coefficients.

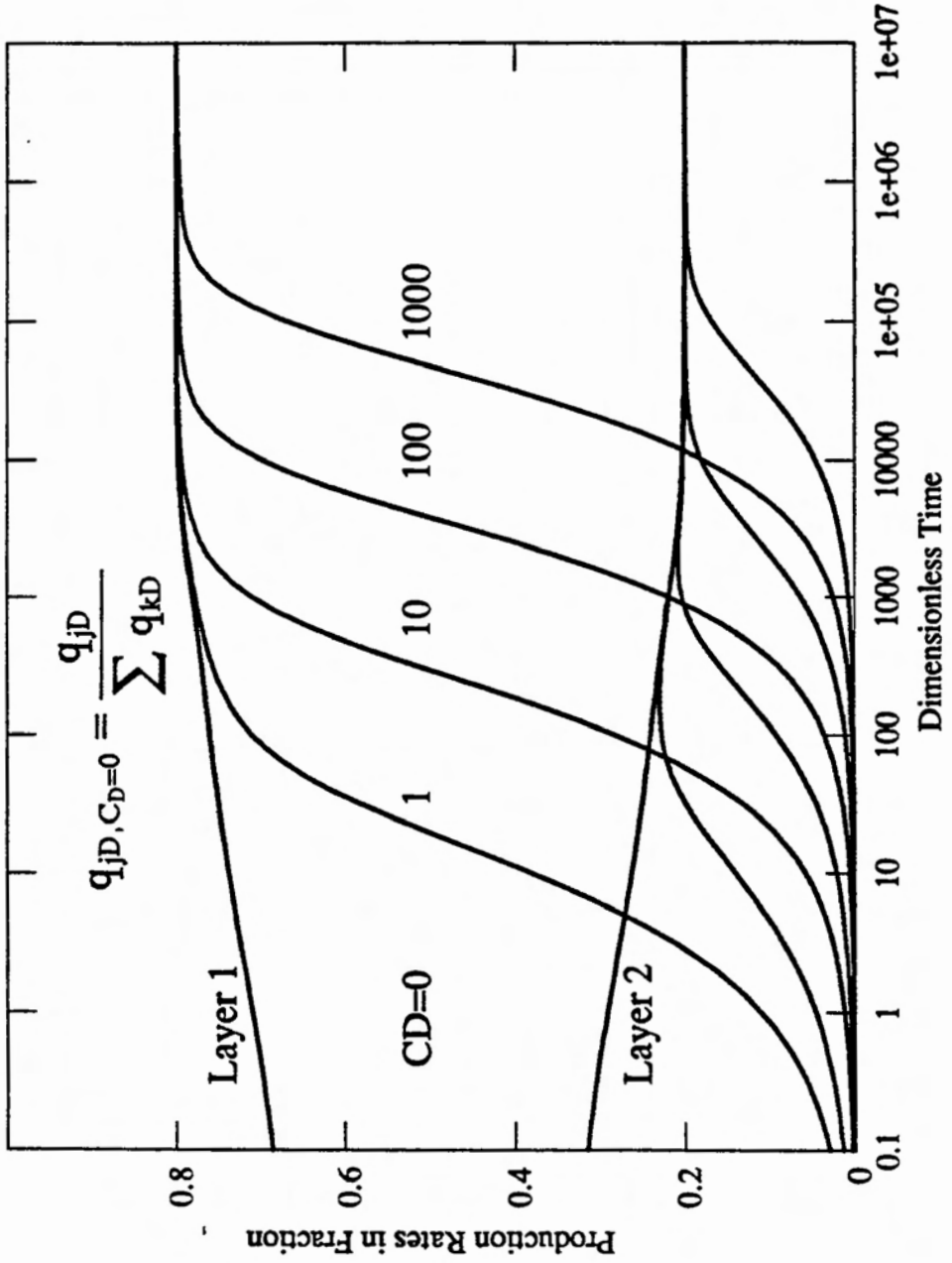

Figure 3.18: Rate Transients for Various Storage Coefficients

3.7 Effect of Layering Order

The order of layers also has some effect on the wellbore response. The change of order will also change the values of the λ's, the parameters representing crossflow between layers, since each layer has different vertical permeability. These modified λ's will affect intermediate and late time response of the multilayered reservoir with crossflow. The early time response does not change because the system is behaving like a commingled system. Fig. 3.19- 3.21 show the effect of layering for a three layered crossflow system with the reservoir parameters in Table 3.6.

Table 3.6: Reservoir Parameters for Studies of the Effect of the Order of the Layers

Case	k_1(md)	k_2(md)	k_3(md)	s_1	s_2	s_3
A	1000	10	1000	5	1	3
B	10	1000	1000	1	5	3
C	10	1000	1000	1	3	5

Considering that the heterogeneities in permeability are 100 fold, it may be said that there is little difference in response among the three sample cases. This is same as the observation of Gao (1983 b). If the heterogeneities in skin factor and vertical permeability are not big, the effect of layering order in a multilayered reservoir with crossflow is not significant. However, when the heterogeneities in vertical permeability is very big and the least permeable layer is placed between more permeable layers as in case B, the system behaves like a commingled system.

As a special case, when skin is zero in every layer, or more generally, when the skin factors are all of equal magnitude, s, then wellbore pressure at late time and the layer production rate are as follows, as shall be discussed in Section 3.9.

$$ {p_{wD}}^{LT} = \frac{1}{2}\ln t_D + 0.404535 + \overline{s} \tag{3.36} $$

where

$$ \begin{aligned} \overline{s} &= {q_{1D}}^{LT} s_1 + \ldots + {q_{nD}}^{LT} s_n \\ &= ({q_{1D}}^{LT} + \ldots + {q_{nD}}^{LT}) s \end{aligned} \tag{3.37} $$

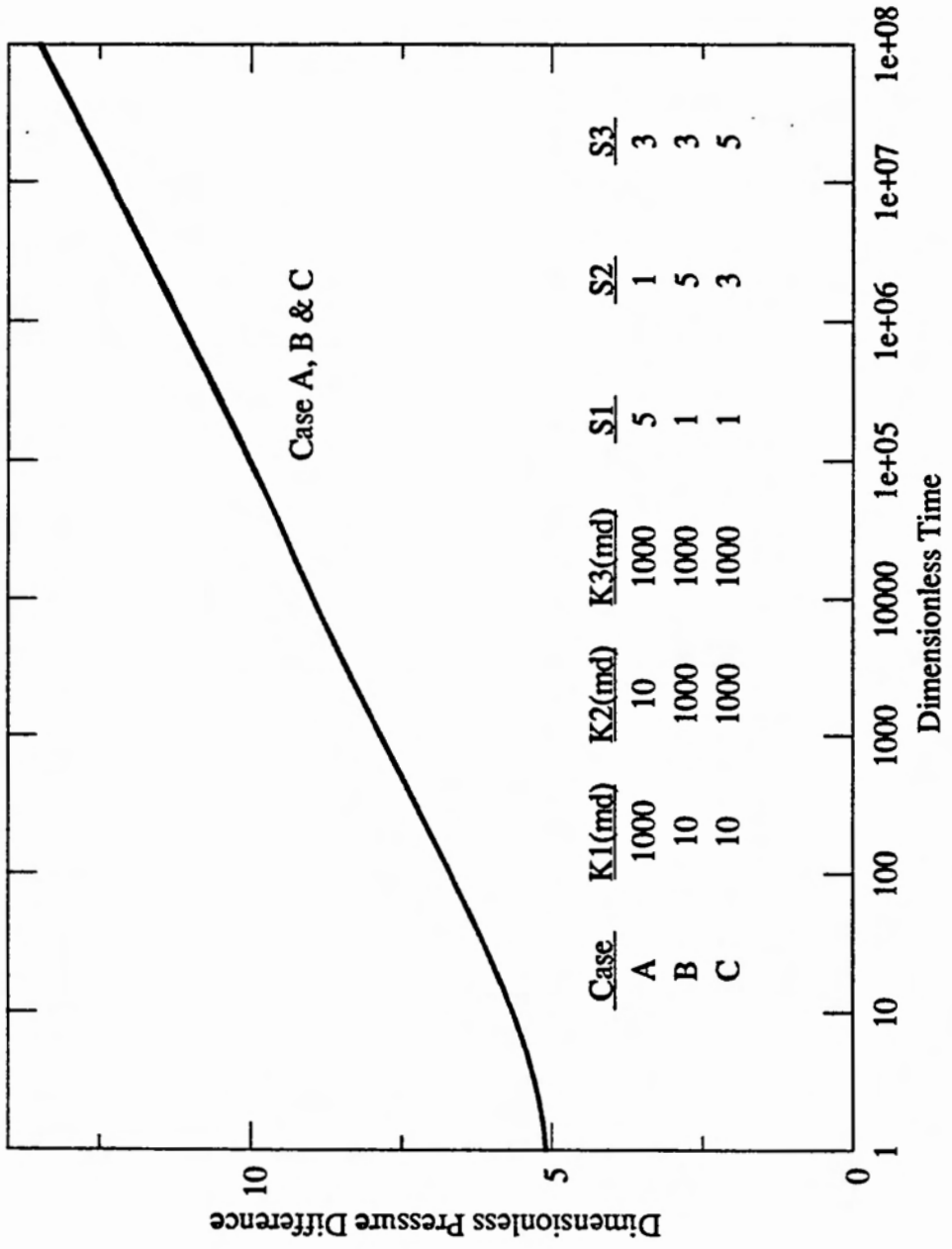

Figure 3.19: Wellbore Pressure Response for Different Layering Orders

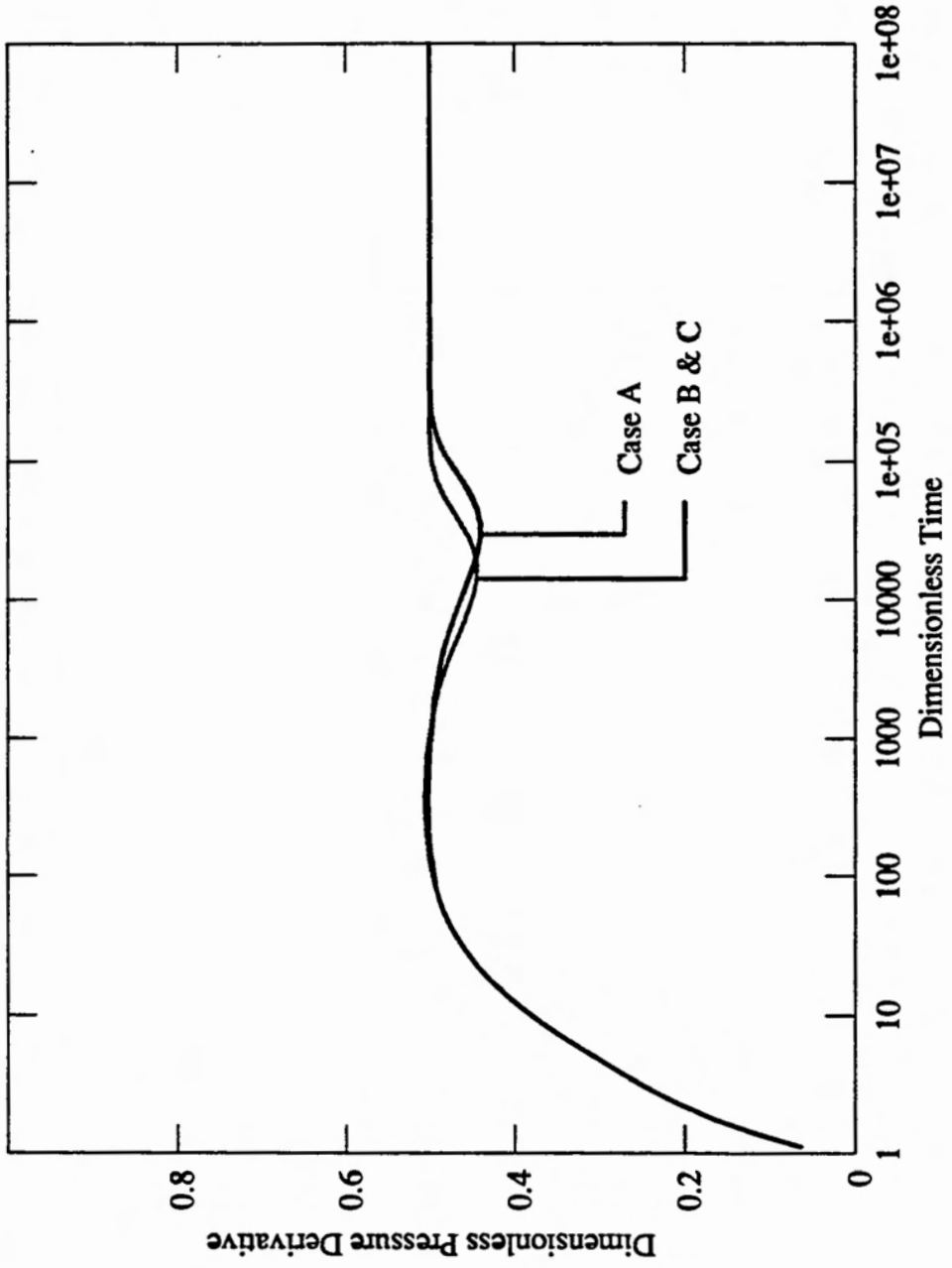

Figure 3.20: Wellbore Pressure Derivatives for Different Layering Orders

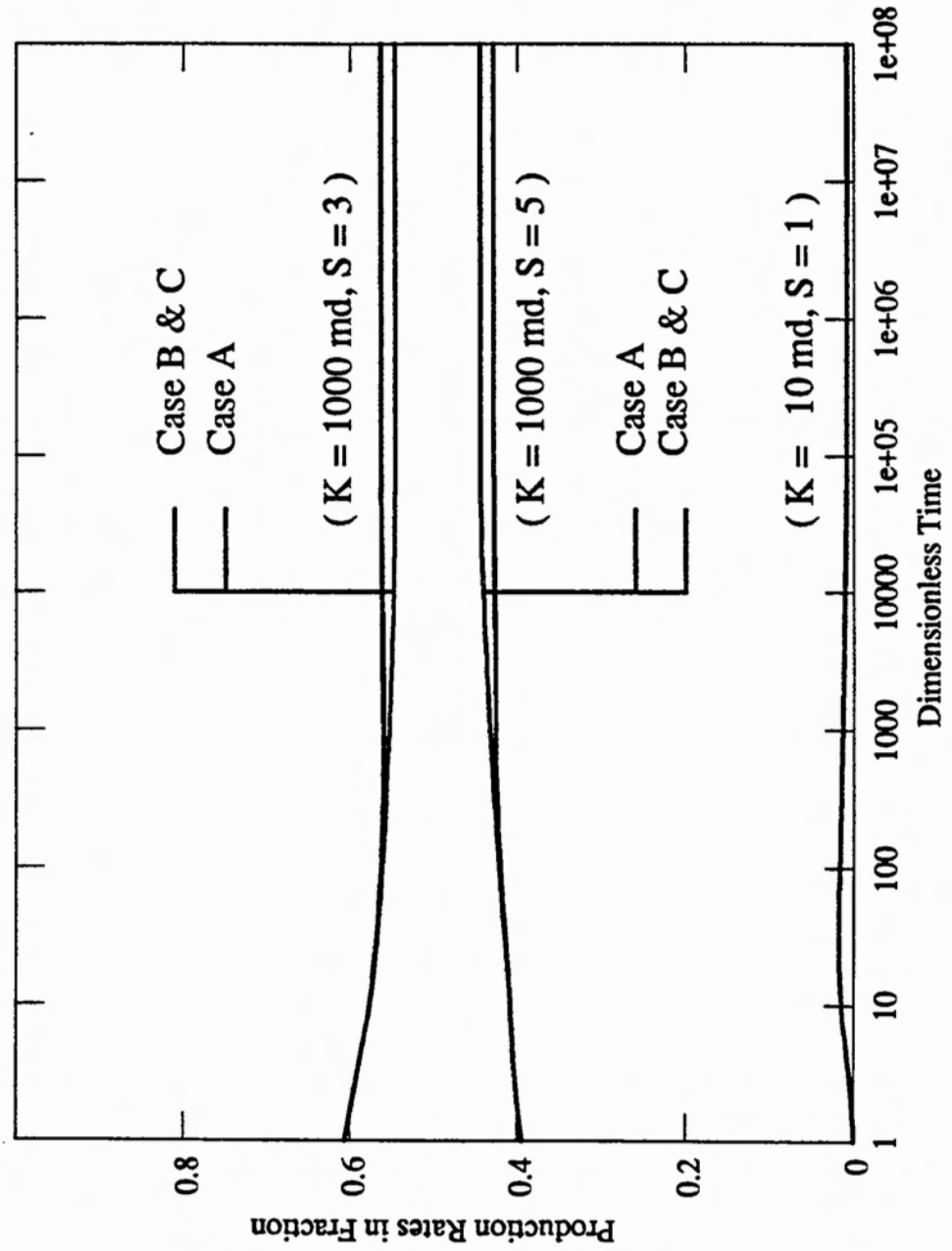

Figure 3.21: Rate Transients for Different Layering Orders

$$= \quad s$$

and

$$q_{jD}{}^{LT} = \kappa_j = \frac{k_1 h_1}{(kh)_t} \tag{3.38}$$

Since the layer production rate is equivalent to κ at late time, the average skin is never affected by the order of layering, neither is wellbore pressure. Thus, when the skin of each layer is all same, there is no effect of layering on the wellbore response in the late time either. If skin factors are different from each other, then layer production rate is not κ but some other constant determined by the skin factors and vertical permeabilities as well as radial permeabilities. Hence the average skin changes with q_{jD} and the wellbore pressure also change with $\overline{s}$.

3.8 Early Time Behavior

As many authors have pointed out, the early time behavior of the crossflow system is identical to that of the commingled system. However, Ehlig-Economides and Joseph (1985) were the first to have proved it rigorously.

The Laplace transformation of the pressure drop and the production rate from each layer in a commingled system, have been solved by Lefkovits, *et al.* (1961). Their solution is for a closed system and is in dimensional form. Assuming that the early time behavior of the system is not affected by the outer boundary conditions, we can more easily analyze the early time behavior by investigating the solutions for an infinite reservoir in a dimensionless form as in Appendix B:

$$\overline{p_{wD}} = \frac{1}{z[C_D z + \sum_{j=1}^{n} \frac{\kappa_j \sigma_j K_1(\sigma_j)}{K_0(\sigma_j)+s_j\sigma_j K_1(\sigma_j)}]} \tag{3.39}$$

$$\overline{q_{jD}} = \frac{\kappa_j \sigma_j K_1(\sigma_j)}{K_0(\sigma_j) + s_j \sigma_j K_1(\sigma_j)} \overline{p_{wD}} \tag{3.40}$$

where

$$\sigma_j = \sqrt{\frac{\omega_j z}{\kappa_j}} \tag{3.41}$$

By the method mentioned in Section 3.6, the effect of wellbore storage can be eliminated. So, in this section, we just consider the case with no wellbore storage.

At early time, z becomes large and so does σ. Thus, using the approximation of the K_0 and K_1 for the large argument:

$$\lim_{\sigma \to \infty} \frac{K_0(\sigma_j)}{\sigma_j K_1(\sigma_j)} \to \frac{1}{\sigma_j} \tag{3.42}$$

The equation for $\overline{q_{jD}}$ becomes:

$$\overline{q_{jD}} = \frac{\frac{\kappa_j \sigma_j}{1+s_j\sigma_j}}{z \sum_k \frac{\kappa_k \sigma_k}{1+s_k\sigma_k}} \tag{3.43}$$

As mentioned earlier in Section 3.1, the limiting forms of the early time layer production rate are constant. Since a multilayered crossflow system can be classified by the combination of skin factors as follows:

1. Case (A) : All skin factors are zero,
2. Case (B) : All skin factors are non-zero, and
3. Case (C) : Some skin factors are zero, while others are not.

the constant values of the early time layer production rate can be determined case by case.

3.8.1 Case A: $s_k = 0$ for all k

Since all skin factors are zero:

$$1 + s_k\sigma_k = 1 \tag{3.44}$$

Then, the production rate of the layer j at early time becomes:

$$\begin{aligned} \overline{q_{jD}} &= \frac{\kappa_j\sigma_j}{z\sum_{k=1}^{n}\kappa_k\sigma_k} \\ &= \frac{\kappa_j\sqrt{\frac{\omega_j z}{\kappa_j}}}{z\sum_{k=1}^{n}\kappa_k\sqrt{\frac{\omega_k z}{\kappa_k}}} \\ &= \frac{\sqrt{\omega_j\kappa_j}}{z\sum_{k=1}^{n}\sqrt{\omega_k\kappa_k}} \end{aligned} \tag{3.45}$$

and, if transformed into real space, it becomes:

$$q_{jD} = \frac{\sqrt{\omega_j\kappa_j}}{\sum_{k=1}^{n}\sqrt{\omega_k\kappa_k}} \tag{3.46}$$

Thus, at early time, each layer produces at a constant rate determined by the fraction of $\sqrt{\omega_j\kappa_j}$. An Example for case A is shown in Fig. 3.22.

3.8.2 Case B: $s_k \neq 0$ for all k

At early time, $\sigma_k = \sqrt{\frac{\omega_k z}{\kappa_k}}$ is much greater than one. If s_k is a reasonably big number, then:

$$1 + s_k\sigma_k \simeq s_k\sigma_k \tag{3.47}$$

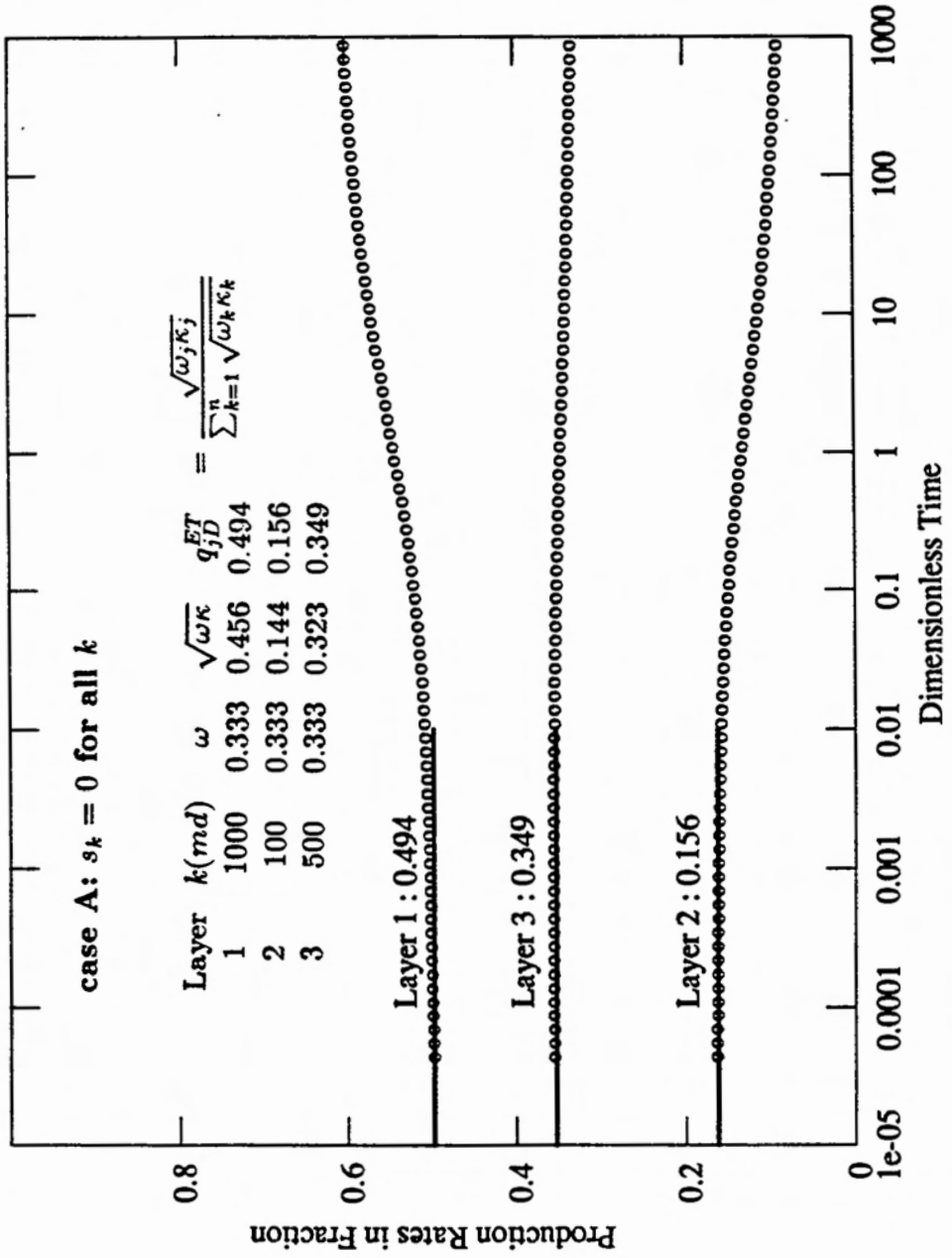

Figure 3.22: Early Time Limiting Layer Production Rates for Case A

Thus the production rate of the layer j at early time becomes:

$$\begin{aligned} \overline{q_{jD}} &= \frac{\frac{\kappa_j \sigma_j}{s_j \sigma_j}}{z \sum_{k=1}^{n} \frac{\kappa_k \sigma_k}{s_k \sigma_k}} \\ &= \frac{\kappa_j / s_j}{z \sum_{k=1}^{n} \kappa_k / s_k} \end{aligned} \tag{3.48}$$

and, if transformed into real space, it becomes:

$$q_{jD} = \frac{\kappa_j / s_j}{\sum_{k=1}^{n} \kappa_k / s_k} \tag{3.49}$$

which is also a constant rate determined by the fraction of $\frac{\kappa_j}{s_j}$. Example for case B is shown in Fig. 3.23.

A question might be raised about the limiting production rates of the layers with very small non-zero skin factors. The answer for the question can be sought in the validity of the approximation of Eq. 3.47.

$$1 + s_k \sigma_k \simeq s_k \sigma_k \tag{3.50}$$

Eq. 3.47 is valid only $s_k \sigma_k$ is much larger than 1. For example, if we assume that it is valid when $s_k \sigma_k$ is greater than 100 and s_k is a very small number like 0.0001, then:

$$\begin{aligned} s_k \sigma_k &= 0.0001 \sqrt{\frac{\omega_k z}{\kappa_k}} \\ &\simeq 0.0001 \sqrt{z} \\ &> 100 \end{aligned} \tag{3.51}$$

Eq. 3.47 is valid only when z is greater than 10^{12}. As stated in Chapter 2, the governing equation for a multilayer crossflow system is solved in Laplace space first and inversely transformed into real domain using the Stehfest algorithm. Such a big argument, $z = 10^{12}$, is generated in the Stehfest algorithm when t_D is as small as 10^{-12}, which is too small a time in most well testing analysis. Actually, at early time when $t_D \simeq 0.001$, $s_k \sigma_k$ is much smaller than 1, and Eq. 3.44 is a more proper approximation than Eq. 3.47 and the system behaves as if the skin factors are zero.

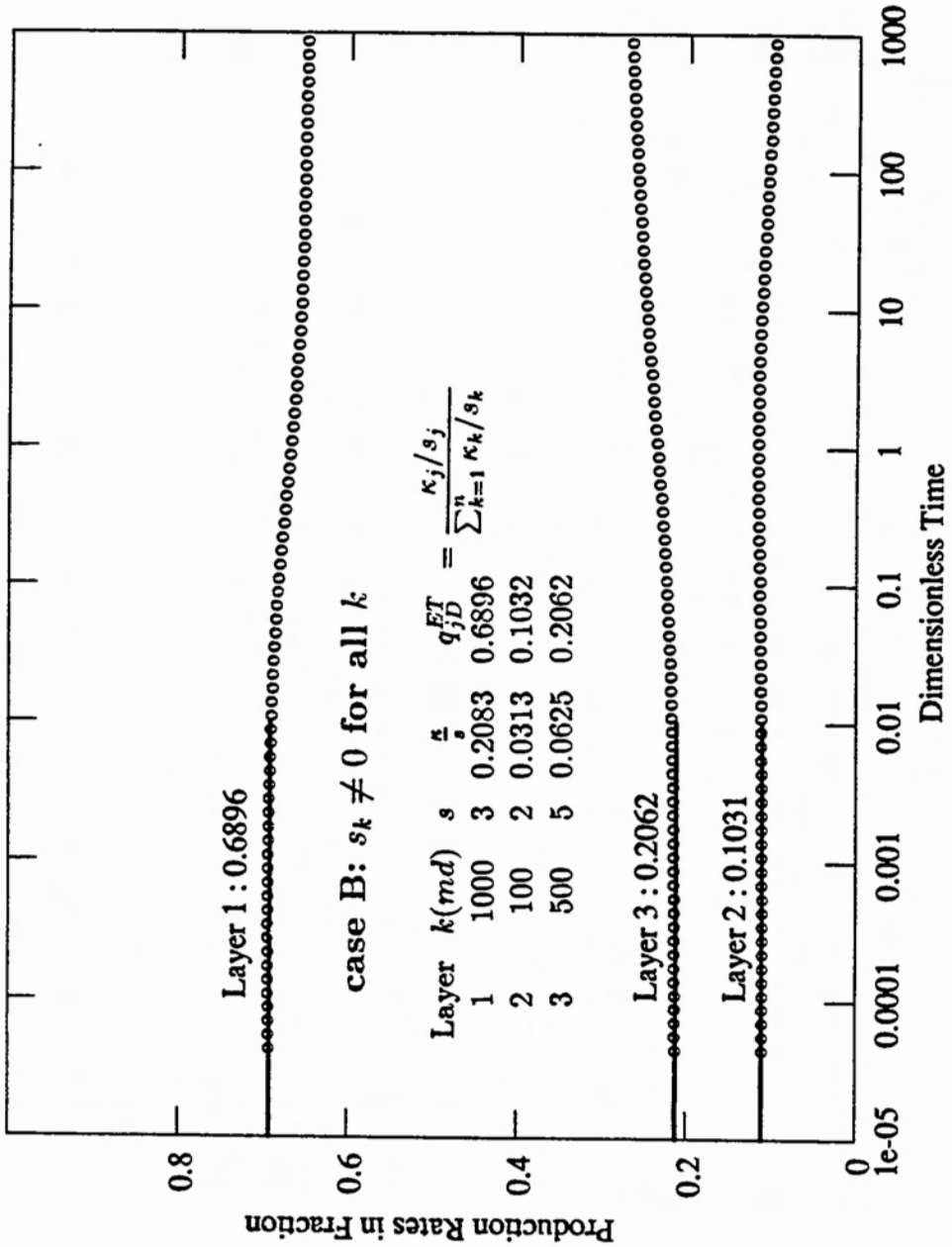

Figure 3.23: Early Time Limiting Layer Production Rates for Case B

3.8.3 Case C: some $s_k = 0$ and others are not

From the previous subsections, we know that:

$$\frac{\kappa_j \sigma_j}{1 + s_j \sigma_j} \simeq \kappa_j \sigma_j \tag{3.52}$$

if the skin factor of the layer is zero, and that:

$$\frac{\kappa_j \sigma_j}{1 + s_j \sigma_j} \simeq \frac{\kappa_j}{s_j} \tag{3.53}$$

if the skin factor of the layer is non-zero.

Thus, the layer production rate in case C should be considered separately based on whether the layer has zero or non-zero skin.

In the first case, when $s_j = 0$, the layer production rate of layer j becomes a constant.

$$\begin{aligned}
\overline{q_{jD}} &= \frac{\frac{\kappa_j \sigma_j}{1+s_j \sigma_j}}{z \sum_{k=1}^{n} \frac{\kappa_k \sigma_k}{1+s_k \sigma_k}} && (3.54)\\
&= \frac{\kappa_j \sigma_j}{z[\sum_{s_k \neq 0} \kappa_k / s_k + \sum_{s_k = 0} \kappa_k \sigma_k]} && (3.55)\\
&= \frac{\kappa_j \sqrt{\frac{\omega_j z}{\kappa_j}}}{z[\sum_{s_k \neq 0} \kappa_k / s_k + \sum_{s_k = 0} \kappa_k \sqrt{\frac{\omega_k z}{\kappa_k}}]} \\
&= \frac{\sqrt{\omega_j \kappa_j}}{\sqrt{z}[\sum_{s_k \neq 0} \kappa_k / s_k + \sum_{s_k = 0} \sqrt{\omega_k \kappa_k z}]} \\
&= \frac{\sqrt{\omega_j \kappa_j} / \sum_{s_k = 0} \sqrt{\omega_k \kappa_k}}{\sqrt{z}(\sqrt{z} + a)}
\end{aligned}$$

where

$$a = \frac{\sum_{s_k \neq 0} \frac{\kappa_k}{s_k}}{\sum_{s_k = 0} \sqrt{\omega_k \kappa_k}} \tag{3.56}$$

From Abramowitz and Stegun (1970),

$$\frac{1}{\sqrt{z}(\sqrt{z} + a)} \rightarrow e^{a^2 t_D} erfc(a\sqrt{t_D}) \tag{3.57}$$

Thus, final expression of the layer production becomes:

$$q_{jD} = \frac{\sqrt{\omega_j \kappa_j}}{\sum_{s_k = 0} \sqrt{\omega_k \kappa_k}} e^{a^2 t_D} erfc(a\sqrt{t_D}) \tag{3.58}$$

At very early time ($t_D \simeq 0$),

$$e^0 = 1 \tag{3.59}$$

$$erfc(0) = 1 \tag{3.60}$$

Thus, the production rate of layer j at very early time becomes a constant, determined as follows:

$$\begin{aligned} \lim_{t_D \to 0} q_{jD} &= \lim_{t_D \to 0} \frac{\sqrt{\omega_j \kappa_j}}{\sum_{s_k=0} \sqrt{\omega_k \kappa_k}} e^{a^2 t_D} erfc(a\sqrt{t_D}) \qquad (3.61) \\ &= \frac{\sqrt{\omega_j \kappa_j}}{\sum_{s_k=0} \sqrt{\omega_k \kappa_k}} \end{aligned}$$

In the second case, when $s_j \neq 0$, the production rate of layer j becomes zero.

$$\begin{aligned} \overline{q_{jD}} &= \frac{\frac{\kappa_j \sigma_j}{1+s_j \sigma_j}}{z \sum_{k=1}^{n} \frac{\kappa_k \sigma_k}{1+s_k \sigma_k}} \qquad (3.62) \\ &= \frac{\kappa_j / s_j}{z[\sum_{s_k \neq 0} \kappa_k / s_k + \sum_{s_k=0} \kappa_k \sigma_k]} \qquad (3.63) \\ &= \frac{\kappa_j / s_j}{z[\sum_{s_k \neq 0} \kappa_k / s_k + \sum_{s_k=0} \sqrt{\omega_k \kappa_k z}]} \\ &= \frac{\frac{\kappa_j}{s_j} / (\sum_{s_k=0} \sqrt{\kappa_k \omega_k})}{z[\sqrt{z} + \frac{\sum_{s_k \neq 0} \kappa_k / s_k}{\sum_{s_k=0} \sqrt{\omega_k \kappa_k}}]} \\ &= \frac{\kappa_j / s_j \sum_{s_k=0} \sqrt{\omega_k \kappa_k}}{(\sum_{s_k \neq 0} \kappa_k / s_k)^2} \frac{(\sum_{s_k \neq 0} \frac{\kappa_k}{s_k} / \sum_{s_k=0} \sqrt{\omega_k \kappa_k})^2}{z[\sqrt{z} + \frac{\sum_{s_k \neq 0} \kappa_k / s_k}{\sum_{s_k=0} \sqrt{\omega_k \kappa_k}}]} \qquad (3.64) \end{aligned}$$

By defining b as follows:

$$b = \frac{\sum_{s_k \neq 0} \frac{\kappa_k}{s_k}}{\sum_{s_k=0} \sqrt{\omega_k \kappa_k}} \tag{3.65}$$

we have a simpler form for $\overline{q_{jD}}$:

$$\overline{q_{jD}} = \frac{\kappa_j / s_j \sum_{s_k=0} \sqrt{\omega_k \kappa_k}}{(\sum_{s_k \neq 0} \kappa_k / s_k)^2} \frac{b^2}{z[\sqrt{z} + b]} \tag{3.66}$$

From Abramowitz and Stegun (1970),

$$\frac{b^2}{z[\sqrt{z} + b]} \to b[1 - e^{b^2 t_D} erfc(b\sqrt{t_D})] \tag{3.67}$$

Thus, the inversely transformed expression for q_{jD} becomes:

$$\begin{aligned} q_{jD} &= \frac{\kappa_j/s_j \sum_{s_k=0} \sqrt{\omega_k \kappa_k}}{(\sum_{s_k \neq 0} \kappa_k/s_k)^2} b[1 - e^{b^2 t_D} erfc(b\sqrt{t_D})] \\ &= \frac{\kappa_j/s_j}{\sum_{s_k \neq 0} \kappa_k/s_k}[1 - e^{b^2 t_D} erfc(b\sqrt{t_D})] \end{aligned} \tag{3.68}$$

At very early time, q_{jD} becomes zero, since

$$e^0 = 1 \tag{3.69}$$

$$erfc(0) = 1 \tag{3.70}$$

An example for case C is shown in Fig. 3.24.

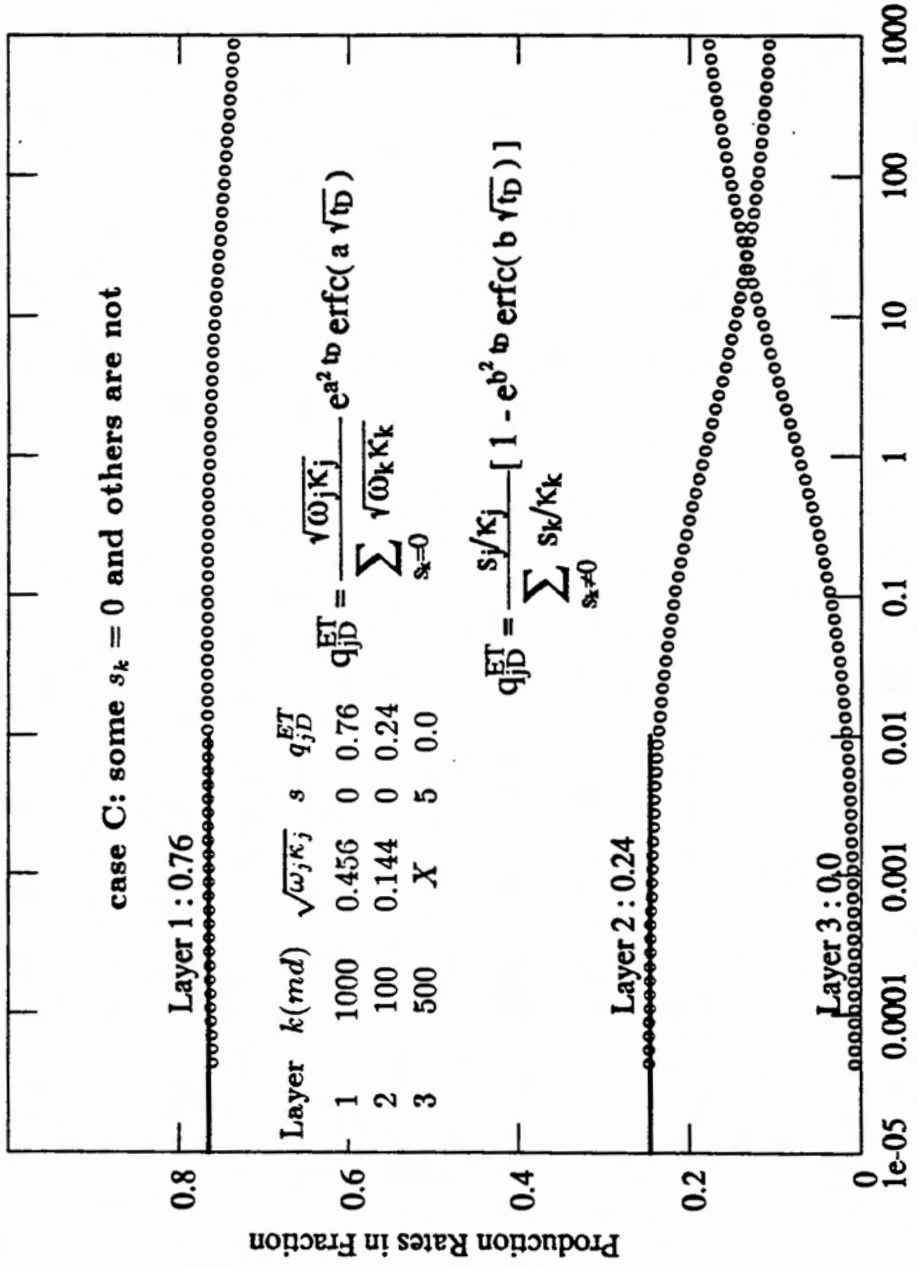

Figure 3.24: Early Time Limiting Layer Production Rates for Case C

3.9 Late Time Behavior

Unlike a commingled system, a crossflow system shows many advantageous characteristics in the late time behavior of wellbore pressure and layer production rate. The first is that layer production rates become constant, the second is that the vertical pressure difference between layers becomes constant and the last is that wellbore pressure can be approximated as a semilog straight line of the equivalent homogeneous system. All these can be proven mathematically in a two layered system. However, they still hold for multilayered systems when there are more than two layers.

3.9.1 Constant Terminal Layer Production Rate

Bourdet (1985) derived the solution for wellbore pressure in double layered reservoir, which is introduced briefly in Appendix C. Following Bourdet:

$$p_{\overline{1D}} = a_1 B_1 K_0(\sigma_1 r_D) + a_2 B_2 K_0(\sigma_2 r_D) \tag{3.71}$$

$$p_{\overline{2D}} = B_1 K_0(\sigma_1 r_D) + B_2 K_0(\sigma_2 r_D) \tag{3.72}$$

where each variable is defined as:

$$a_1 = 1 + (\frac{1}{\lambda})[\omega_2 z - \kappa_2 \sigma_1^2] \tag{3.73}$$

$$a_2 = 1 + (\frac{1}{\lambda})[\omega_2 z - \kappa_2 \sigma_2^2] \tag{3.74}$$

$$\sigma_1^2 = \frac{1}{2}(\frac{\omega_2 z + \lambda}{\kappa_2} + \frac{\omega_1 z + \lambda}{\kappa_1} + \Delta) \tag{3.75}$$

$$\sigma_2^2 = \frac{1}{2}(\frac{\omega_2 z + \lambda}{\kappa_2} + \frac{\omega_1 z + \lambda}{\kappa_1} - \Delta) \tag{3.76}$$

$$\Delta = \sqrt{(\frac{\omega_2 z + \lambda}{\kappa_2} - \frac{\omega_1 z + \lambda}{\kappa_1})^2 + \frac{4\lambda^2}{\kappa_1 \kappa_2}} \tag{3.77}$$

By applying inner boundary conditions, we can get:

$$\sigma_1 K_1(\sigma_1) B_1 = -\frac{1}{cz}[a_2(K_1^0(\sigma_2) + s_1) - (K_1^0(\sigma_2) + s_2)] \tag{3.78}$$

$$\sigma_2 K_1(\sigma_2) B_2 = -\frac{1}{cz}[a_1(K_1^0(\sigma_1) + s_1) - (K_1^0(\sigma_1) + s_2)] \tag{3.79}$$

where

$$K_1^0(\sigma) = \frac{K_0(\sigma)}{\sigma K_1(\sigma)} \tag{3.80}$$

and

$$\begin{aligned} c &= (\kappa_1 a_2 + \kappa_2)[a_1(K_1^0(\sigma_1) + s_1) - (K_1^0(\sigma_1) + s_2)] \\ &= -(\kappa_1 a_1 + \kappa_2)[a_2(K_1^0(\sigma_2) + s_1) - (K_1^0(\sigma_2) + s_2)] \end{aligned} \tag{3.81}$$

Since we are looking for the limiting form at late time, we need to get the limiting values for all the variables for small Laplacian argument z.

$$\lim_{z\to 0}\Delta = \lim_{z\to 0}[\frac{\lambda}{\kappa_2} + \frac{\lambda}{\kappa_1} + (\frac{\omega_2}{\kappa_2} - \frac{\omega_1}{\kappa_1})\frac{\frac{1}{\kappa_2} - \frac{1}{\kappa_1}}{\frac{1}{\kappa_2} + \frac{1}{\kappa_1}}z + O(z^2)] \tag{3.82}$$

$$\begin{aligned} \lim_{z\to 0}\sigma_1^2 &= \lim_{z\to 0}[\frac{\lambda}{\kappa_2} + \frac{\lambda}{\kappa_1} + \frac{\frac{\omega_2}{\kappa_2^2} + \frac{\omega_1}{\kappa_1^2}}{\frac{1}{\kappa_2} + \frac{1}{\kappa_1}}z + O(z^2)] \\ &\to \frac{\lambda}{\kappa_2} + \frac{\lambda}{\kappa 1} \end{aligned} \tag{3.83}$$

$$\begin{aligned} \lim_{z\to 0}\sigma_2^2 &= \lim_{z\to 0}[\frac{\frac{\omega 1+\omega 2}{\kappa 1\kappa 2}}{\frac{1}{\kappa_1} + \frac{1}{\kappa_2}}z + O(z^2)] \\ &\to z \end{aligned} \tag{3.84}$$

$$\begin{aligned} \lim_{z\to 0}a_1 &= \lim_{z\to 0} 1 + (\frac{1}{\lambda})[\omega_2 z - \kappa_2\sigma_1^2] \\ &= \lim_{z\to 0} 1 + (\frac{1}{\lambda})[\omega_2 z - \kappa_2(\frac{\lambda}{\kappa_1} + \frac{\lambda}{\kappa_2})] \\ &\to -\frac{\kappa_2}{\kappa_1} \end{aligned} \tag{3.85}$$

$$\begin{aligned} \lim_{z\to 0}a_2 &= \lim_{z\to 0} 1 + (\frac{1}{\lambda})[\omega_2 z - \kappa_2\sigma_2^2] \\ &= \lim_{z\to 0} 1 + (\frac{1}{\lambda})[\omega_2 z - \kappa_2 z] \\ &\to 1 \end{aligned} \tag{3.86}$$

$$\begin{aligned}\lim_{z\to 0} c &= \lim_{z\to 0}(\kappa_1 a_2+\kappa_2)[a_1(K_1^0(\sigma_1)+s_1)-(K_1^0(\sigma_1)+s_2)] \\ &\quad -(\kappa_1 a_1+\kappa_2)[a_2(K_1^0(\sigma_2)+s_1)-(K_1^0(\sigma_2)+s_2)] \\ &\to -\frac{\kappa_2}{\kappa_1}(K_1^0(\sigma_1)+s_1)-(K_1^0(\sigma_1)+s_2) \qquad (3.87)\end{aligned}$$

Substituting these limiting values into Eq. 3.78 and 3.79 yields:

$$\begin{aligned}[\sigma_1 K_1(\sigma_1)B_1]^{LT} &= -\frac{1}{cz}\left[(K_1^0(\sigma_2)+s_1)-(K_1^0(\sigma_2)+s_2)\right] \\ &= \frac{\kappa_1}{z}\frac{(s_1-s_2)}{K_1^0(\sigma_1)+\kappa_1 s_2+\kappa_2 s_1} \qquad (3.88)\end{aligned}$$

$$\begin{aligned}[\sigma_2 K_1(\sigma_2)B_2]^{LT} &= \frac{1}{cz}\left[(-\frac{\kappa_2}{\kappa_1})(K_1^0(\sigma_1)+s_1)-(K_1^0(\sigma_1)+s_2)\right] \qquad (3.89) \\ &= \frac{1}{z}\end{aligned}$$

Then, the production rate of layer 2 becomes:

$$\begin{aligned}(q_{\overline{2D}})^{LT} &= -\kappa_2\frac{\partial p_{\overline{2D}}}{\partial r_D}|_{r_D=1} \\ &= \kappa_2[B_1\sigma_1 K_1(\sigma_1)+B_2\sigma_2 K_1(\sigma_2)]^{LT} \qquad (3.90) \\ &= \frac{\kappa_2}{z}[1+\frac{\kappa_1(s_1-s_2)}{K_1^0(\sigma_1)+\kappa_1 s_2+\kappa_2 s_1}]\end{aligned}$$

Similarly:

$$(q_{\overline{1D}})^{LT} = \frac{\kappa_1}{z}[1+\frac{\kappa_2(s_2-s_1)}{K_1^0(\sigma_1)+\kappa_1 s_2+\kappa_2 s_1}] \qquad (3.91)$$

Since all the values are constant except z, transformation into real domain yields constant values:

$$(q_{1D})^{LT} = \kappa_1[1+\frac{\kappa_2(s_2-s_1)}{K_1^0(\sigma_1)+\kappa_1 s_2+\kappa_2 s_1}] \qquad (3.92)$$

$$(q_{2D})^{LT} = \kappa_2[1+\frac{\kappa_1(s_1-s_2)}{K_1^0(\sigma_1)+\kappa_1 s_2+\kappa_2 s_1}] \qquad (3.93)$$

These formulae for layer production rate at late time imply several things:

1. The terminal production rate from each layer is constant.

2. If $s_1 = s_2$, then the layer production rate is proportional to the productivity ratio.

3. If $s_1 \neq s_2$, then the layer with smaller skin produces more than κ, suggesting that the formation crossflow occurs from the layer with larger skin to the layer with smaller skin, as explained in Section 3.4.

When there are more than two layers, the expression for the pressure is not available in a closed form, and above derivation is not possible. However, we still can try the approximated forms for the terminal layer production rate, since the expressions are very symmetrical. Taking the similar forms, we can suggest:

$$q_{jD}{}^{LT} = \kappa_j[1 + \sum_{k \neq j} \frac{\kappa_k(s_k - s_j)}{K_1^0(\sigma_{kj}) + \kappa_k s_j + \kappa_j s_k}] \tag{3.94}$$

where

$$K_1^0(\sigma_{kj}) = \frac{K_0(\sigma_{kj})}{\sigma_{kj} K_1(\sigma_{kj})} \tag{3.95}$$

$$\sigma_{kj} = \sqrt{\frac{\lambda_{kj}}{\kappa_k} + \frac{\lambda_{kj}}{\kappa_j}} \tag{3.96}$$

$$\lambda_{kj} = \frac{2r_w^2}{(kh)_t \sum_{i=k}^{j-1} (\frac{h_i}{k_{v_i}} + \frac{h_{i\pm1}}{k_{v_{i\pm1}}})} \tag{3.97}$$

The sign $\pm$ is determined by the order of k and j. If k is smaller than j, then the sign is positive.

For example, $q_{1D}{}^{LT}$ in a three layered system can be expressed as:

$$q_{1D}{}^{LT} = \kappa_1[1 + \frac{\kappa_2(s_2 - s_1)}{K_1^0(\sigma_{12}) + \kappa_1 s_2 + \kappa_2 s_1} + \frac{\kappa_3(s_3 - s_1)}{K_1^0(\sigma_{13}) + \kappa_1 s_3 + \kappa_3 s_1}] \tag{3.98}$$

where

$$\sigma_{12} = \sqrt{\frac{\lambda_{12}}{\kappa_1} + \frac{\lambda_{12}}{\kappa_2}} \tag{3.99}$$

$$\sigma_{13} = \sqrt{\frac{\lambda_{13}}{\kappa_1} + \frac{\lambda_{13}}{\kappa_3}} \tag{3.100}$$

$$\lambda_{12} = \frac{2r_w^2}{(kh)_t(\frac{h_1}{k_{v_1}} + \frac{h_2}{k_{v_2}})} \tag{3.101}$$

$$\lambda_{13} = \frac{2r_w^2}{(kh)_t(\frac{h_1}{k_{v_1}} + 2\frac{h_2}{k_{v_2}} + \frac{h_3}{k_{v_3}})} \tag{3.102}$$

Fig. 3.25 and Fig. 3.26 compares the real production rate history and the terminal production rate for a two layered and a three layered system each. Fig. 3.25 is for a two layered case and the terminal production rate was calculated from Eq. 3.92 and Eq. 3.93. Both show an exact match naturally. However, Eq. 3.94 was applied in approximating the terminal production rates for a three layered case as in Fig. 3.26, It also showed a very nice match. These approximations become less credible when the reservoir is composed of many layers, as might be guessed.

3.9.2 Constant Vertical Pressure Gradient

The layer pressure at an arbitrary point ($r = r_D$) is given by Eq. 3.71 and Eq. 3.72:

$$\overline{p_{1D}} = a_1 B_1 K_0(\sigma_1 r_D) + a_2 B_2 K_0(\sigma_2 r_D) \tag{3.103}$$

$$\overline{p_{2D}} = B_1 K_0(\sigma_1 r_D) + B_2 K_0(\sigma_2 r_D) \tag{3.104}$$

Define the pressure difference between the layers as $\Delta\overline{p_D}$:

$$\begin{aligned} \Delta\overline{p_D} &= \overline{p_{1D}} - \overline{p_{2D}} \\ &= (a_1 - 1) B_1 K_0(\sigma_1 r_D) + (a_2 - 1) B_2 K_0(\sigma_2 r_D) \end{aligned} \tag{3.105}$$

At late time, from Eq. 3.85 and Eq. 3.86:

$$a_1 = -\frac{\kappa 2}{\kappa 1} \tag{3.106}$$

$$a_2 = 1 \tag{3.107}$$

Thus the second term in the right hand side drops out and $\Delta\overline{p_D}^{LT}$ becomes:

$$\begin{aligned} \Delta\overline{p_D}^{LT} &= (-\frac{\kappa_2}{\kappa_1} - 1) B_1 K_0(\sigma_1 r_D) \\ &= -\frac{1}{\kappa_1} B_1 K_0(\sigma_1 r_D) \end{aligned} \tag{3.108}$$

B_1 can be obtained from Eq. 3.88:

$$[\sigma_1 B_1 K_1(\sigma_1)]^{LT} = \frac{\kappa_1}{z} \frac{s_1 - s_2}{K_1^0(\sigma_1) + \kappa_1 s_2 + \kappa_2 s_1} \tag{3.109}$$

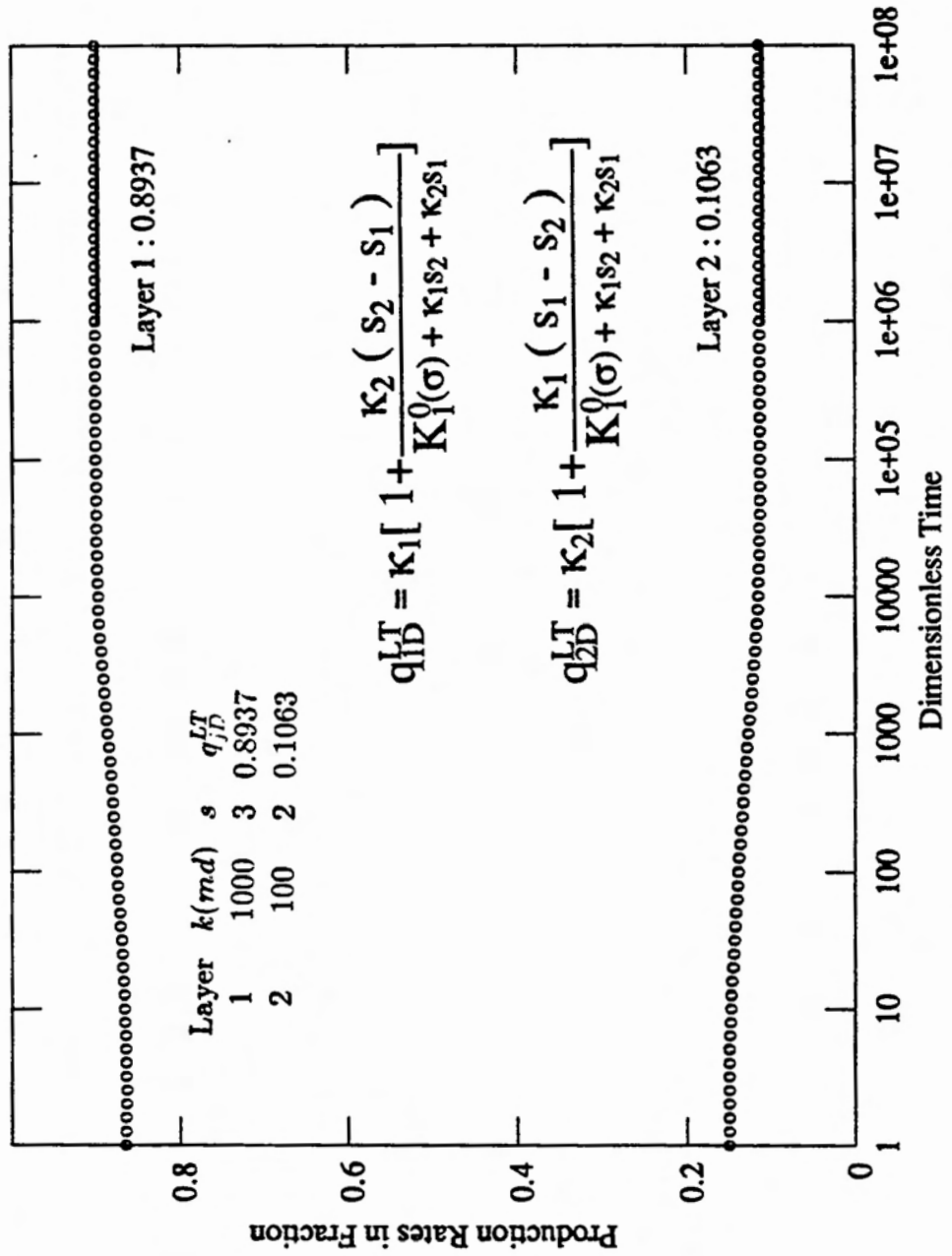

Figure 3.25: Layer Production Rates at Late Time for a Two Layered Reservoir : Exact Solution

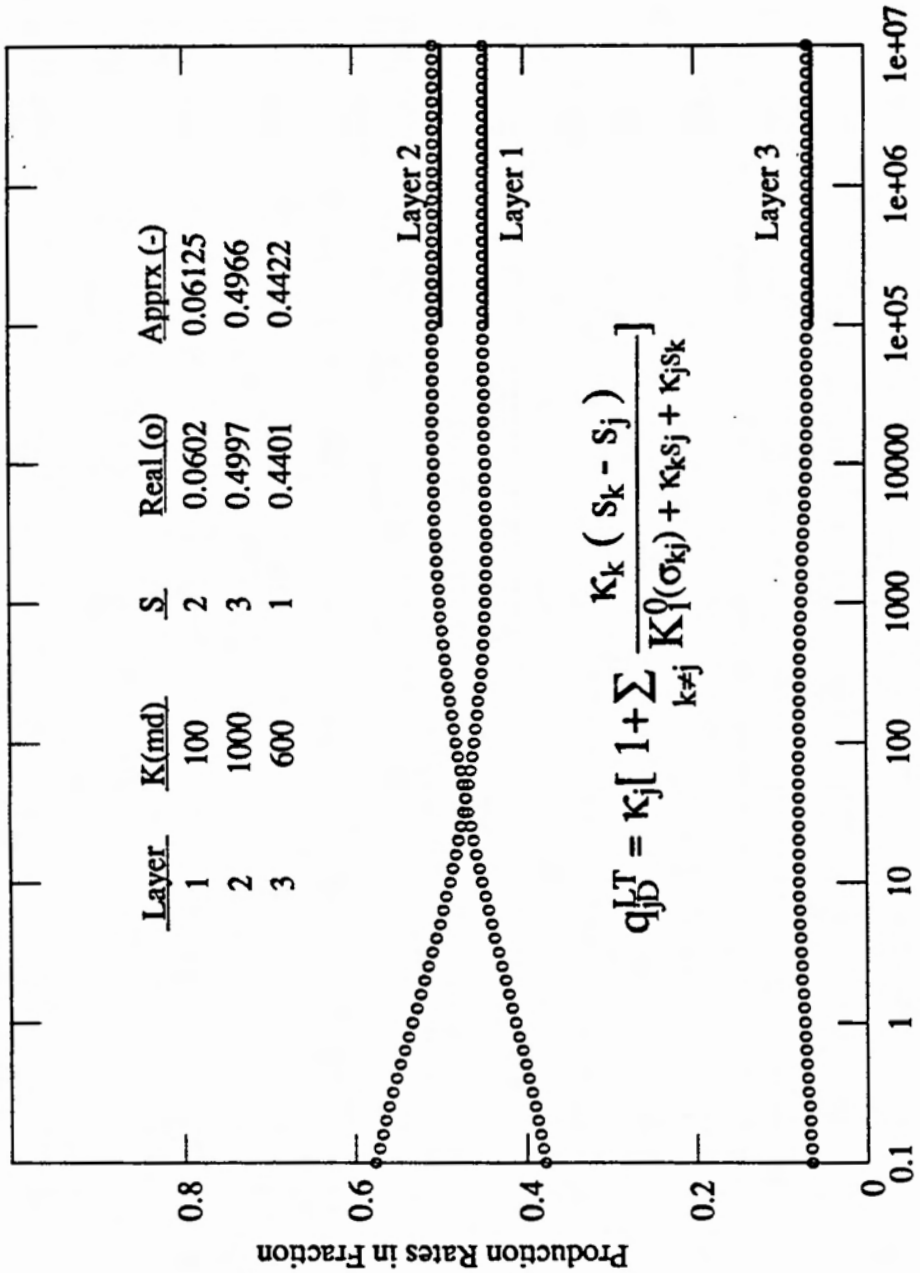

Figure 3.26: Layer Production Rates at Late Time for a Three Layered Reservoir: Approximate Solution

Thus, $\Delta\overline{p_D}^{LT}$ becomes:

$$\begin{aligned}\Delta\overline{p_D}^{LT} &= -\frac{1}{\kappa_1}B_1K_0(\sigma_1 r_D) \\ &= \frac{1}{z}\frac{s_2-s_1}{K_1^0(\sigma_1)+\kappa_1 s_2+\kappa_2 s_1}\frac{K_0(\sigma_1 r_D)}{\sigma_1 K_1(\sigma_1)}\end{aligned} \tag{3.110}$$

Transformation of the above equation into the real domain yields:

$$\Delta p_D{}^{LT} = \frac{s_2-s_1}{K_1^0(\sigma_1)+\kappa_1 s_2+\kappa_2 s_1}\frac{K_0(\sigma_1 r_D)}{\sigma_1 K_1(\sigma_1)} \tag{3.111}$$

This implies two things:

1. At a specified distance from the wellbore ($r = r_D$), all the variables become constant at late time. Thus the pressure difference or the vertical pressure gradient becomes constant, and

2. The direction of the formation crossflow at late time is entirely determined by the magnitude of the skin factors.

For example, in the case when s_1 is bigger than s_2, Δp_D becomes negative. However, from the definition of the dimensionless pressure:

$$\begin{aligned}\Delta p_D &= p_{1D} - p_{2D} \\ &= \frac{2\pi(kh)_t(p_i-p_1)}{q_t\mu} - \frac{2\pi(kh)_t(p_i-p_2)}{q_t\mu} \\ &= \frac{2\pi(kh)_t(p_2-p_1)}{q_t\mu} < 0\end{aligned} \tag{3.112}$$

Thus, the real pressure in layer 1 is bigger than the pressure in layer 2. Thus the direction of formation crossflow is from layer 1 to layer 2. In other words, the formation crossflow is from the layer with bigger skin to the layer with smaller skin.

Examples can be seen in Fig. 3.10 in Section 3.3, which shows that skin factors alone determine the direction of formation crossflow at late time. However, this might not be accurate because the crossflow effect is not treated two-dimensionally, as stated in Chapter 2.

In Fig. 3.27, an example was given where each layer was divided into three sublayers to study the effect of two-dimensional crossflow, for a two layered reservoir with

parameters listed in Table 3.7. In the beginning, the pressure in layer 2 (sublayers 4, 5 and 6) is higher than that in layer 1 (sublayers 1, 2 and 3), since layer 1 has bigger permeability than layer 2, as mentioned in Section 3.3. At late time ($t > 1$ hr), however, the pressure in layer 1 is greater than that in layer 2, since layer 1 has bigger skin than layer 2. Notice that the pressure difference between two layers are constant throughout late time stage, which justifies the one-dimensional approximation of the crossflow using the semi-permeable wall model.

Table 3.7: Reservoir Parameters for the Example Showing the Constant Pressure Difference in Vertical Direction at Late Time with Two-Dimensional Crossflow

Layer	Sublayer	k(md)	k_v(md)	s
	1	500	50	3
1	2	500	50	3
	3	500	50	3
	4	100	50	0
2	5	100	50	0
	6	100	50	0

3.9.3 Wellbore Pressure as a Semilog Straight Line

Wellbore pressure in a multilayered reservoir is defined as:

$$\overline{p_{wD}} = \overline{p_{jD}} - s_j \frac{\partial \overline{p_{jD}}}{\partial r_D}|_{r_D=1} \qquad (j = 1, \ldots, n) \tag{3.113}$$

or for the second layer:

$$\begin{aligned} \overline{p_{wD}} &= \overline{p_{2D}} - s_2 \frac{\partial \overline{p_{2D}}}{\partial r_D}|_{r_D=1} \\ &= B_1 K_0(\sigma_1) + B_2 K_0(\sigma_2) + s_2[\sigma_1 B_1 K_1(\sigma_1) + \sigma_2 B_2 K_1(\sigma_2)] \end{aligned} \tag{3.114}$$

However:

$$\begin{aligned} \overline{q_{2D}} &= -\kappa_2 \frac{\partial \overline{p_{2D}}}{\partial r_D}|_{r_D=1} \\ &= \kappa_2[\sigma_1 B_1 K_1(\sigma_1) + \sigma_2 B_2 K_1(\sigma_2)] \end{aligned} \tag{3.115}$$

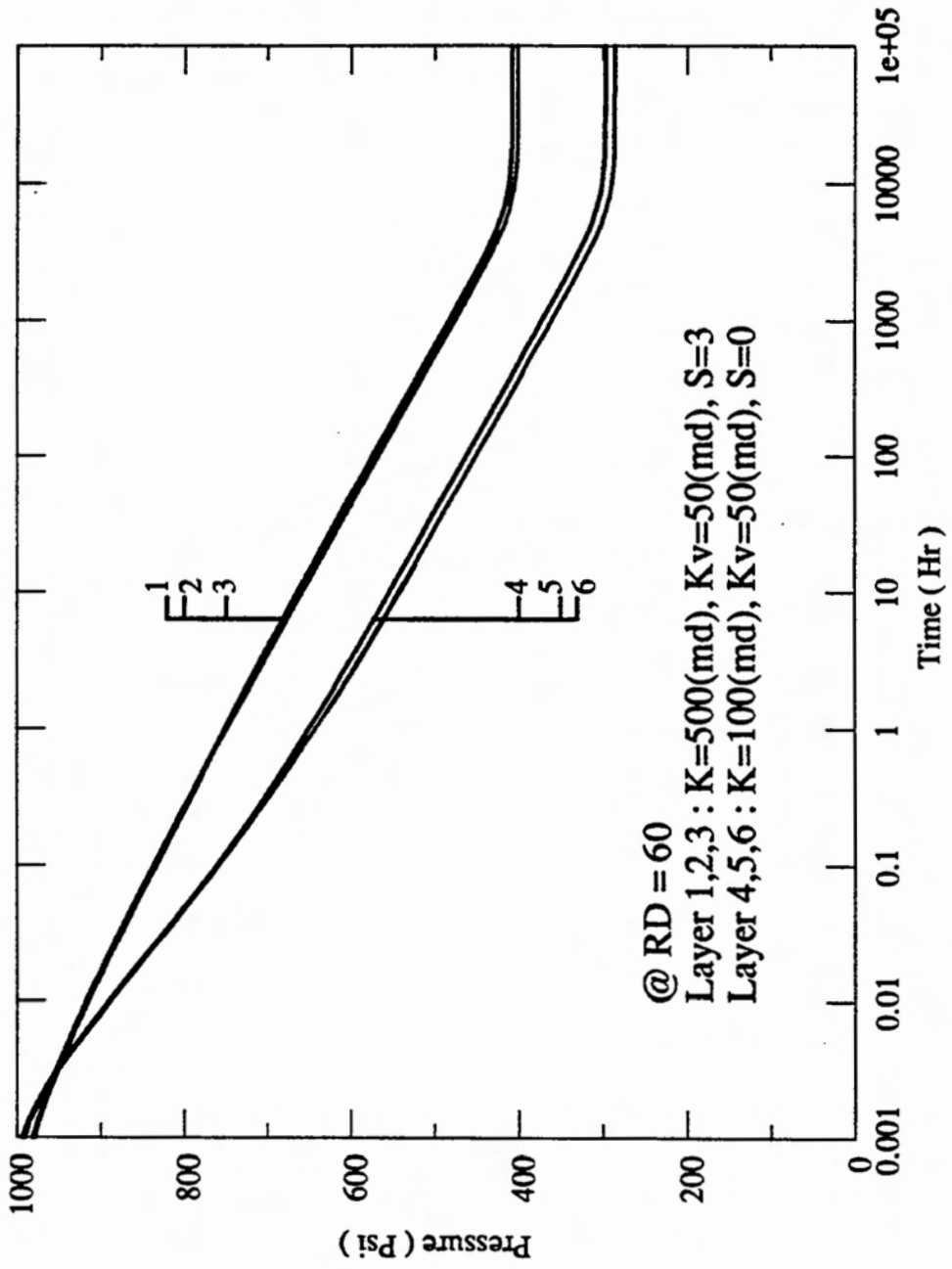

Figure 3.27: Layer Production Rate at Late Time for a Two Layered Reservoir with 2D Approximation of Crossflow

Thus, $\overline{p_{wD}}$ becomes:

$$\overline{p_{wD}} = B_1 K_0(\sigma_1) + B_2 K_0(\sigma_2) + \frac{s_2}{\kappa_2}\overline{q_{2D}} \tag{3.116}$$

At late time, z becomes very small. From 3.84 and Eq. 3.89:

$$[\sigma_2 B_2 K_1(\sigma_2)]^{LT} = \frac{1}{z} \tag{3.117}$$

$$[\sigma_2]^{LT} = \sqrt{z} \tag{3.118}$$

From Abramowitz and Stegun (1970):

$$\lim_{x\to 0} K_0(x) = -\ln\frac{x}{2} - \gamma \tag{3.119}$$

$$\lim_{x\to 0} K_1(x) = \frac{1}{x} \tag{3.120}$$

Thus the second term of the right hand side of Eq. 3.116 becomes:

$$\begin{aligned}[B_2 K_0(\sigma_2)]^{LT} &= \frac{1}{z}\frac{K_0(\sigma_2)}{\sigma_2 K_1(\sigma_2)} \\ &= \frac{1}{z}\frac{-\ln(\sigma_2/2) - \gamma}{\sigma_2 \frac{1}{\sigma_2}} \\ &= -\frac{1}{z}[\frac{1}{2}\ln\frac{z}{4} + \gamma]\end{aligned} \tag{3.121}$$

Similarly, for the first term:

$$[\sigma_1 B_1 K_1(\sigma_1)]^{LT} = \frac{\kappa_1}{z}\frac{s_1 - s_2}{K_1^0(\sigma_1) + \kappa_1 s_2 + \kappa_2 s_1} \tag{3.122}$$

$$\begin{aligned}[B_1 K_0(\sigma_1)]^{LT} &= \frac{K_0(\sigma_1)}{\sigma_1 K_1(\sigma_1)}\frac{\kappa_1}{z}\frac{s_1 - s_2}{K_1^0(\sigma_1) + \kappa_1 s_2 + \kappa_2 s_1} \\ &= K_1^0(\sigma_1)\frac{\frac{\kappa_1}{z}(s_1 - s_2)}{K_1^0(\sigma_1) + \kappa_1 s_2 + \kappa_2 s_1}\end{aligned} \tag{3.123}$$

From Eq. 3.91:

$$\overline{q_{1D}}^{LT} = \frac{\kappa_1}{z}[1 + \frac{\kappa_2(s_2 - s_1)}{K_1^0(\sigma_1) + \kappa_1 s_2 + \kappa_2 s_1}] \tag{3.124}$$

By rearranging the above equation:

$$K_1^0(\sigma_1) + \kappa_1 s_2 + \kappa_2 s_1 = \frac{\kappa_2(s_2 - s_1)}{\frac{z\overline{q_{1D}}^{LT}}{\kappa_1} - 1} \tag{3.125}$$

Solving for $K_1^0(\sigma_1)$ yields:

$$\begin{aligned} K_1^0(\sigma_1) &= \frac{\kappa_1\kappa_2(s_2-s_1)}{z\overline{q_{1D}}^{LT}-\kappa_1} - \kappa_1 s_2 - \kappa_2 s_1 \\ &= \frac{\kappa_1\kappa_2(s_2-s_1) - \kappa_1 s_2(z\overline{q_{1D}}^{LT}-\kappa_1) - \kappa_2 s_1(z\overline{q_{1D}}^{LT}-\kappa_1)}{z\overline{q_{1D}}^{LT}-\kappa_1} \end{aligned} \tag{3.126}$$

Since:

$$\frac{1}{z} = \overline{q_{1D}}^{LT} + \overline{q_{2D}}^{LT} \tag{3.127}$$

$$\begin{aligned} 1 &= z\overline{q_{1D}}^{LT} + z\overline{q_{2D}}^{LT} \\ &= \kappa_1 + \kappa_2 \end{aligned} \tag{3.128}$$

$$z\overline{q_{1D}}^{LT} - \kappa_1 = \kappa_2 - z\overline{q_{2D}}^{LT} \tag{3.129}$$

$K_1^0(\sigma_1)$ can be expressed as:

$$\begin{aligned} K_1^0(\sigma_1) &= \frac{\kappa_1\kappa_2(s_2-s_1) - \kappa_1 s_2(\kappa_2 - z\overline{q_{2D}}^{LT}) - \kappa_2 s_1(z\overline{q_{1D}}^{LT}-\kappa_1)}{z\overline{q_{1D}}^{LT}-\kappa_1} \\ &= \frac{z(\kappa_1 s_2\overline{q_{2D}}^{LT} - \kappa_2 s_1\overline{q_{1D}}^{LT})}{z\overline{q_{1D}}^{LT}-\kappa_1} \end{aligned} \tag{3.130}$$

Also from Eq. 3.90:

$$\overline{q_{2D}}^{LT} = \frac{\kappa_2}{z}[1 + \frac{\kappa_1(s_1-s_2)}{K_1^0(\sigma_1)+\kappa_1 s_2 + \kappa_2 s_1}] \tag{3.131}$$

By rearranging the above equation:

$$\begin{aligned} [\frac{\kappa_1(s_2-s_1)}{K_1^0(\sigma_1)+\kappa_1 s_2+\kappa_2 s_1}] &= \frac{\overline{q_{2D}}^{LT} - \frac{\kappa_2}{z}}{\kappa_2/z} \\ &= \frac{1}{\kappa_2}(z\overline{q_{2D}}^{LT} - \kappa_2) \\ &= \frac{-z\overline{q_{1D}}^{LT} + \kappa_1}{\kappa_2} \\ &= -\frac{1}{\kappa_2}(z\overline{q_{1D}}^{LT} - \kappa_1) \end{aligned} \tag{3.132}$$

Substitution of Eq. 3.126 and Eq. 3.132 into Eq. 3.123 yields:

$$\begin{aligned} B_1 K_0(\sigma_1) &= K_1^0(\sigma_1)\frac{\frac{\kappa_1}{z}(s_1-s_2)}{K_1^0(\sigma_1)+\kappa_1 s_2+\kappa_2 s_1} \\ &= \frac{z(\kappa_1 s_2\overline{q_{2D}}^{LT} - \kappa_2 s_1\overline{q_{1D}}^{LT})}{z\overline{q_{1D}}^{LT}-\kappa_1}\frac{-1}{z\kappa_2}(z\overline{q_{1D}}^{LT}-\kappa_1) \\ &= -\frac{\kappa_1}{\kappa_2}s_2\overline{q_{2D}}^{LT} + s_1\overline{q_{1D}}^{LT} \end{aligned} \tag{3.133}$$

Substitution of Eq. 3.121 and Eq. 3.133 into Eq. 3.116 yields:

$$\begin{aligned}
\overline{p_{wD}}^{LT} &= B_1K_0(\sigma_1) + B_2K_0(\sigma_2) + \frac{s_2}{\kappa_2}\overline{q_{2D}}^{LT} \qquad (3.134)\\
&= -\frac{\kappa_1}{\kappa_2}s_2\overline{q_{2D}}^{LT} + s_1\overline{q_{1D}}^{LT} + B_2K_0(\sigma_2) + \frac{s_2}{\kappa_2}\overline{q_{2D}}^{LT}\\
&= B_2K_0(\sigma_2) + s_1\overline{q_{1D}}^{LT} + s_2\overline{q_{2D}}^{LT}\\
&= -\frac{1}{z}[\frac{1}{2}\ln\frac{z}{4} + \gamma] + s_1\overline{q_{1D}}^{LT} + s_2\overline{q_{2D}}^{LT}\\
&= -\frac{1}{2}\frac{\ln z}{z} + \frac{\ln 2 - \gamma}{z} + s_1\overline{q_{1D}}^{LT} + s_2\overline{q_{2D}}^{LT}
\end{aligned}$$

From Abramowitz and Stegun (1970):

$$\frac{\ln z}{z} \rightarrow -\ln t_D - \gamma \qquad (\gamma = 0.5772) \qquad (3.135)$$

The inversely transformed equation for wellbore pressure becomes:

$$\begin{aligned}
{p_{wD}}^{LT} &= -\frac{1}{2}(-\ln t_D - \gamma) + \ln 2 - \gamma + s_1{q_{1D}}^{LT} + s_2{q_{2D}}^{LT} \qquad (3.136)\\
&= \frac{1}{2}\ln t_D + 0.404535 + s_1{q_{1D}}^{LT} + s_2{q_{2D}}^{LT}\\
&= \frac{1}{2}\ln t_D + 0.404535 + \overline{s}
\end{aligned}$$

Thus, the late time behavior of wellbore pressure is exactly same as the semilog straight line of the equivalent homogeneous line.

Chapter 4

Determination of the Reservoir Parameters

Conventional well test analysis is performed by matching the measured data, commonly the wellbore pressure, graphically with the mathematically or numerically computed data either on a semilog or on a log-log scale. The pressure response of some reservoir models at late time can be approximated as a straight line on a semilog plot, from which we can directly calculate several reservoir parameters. When the test is too short for a semilog straight line to develop or when the reservoir model does not produce a semilog straight line inherently, log-log type curve matching technique is applied to analyze the measured data.

If type curve matching is to be done manually, a lot of uncertainty and subjectivity may be involved, because many of the type curves generated with different reservoir parameters may look very similar in some cases. This gets more difficult if we consider the deviation of the well test data from the type curve due to the small measurement error. Besides, it is almost impossible in the sense of simplicity and efficiency to represent all the type curves graphically when there are too many unknown reservoir parameters, because the curves are to be shown only two-dimensionally. For example, even in the simplest case of the multilayered system when all the other parameters are known except the permeability of the individual layers, there are too many possible cases to allocate the total productivity to each layer. In this case, many trials and

errors are required to get an acceptable match, hence considerable analysis time and human efforts will be wasted.

Automated type curve matching with the aid of computers has been widely used since its introduction and claimed by many authors to be powerful and have many advantages compared to the conventional analysis. Some of the advantages are:

1. Calculation is fast and numerically free of error. The analysts can have as high resolution as they want. It also saves the analysts a lot of time and labor doing calculations needed in building a Horner plot or Miller-Dyes-Hutchinson plot.

2. Because the method uses the entire well test data, even the data from the test of short duration that does not produce a proper semilog straight line can be analyzed. Similarly, it also eliminates the danger of the subjectivity in the choice of a correct semilog straight line.

3. The method does not necessarily require maintaining the restrictive test conditions such as a constant rate production or constant wellbore pressure. It can also handle complex reservoir models for which analytical solution is hard to obtain.

4.1 Nonlinear Parameter Estimation

The idea of most parameter estimation methods is to find values of unknown parameters so that the objective function for those values be minimized or maximized. The objective function should be defined as a proper measure of the discrepancy of two data sets; one is observed or measured data and the other is calculated data either analytically or numerically from the reservoir model. Example of the objective function to be minimized is the sum of square of the residuals and to be maximized is the likely hood function (Bard, 1974). In this study, one of the most widely accepted objective function, the sum of squares of residuals (SSR), will be minimized.

For example, in case of matching both wellbore pressure and production rate from each layer, the SSR can be defined as:

$$SSR(\vec{\theta}) = \sum_{i=1}^{N_d} a_i[\Delta p_{wf}^m(t_i) - \Delta p_{wf}^c(\vec{\theta}, t_i)]^2 + \sum_{i=1}^{N_d}\sum_{l=1}^{N_l} b_{il}[q_l^m(t_i) - q_l^c(\vec{\theta}, t_i)]^2 \qquad (4.1)$$

where:

$\vec{\theta}$	a set of unknown parameters
$\Delta p_{wf}(t_i)$	pressure drop at the wellbore at time t_i
$q_l(t_i)$	production rate from layer l at time t_i
N_d	number of data
N_l	number of layers
m	measured data
c	calculated data
a_i, b_{il}	proper weighting constant

If the unknown parameters ($\vec{\theta}$) are close enough to the real value, the objective function (SSR) will be negligibly small and there will be no big change in $\vec{\theta}$ for the next iteration (convergence).

The minimization process is done in a systematic and iterative way. Initially we should guess values of $\vec{\theta_0}$ and apply the regression technique to determine $\vec{\theta_1}$, for which we hope the objective function gets smaller ($SSR(\vec{\theta_0}) > SSR(\vec{\theta_1})$). We substitute $\vec{\theta_1}$ for $\vec{\theta_0}$ and continue this process again until $SSR(\vec{\theta})$ becomes negligibly small after several iterations.

Many ideas on regression technique have been developed since Legendre suggested the use of the least squares criterion for estimating parameters in linear curve fitting (Bard, 1974), such as Steepest Descent method, Gauss-Newton method, Marquardt method and Gauss-Marquardt modification. However none of them has been proved to be best in all nonlinear parameter estimation problems. Each method must be compared in particular cases (Rosa and Horne, 1983). In this study, the Gauss-Newton method is selected as the regression method for three reasons:

1. It is not the purpose of this study to find the best regression method,

2. Gauss-Newton method is easy to apply and it always worked satisfactorily for the problems in this study, and

3. Hessian matrix is always positive definite, which guarantees the presence of the minimum point of the objective function.

Gauss-Newton Regression

Suppose the objective function is defined as in Eq. 4.1 and call it $S(\vec{\theta})$. By applying the second order Taylor expansion, $S(\vec{\theta})$ can be approximated as:

$$\begin{aligned} S(\vec{\theta_1}) &= S(\vec{\theta_0}) + \sum_{j=1}^{Np} (\delta\theta_j) \frac{\partial S(\vec{\theta_0})}{\partial \theta_j} \\ &\quad + \frac{1}{2} \sum_{j=1}^{Np} \sum_{k=1}^{Np} (\delta\theta_j)(\delta\theta_k) \frac{\partial^2 S(\vec{\theta_0})}{\partial \theta_j \partial \theta_k} \end{aligned} \tag{4.2}$$

where

N_p	number of unknown parameters
$\vec{\theta_0}$	a set of initial estimates of N_p parameters
$\vec{\theta_1}$	a set of parameter values after the first iteration
$\delta\theta_j$	$\theta_{1,j} - \theta_{0,j}$
$\theta_{0,j}$	the value of j_{th} parameter of the initial estimates
$\theta_{1,j}$	the value of j_{th} parameter after the first iteration

Define G and H such that:

$$G_j = \frac{\partial S(\vec{\theta_0})}{\partial \theta_j} \tag{4.3}$$

$$H_{jk} = \frac{\partial^2 S(\vec{\theta_0})}{\partial \theta_j \partial \theta_k} \tag{4.4}$$

Then from Eq. 4.1:

$$\begin{aligned} G_j &= -2\sum_{i=1}^{Nd} a_i[\Delta p_{wf}^m(t_i) - \Delta p_{wf}^c(\vec{\theta_0}, t_i)]\frac{\partial \Delta p_{wf}^c(\vec{\theta_0}, t_i)}{\partial \theta_j} \\ &\quad -2\sum_{i=1}^{Nd}\sum_{l=1}^{Nl} b_{i,j}[q_l^m(t_i) - q_l^c(\vec{\theta_0}, t_i)]\frac{\partial q_l^c(\vec{\theta_0}, t_i)}{\partial \theta_j} \end{aligned} \tag{4.5}$$

$$\begin{aligned} H_{jk} &= 2\sum_{i=1}^{Nd} a_i \left(\frac{\partial \Delta p_{wf}^c(\vec{\theta_0}, t_i)}{\partial \theta_j} \frac{\partial \Delta p_{wf}^c(\vec{\theta_0}, t_i)}{\partial \theta_k} \right) \\ &\quad -2\sum_{i=1}^{Nd} a_i \left((\Delta p_{wf}^m(t_i) - \Delta p_{wf}^c(\vec{\theta_0}, t_i)) \frac{\partial^2 \Delta p_{wf}^c(\vec{\theta_0}, t_i)}{\partial \theta_j \partial \theta_k} \right) \\ &\quad + 2\sum_{i=1}^{Nd}\sum_{l=1}^{Nl} b_{ij} \left(\frac{\partial q_l^c(\vec{\theta_0}, t_i)}{\partial \theta_j} \frac{\partial q_l^c(\vec{\theta_0}, t_i)}{\partial \theta_k} - [q_l^m(t_i) - q_l^c(\vec{\theta_0}, t_i)] \frac{\partial^2 q_l^c(\vec{\theta_0}, t_i)}{\partial \theta_j \partial \theta_k} \right) \end{aligned} \tag{4.6}$$

Then $S(\vec{\theta_1})$ can be written as:

$$S(\vec{\theta_1}) = S(\vec{\theta_0}) + \sum_{j=1}^{Np} \delta\theta_j G_j + \frac{1}{2}\sum_{j=1}^{Np}\sum_{k=1}^{Np} \delta\theta_j \delta\theta_k H_{jk} \tag{4.7}$$

or in a matrix form:

$$S(\vec{\theta_1}) = S(\vec{\theta_0}) + \vec{\delta\theta}^T \underline{\underline{G}} + \frac{1}{2}\vec{\delta\theta}^T \underline{\underline{H}} \vec{\delta\theta} \tag{4.8}$$

For $S(\vec{\theta_1})$ to have a minimum point, $\underline{\underline{H}}$ (Hessian matrix) must be positive definite. Since in Gauss-Newton method, all the second derivatives are neglected, the elements in Hessian matrix reduce to:

$$\begin{aligned} H_{jk} &= 2\sum_{i=1}^{Nd} a_i \left(\frac{\partial \Delta p_{wf}^c(\vec{\theta_0}, t_i)}{\partial \delta\theta_j} \frac{\partial \Delta p_{wf}^c(\vec{\theta_0}, t_i)}{\partial \delta\theta_k} \right) \\ &\quad +2\sum_{i=1}^{Nd}\sum_{l=1}^{Nd} b_{ij} \left(\frac{\partial q_l^c(\vec{\theta_0}, t_i)}{\partial \delta\theta_j} \frac{\partial q_l^c(\vec{\theta_0}, t_i)}{\partial \delta\theta_k} \right) \end{aligned} \tag{4.9}$$

The symmetry and the positive diagonal elements guarantees the Hessian matrix to be positive definite. At the minimum point:

$$\begin{aligned} \frac{\partial S}{\partial(\delta\vec{\theta})} &= \underline{\underline{G}} + \underline{\underline{H}}\delta\vec{\theta} \\ &= 0 \end{aligned} \tag{4.10}$$

Thus, we can solve for $\delta\vec{\theta}$ that minimizes SSR.

$$\begin{aligned} \delta\vec{\theta} &= \vec{\theta_1} - \vec{\theta_0} \\ &= -\underline{\underline{H}}^{-1}\underline{\underline{G}} \end{aligned} \tag{4.11}$$

After the first iteration, the set of parameters, $\vec{\theta_1}$, becomes:

$$\vec{\theta_1} = \vec{\theta_0} + \delta\vec{\theta} \tag{4.12}$$

Above was the process for the first iteration. Since we approximated the objective function using Taylor series, $\vec{\theta_1}$ is not the real answer and we need to iterate the process several times. With substitution of $\vec{\theta_1}$ in place of $\vec{\theta_0}$, iterate the whole process and continue until SSR becomes negligible.

4.2 Initial Estimation

Initial values are extremely important in parameter estimation. Depending on how good the initial estimation is, the optimization process may converge to the real answer, or to the wrong answer (local minimum) or may not converge at all. Even the speed of the convergence is affected by the initial guess.

4.2.1 Old Methods

For multilayered systems, several methods for the initial estimation have been suggested by earlier authors. Kucuk, *et al.* (1985) suggested the sandface flow rate convolution method, which is in essence a multirate test applied to a multilayered reservoir without formation crossflow (commingled system). They assumed the coupling of wellbore pressure and production rate would yield a semilog straight line by noticing that the wellbore pressure is a function of the reservoir parameters while the layer production rate is a function of the layer parameters only.

From the Appendix B, the wellbore pressure and the layer production rate for the commingled system is:

$$\overline{p_{wD}} = \frac{1}{z[C_D z + \sum_{j=1}^{n} \frac{\kappa_j \sigma_j K_1(\sigma_j)}{K_0(\sigma_j)+s_j\sigma_j K_1(\sigma_j)}]} \tag{4.13}$$

$$\overline{q_{jD}} = \frac{\kappa_j \sigma_j K_1(\sigma_j)\overline{p_{wD}}}{K_0(\sigma_j) + s_j \sigma_j K_1(\sigma_j)} \tag{4.14}$$

where:

$$\sigma_j = \sqrt{\frac{\omega_j z}{\kappa_j}} \tag{4.15}$$

Coupling of $\overline{p_{wD}}$ and $\overline{q_{jD}}$ yields:

$$\begin{aligned} \frac{\overline{p_{wD}}}{z\overline{q_{jD}}} &= \frac{K_0(\sigma_j) + s_j\sigma_j K_1(\sigma_j)}{z\kappa_j\sigma_j K_1(\sigma_j)} \\ &= \frac{1}{z\kappa_j}[K_1^0(\sigma_j) + s_j] \end{aligned} \tag{4.16}$$

This is identical to the pressure response of a single layered system, where the reservoir parameters are same as the parameters of layer j. With this equation, we can determine κ_j and s_j using conventional well test analysis.

Ehlig-Economides and Joseph (1985) used the same idea in a multilayered crossflow system by noting that early time behavior of the crossflow system is identical to that of a commingled system. They analyzed early time data to determine layer properties, κ_j and s_j. The problem is that the early time interval should be long enough that the equation develop a semilog straight line. Thus this method for the crossflow system will not be adequate when the vertical permeabilities of the layers are big.

Both authors have applied the same principle but Kucuk, *et al.* (1985) only obtained the rough result in estimating the layer properties while Economides and Joseph obtained satisfactory result. The difference is in their methods of data acquisition. The idea of data acquisition of Kucuk, *et al.* (1985) is as follows:

1. Place the tool at the top of the uppermost layer and start production. The test time should be long enough to identify the average parameters of the total system, but not too long to detect the outer boundary conditions.

2. Survey the production profile to decide the number and the location of layers.

3. Position the tool at the top of bottom layer and measure the pressure and the flow rate from the bottom layer with changing the production rate at the wellhead.

4. Position the tool at the top of next higher layer and measure the pressure and the flow rate from all the layers below spinner.

5. Continue step 4 for all layers identified during step 2.

With this method, they assumed to be able to obtain the average properties of the layers below the tool. For example, when the tool was placed at the top of the k_{th} layer, the data they measured was the bottom hole pressure and the cumulative layer production rate, $\sum_{j=k}^{n} q_{ij}$. And the parameters they could obtain was $(\overline{kh})_k$ and $\overline{s_k}$:

$$(\overline{kh})_t = \sum_{j=k}^{n} k_j h_j \tag{4.17}$$

$$\overline{s_k} = \frac{\sum_{j=k}^{n} s_j q_{ij}}{\sum_{j=k}^{n} q_{ij}} \tag{4.18}$$

where q_{ij} is the stabilized flow rate of the j_{th} layer at the end of the i_{th} flow test.

Since N flow tests are executed for an N-layered reservoir, there will be N estimates of average values for permeability and the skin. With simple algebra, the parameters of individual layer are calculated. However, in reality, there is no semilog straight line in a commingled system, unlike crossflow systems as can be seen in many pressure derivative curves in Chapter 3. The truth is that the pressure curve is only approaching to a semilog straight line. Thus there is a big difference between reality and the assumption that $(\overline{kh})_k$ and $\overline{s}_k$ can be obtained from each flow test. Besides, the method calculates the parameters of the bottom layer first. That is the reason why the estimation of the individual layer is most accurate for the bottom layer. In fact, Kucuk, *et al.* (1985) used the estimate only as an initial values for the unknown reservoir parameter and improved by nonlinear parameter estimation method. However, Ehlig-Economides and Joseph (1985) simply assumed the availability of the production data for the individual layer from the beginning. Thus, unlike Kucuk, *et al.* (1985), they could obtain much better result in estimating layer permeability and skin.

Gao (1985) developed another method to determine the reservoir properties of the individual layer. He suggested that N layers be separated into two sections by a packer and produce only from the upper section, until two different straight lines appear. The first line determines the average permeability of the producing section and the second line determines the permeability and the skin of the entire system. This would be followed by $(N-1)$ drawdown tests, lowering the packer by one formation every time. With these N average values, the individual layer permeability can be calculated. Fig. 4.1 and Fig. 4.2 show this idea, for a four layered reservoir with parameters in Table 4.1.

As Gao observed, Fig. 4.1 shows two obvious semilog straight line when the vertical permeabilities are small ($k_v/k = 0.01$ or 0.0001) and from Fig. 4.2, the gradient of the two lines are 1.35 and 0.5. By conventional method, we can determine $(kh)_t = 27{,}000$ md-ft from the second straight line and $(kh)_1$ can be deduced by the simple

Table 4.1: Reservoir Parameters for the Example of Estimation Using Partial Production Method

Layer	k(md)	s	h(ft)
1	1000	3	10
2	100	2	10
3	600	1	10
4	1000	4	10
Total $(kh)_t = 27000$ md-ft case A: $k_v/k = 1.0$ case B: $k_v/k = 0.01$ case C: $k_v/k = 0.0001$			

relationship with the $(kh)_t$ as follows:

$$\frac{(kh)_t}{(kh)_1} = \frac{1.35}{0.5} \tag{4.19}$$

$$(kh)_1 = \frac{0.5}{1.35}(kh)_t = 10,000\text{md-ft} \tag{4.20}$$

However, if the crossflow effect is very strong ($k_v/k = 1.0$), then we may not observe the first semilog straight line which determines (kh) from the producing zone. Besides, the testing procedure is very difficult, requiring moving the packer during production at a constant rate. As can be seen in Fig. 4.2, the method failed even in the simplest case when the production was only from the first layer and when the vertical permeability of the system was very large ($k_v/k = 1.0$). This is aggravated when the production is from several layers, due to the crossflow effect.

4.2.2 New Methods

This work suggests two new methods to obtain the initial estimate of the reservoir parameters. The first method is applicable only to isotropic two layered reservoirs. The second method is generally applicable for N-layered reservoirs and works better when the reservoir is a commingled system or when the vertical permeabilities are small.

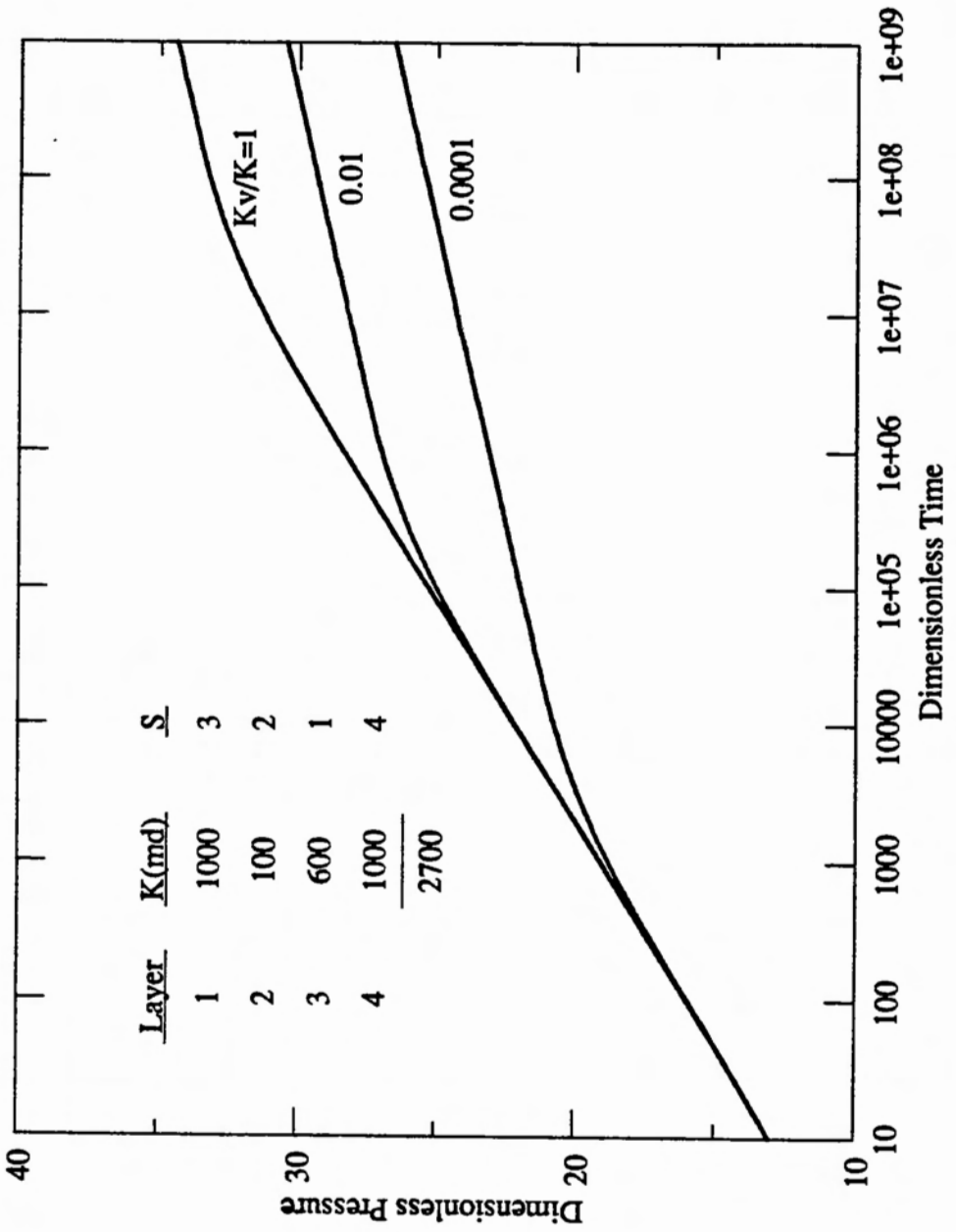

Figure 4.1: Pressure Curves Showing the Application of the Method of Partial Production

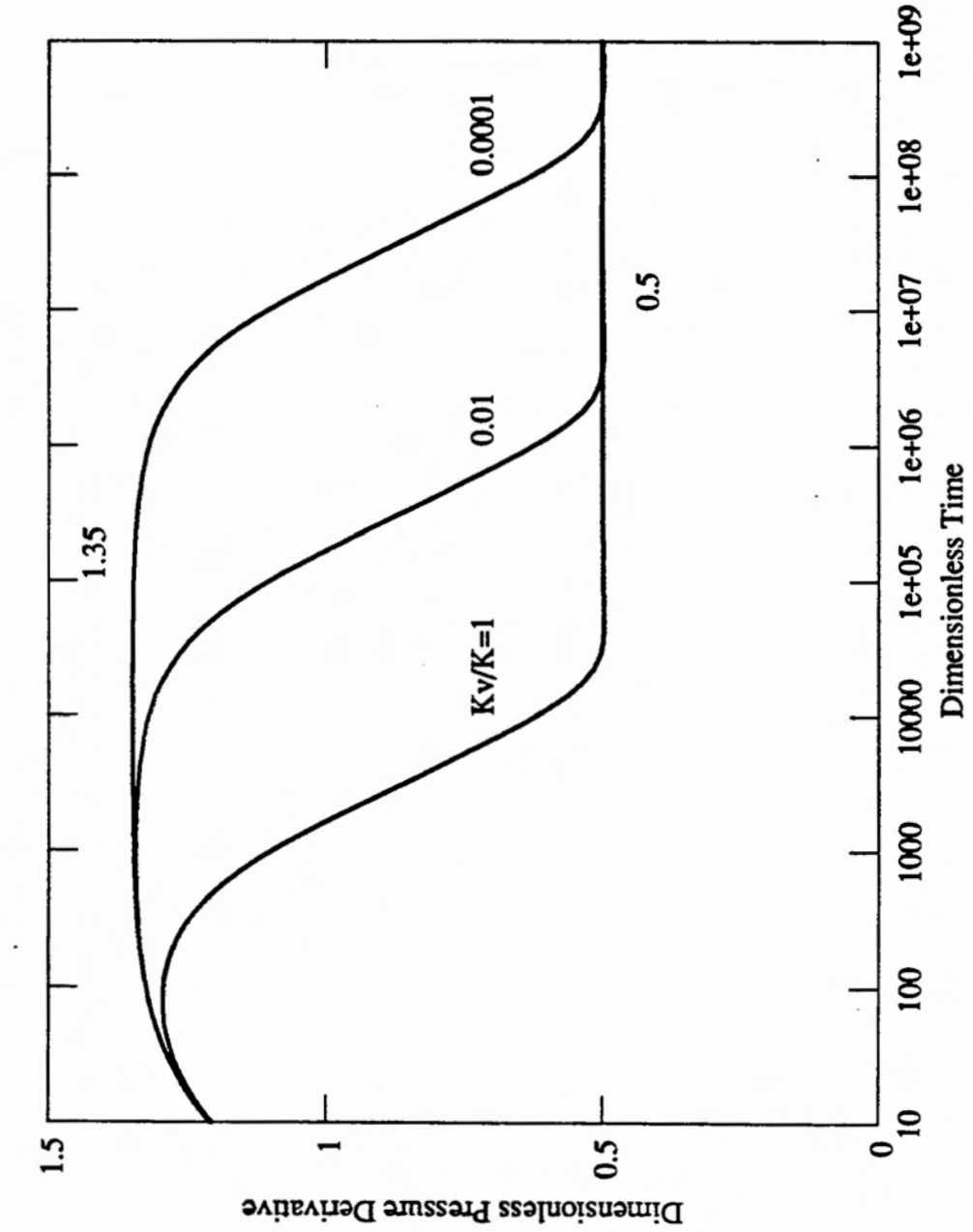

Figure 4.2: Pressure Derivative Curves Showing the Application of the Method of Partial Production

First Method

Data needed in the first method are wellbore pressure and q_{2D}^{LT}, the late time production rate from the bottom layer. The method does not require the entire history of the production rate.

Firstly, measure $(kh)_t$ and $\overline{s}$ for the entire system by the conventional method. By knowing $(kh)_t$ we can nondimensionalize the pressure and the time.

$$p_{wD} = \frac{2\pi(kh)_t(p_i - p_{wf})}{q_t\mu} \tag{4.21}$$

$$t_D = \frac{(kh)_t t}{(\phi h)_t \mu c_t r_w^2} \tag{4.22}$$

Secondly, prepare the semilog plots of the dimensionless pressure and its derivative.

Thirdly, identify the transition period by comparing with the p_D curve of a homogeneous system whose reservoir parameters are $(kh)_t$ and $\overline{s}$. As mentioned in Section 3.1 and Section 3.2, two cases are possible in identifying the transition period:

1. In general, the derivative curve of dimensionless pressure shows small concavity. Locate t_D^* when the small concavity reaches the minimum, which is equivalent to the inflection point in the pressure curve.

2. When the less permeable layer has very small skin and the pressure derivative curve does not show a small concavity, locate t_D^* when p_D curve switches from the commingled system to the homogeneous system.

As long as all the reservoir parameters are same except the skin factors, t_D^*, which represents the most diagnostic transition time is same for both cases. As mentioned in Section 3.4, the transition is entirely determined by the crossflow, which is governed by the parameter λ. Since this method assumes isotropic layers, λ is defined as:

$$\lambda = \frac{r_w^2}{(kh)_t}\left(\frac{k}{h}\right)_{1\frac{1}{2}} \tag{4.23}$$

$$= \frac{r_w^2}{k_1h_1 + k_2h_2}\frac{2}{\frac{k_1}{h_1} + \frac{k_2}{h_2}}$$

$$= \frac{2r_w^2}{h_1^2 + (\frac{k_1}{k_2})h_1h_2 + (\frac{k_2}{k_1})h_1h_2 + h_2^2} \tag{4.24}$$

Since we know r_w, h_1 and h_2, λ is entirely governed by $(\frac{k_1}{k_2})$. Using the type curve method we can determine $(\frac{k_1}{k_2})$. With this ratio and $(kh)_t$, we can calculate k_1 and k_2.

Skin factors can be uniquely calculated by measuring $q_{2D}^{LT}(= 1 - q_{1D}^{LT})$, because we have the relationship between s_1 and s_2 as described in Section 3.9. At late time, the production rate from the first layer is:

$$q_{1D}^{LT} = \kappa_1(1 + \frac{\kappa_2(s_2 - s_1)}{K_1^0(\sigma_1) + \kappa_1 s_2 + \kappa_2 s_1}) \tag{4.25}$$

By rearranging the above equation:

$$q_{1D}^{LT} - \kappa_1 = \frac{\kappa_1\kappa_2(s_2 - s_1)}{K_1^0(\sigma_1) + \kappa_1 s_2 + \kappa_2 s_1} \tag{4.26}$$

$$K_1^0(\sigma_1) + \kappa_1 s_2 + \kappa_2 s_1 = \frac{\kappa_1\kappa_2(s_2 - s_1)}{q_{1D}^{LT} - \kappa_1} \tag{4.27}$$

Moving every term that contains s_2 to the left hand side:

$$\kappa_1 s_2 - \frac{\kappa_1\kappa_2 s_2}{q_{1D}^{LT} - \kappa_1} = -\frac{\kappa_1\kappa_2 s_1}{q_{1D}^{LT} - \kappa_1} - \kappa_2 s_1 - K_1^0(\sigma_1) \tag{4.28}$$

By rearranging the above equation:

$$\kappa_1 s_2(\frac{q_{1D}^{LT} - 1}{q_{1D}^{LT} - \kappa_1}) = -\frac{q_{1D}^{LT}}{q_{1D}^{LT} - \kappa_1}(\kappa_2 s_1) - K_1^0(\sigma_1) \tag{4.29}$$

Since:

$$q_{1D}^{LT} + q_{2D}^{LT} = 1 = \kappa_1 + \kappa_2 \tag{4.30}$$

We can simplify Eq. 4.29 as:

$$q_{2D}^{LT}\kappa_1 s_2 = q_{1D}^{LT}\kappa_2 s_1 + (q_{1D}^{LT} - \kappa_1)K_1^0(\sigma_1) \tag{4.31}$$

The average skin is defined as:

$$\overline{s} = q_{1D}^{LT} s_1 + q_{2D}^{LT} s_2 \tag{4.32}$$

We can obtain:

$$q_{2D}^{LT}\kappa_1 s_2 = \kappa_1\overline{s} - q_{1D}^{LT}\kappa_1 s_1 \tag{4.33}$$

Finally, Eq. 4.31 is further simplified as:

$$q_{1D}^{LT} s_1 = \kappa_1 \overline{s} - (q_{1D}^{LT} - \kappa_1) K_1^0(\sigma_1) \tag{4.34}$$

or using q_{2D}^{LT}:

$$(1 - q_{2D}^{LT}) s_1 = \kappa_1 \overline{s} - (1 - q_{2D}^{LT} - \kappa_1) K_1^0(\sigma_1) \tag{4.35}$$

Similarly, we can get the equation for s_2:

$$q_{2D}^{LT} s_2 = \kappa_2 \overline{s} - (q_{2D}^{LT} - \kappa_2) K_1^0(\sigma_1) \tag{4.36}$$

By knowing $\overline{s}$ and the total productivity from the semilog straight line and κ_1 and κ_2 from the location of t_D^*, we can calculate s_1 and s_2 directly by measuring q_{2D}^{LT}. Since q_{2D}^{LT} is a constant value, we only have to measure q_{2D}^{LT} just once at late time. An example will be given in Section 4.3.

Second Method

The second method is more general. It can be applied to a multilayered reservoir, but needs the entire history of wellbore pressure and layer production.

Firstly, we determine the total productivity and the average skin factor of the reservoir from the semilog straight line.

The second step is to plot the production history of each layer. Production data for this step can be acquired in three ways.

1. Conventional Superposition Method

   Place the production logging tool at the top of the uppermost layer and begin production. Then the measured data will be the sum of the production rate from each layer. After the production rate becomes stable, lower the tool slowly and survey the production profile to decide the number of layers and the formation thickness. Place the tool at the top of the bottom layer. Start measuring the sandface flow rate after changing the total production rate at the wellhead. Naturally, the production rate from the bottom layer would be different from the rate before changing the total production rate, which is not measured. However,

in a dimensionless scale, when each rate is divided by the total production rate at the measurement time, the two curves would be identical except the very early time of adjustment to the new production rate. Raise the tool to the top of the next higher layer. Start measuring after changing the total production rate. The measured date would be the summation of the production rate of the layers below the logging tool. Non-dimensionalize by dividing the measured data by the total production rate at the measurement time. Subtract the dimensionless production rate of the bottom layer from the nondimensionalized data of current stage, and we will get the dimensionless production rate of the next higher layer from the bottom. Repeat the same process until we get the rate history of all the layers. An example of the superposition method is shown in Fig. 4.3. The demerits of this method are a longer testing time and the wiggling effect after changing the total production rate at the wellhead.

2. Multi-Spinner Without Superposition

   Locate the spinners at the top of each layer and start measuring. If there are four layers in the system, then we will get four sets of production data. Each will represent the summation of the production rates below the tool. By subtracting, we can easily determine the production rate of each layer. An example is shown in Fig. 4.4, with the schematic diagram of the multi-spinner method. The demerits are that we have to know the number of the layers and the thickness of the formations prior to placing the spinners.

3. Single Spinner Without Superposition

   The multi-spinner method can be replaced by a single spinner method, where the spinner measures the production rate below the tool, constantly moving upward and downward. Then the data we get will be a spike-like curve which is composed of four different production curves, as can be seen in schematic diagram in Fig. 4.5. The demerit, besides the one in the multi-spinner method, is that the accuracy of the measurement gets worse by moving the spinner constantly and that we might lose data from the very early time portion by the limit of the moving speed of the spinner.

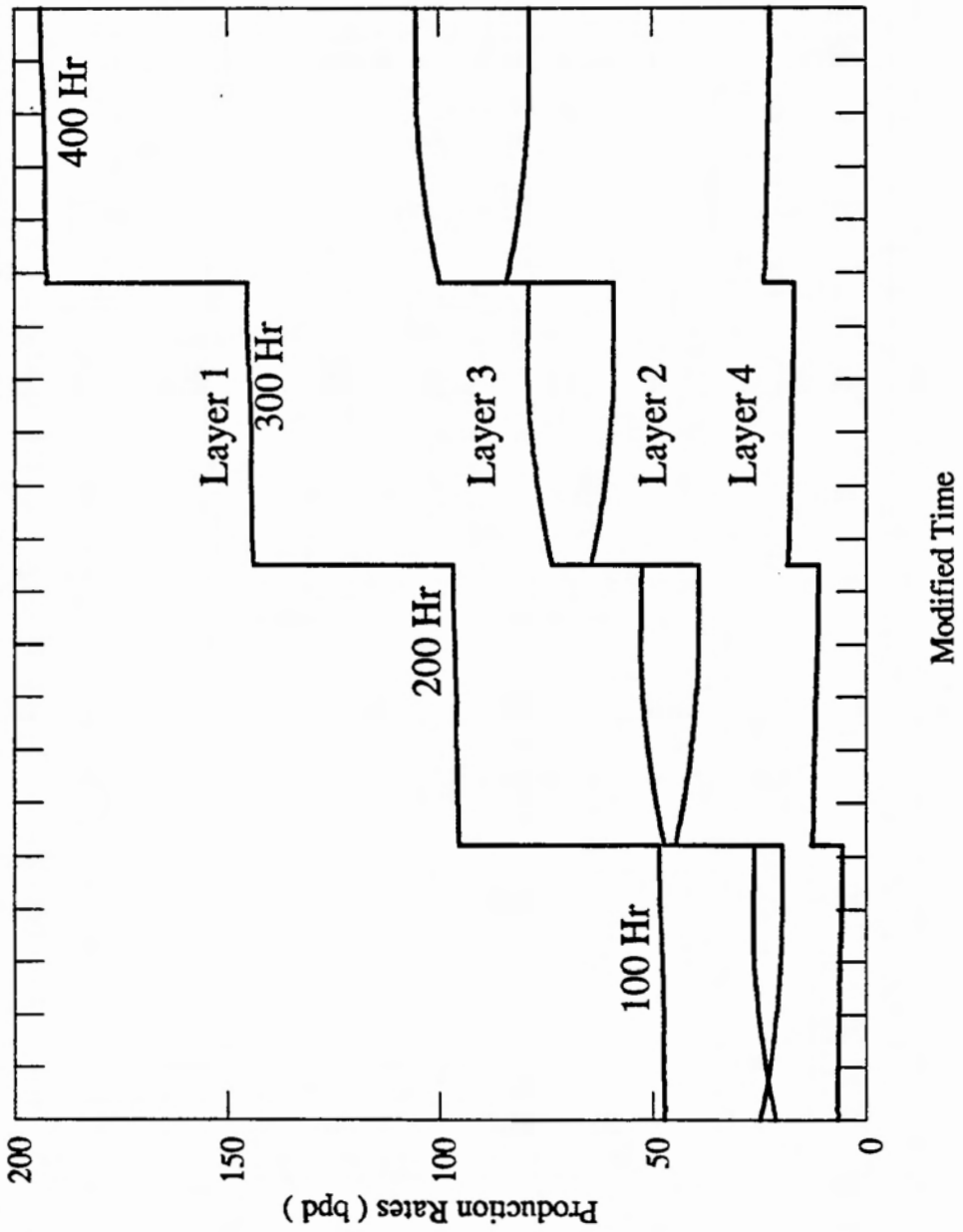

Figure 4.3: Example of Data Acquisition : Conventional Superposition Method

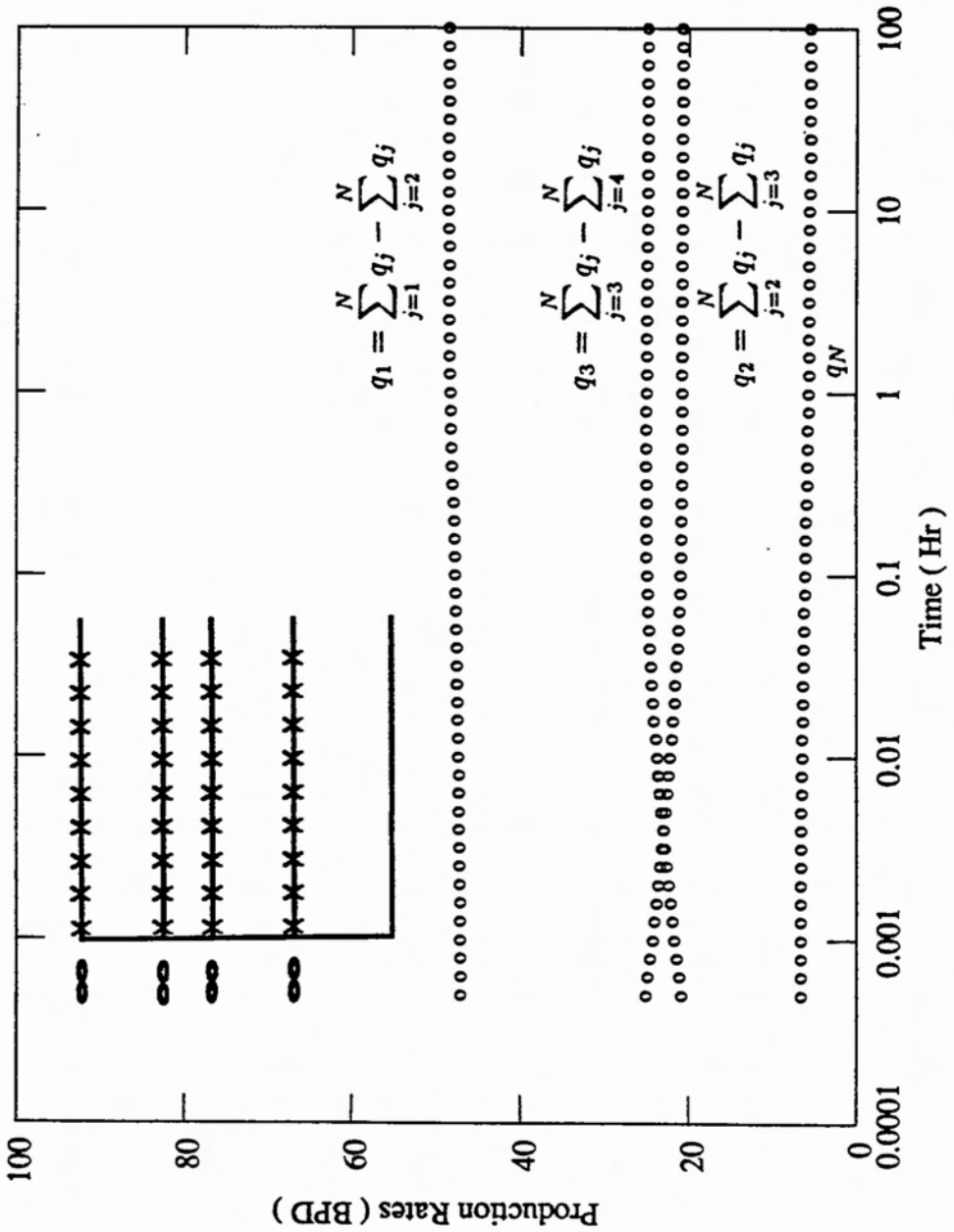

Figure 4.4: Example of Data Acquisition : Multi-Spinner Method

Even if the system has the wellbore storage effect, it can be minimized by the method suggested in Section 3.6.

$$q_{jD,C_D=0} = \frac{q_{jD}}{\sum_{j=1}^{n} q_{jD}} \tag{4.37}$$

This idea is to notice that $q_{jD,C_D=0}$ is an S-shaped curve in which both ends (${q_{jD,C_D=0}}^{ET}$ and ${q_{jD,C_D=0}}^{LT}$) are constant. As mentioned in Section 3.4, the crossflow term, λ, determines the time when transition starts and ends. The smaller λ is, the greater will be the portion of data identical to the response of commingled systems. At late time, the layer production rate of a commingled system is:

$$\overline{q_{jD}}^{LT} = \lim_{z\to 0} \frac{\frac{\kappa_j}{-\ln\sigma_j + s_j}}{z\sum_{k=1}^{n} \frac{\kappa_k}{-\ln\sigma_k + s_k}} \tag{4.38}$$

where:

$$\sigma_j = \sqrt{\frac{\omega_j z}{\kappa_j}} \tag{4.39}$$

This value is not a constant, but slightly changing with time z. At very late time, the terminal production rate from each layer eventually converges to κ_j, the productivity ratio, by the following derivation.

At very late time, z becomes extremely small. Thus:

$$\begin{aligned} \lim_{z\to 0}(-\ln\sigma_j + s_j) &= \lim_{z\to 0}\left(\ln\sqrt{\frac{\kappa_j}{\omega_j z}} + s_j\right) \\ &= \lim_{z\to 0}\left(\frac{1}{2}\ln\frac{1}{z} + \ln\sqrt{\frac{\kappa_j}{\omega_j}} + s_j\right) \\ &\to \frac{1}{2}\ln\frac{1}{z} \end{aligned} \tag{4.40}$$

and the terminal production rate from layer j becomes:

$$\begin{aligned} \overline{q_{jD}}^{LT} &= \lim_{z\to 0}\left(\frac{\frac{\kappa_j}{\frac{1}{2}\ln\frac{1}{z}}}{z\sum_{k=1}^{n}\frac{\kappa_k}{\frac{1}{2}\ln\frac{1}{z}}}\right) \\ &= \lim_{z\to 0}\left(\frac{\kappa_j}{z\sum_{k=1}^{n}\kappa_k}\right) \\ &\to \frac{\kappa_j}{z} \end{aligned} \tag{4.41}$$

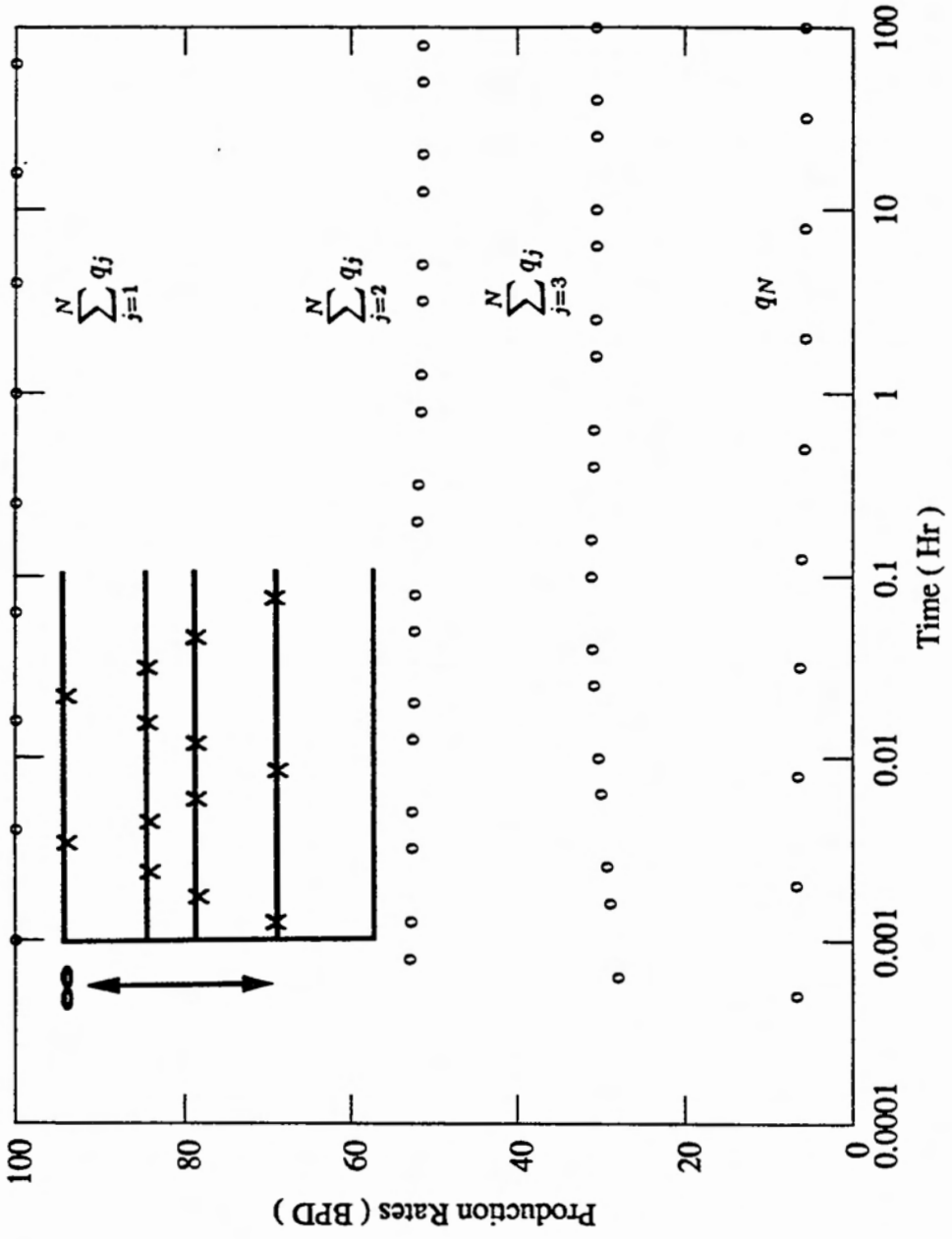

Figure 4.5: Example of Data Acquisition : Single Spinner Method

When it is converted back to the real domain, the production rate from each layer is identical to the productivity ratio of the layer:

$$q_{jD}{}^{LT} = \kappa_j \tag{4.42}$$

Usually the time when q_{jD}^{LT} in a commingled system approaches κ_j is too big for a computer to deal with.

Next, we can extrapolate the layer production data of the early and the intermediate period of the crossflow system to simulate the production history of the commingled system. This is the subjective part in the application of the second method.

At early time, the limiting value of the layer production rate is determined by the skin conditions as discussed in Section 3.8. For example, when the skin values of each layer are all non-zero, the early time limiting production from each layer is given by:

$$q_{jD}^{ET} = \frac{\frac{\kappa_j}{s_j}}{\sum_{k=1}^{n} \frac{\kappa_k}{s_k}} \tag{4.43}$$

At late time, q_{jD}^{LT} is also a constant which is determined by permeability, skin and λ as discussed in Section 3.9.

All skin factors can be expressed in terms of q_{jD}^{ET} and κ_j:

$$q_{1D}^{ET} = \frac{\frac{\kappa_1}{s_1}}{\sum_{k=1}^{n} \frac{\kappa_k}{s_k}} \tag{4.44}$$

$$q_{jD}^{ET} = \frac{\frac{\kappa_j}{s_j}}{\sum_{k=1}^{n} \frac{\kappa_k}{s_k}} \tag{4.45}$$

Then s_j can be expressed in terms of s_1:

$$s_j = \frac{q_{1D}^{ET}}{q_{jD}^{ET}} \frac{\kappa_j}{\kappa_1} s_1 \tag{4.46}$$

Since average skin value is defined as:

$$\overline{s} = \sum_{k=1}^{n} q_{kD}^{LT} s_k \tag{4.47}$$

Substitute Eq. 4.46 into Eq. 4.47:

$$\overline{s} = \sum_{k=1}^{n} q_{kD}^{LT} \frac{q_{1D}^{ET}}{q_{kD}^{ET}} \frac{\kappa_k}{\kappa_1} s_1 \tag{4.48}$$

Thus s_1 can be expressed as:

$$s_1 = \frac{\overline{s}}{\sum_{k=1}^{n} q_{kD}^{LT} \frac{q_{1D}^{ET}}{q_{kD}^{ET}} \frac{\kappa_k}{\kappa_1}} \tag{4.49}$$

By knowing q_{jD}^{ET} and q_{jD}^{LT}, we can calculate all the skin values using Eq. 4.46:

$$\begin{aligned} s_j &= \frac{q_{1D}^{ET}}{q_{jD}^{ET}} \frac{\kappa_j}{\kappa_1} s_1 \\ &= \frac{\frac{q_{1D}^{ET}}{q_{jD}^{ET}} \frac{\kappa_j}{\kappa_1} \overline{s}}{\sum_{k=1}^{n} q_{kD}^{LT} \frac{q_{1D}^{ET}}{q_{kD}^{ET}} \frac{\kappa_k}{\kappa_1}} \end{aligned} \tag{4.50}$$

Thus κ_j and s_j for every layer is determined. Several examples of the second method will be given in Section 4.3.

4.3 Examples of New Initial Estimation

As mentioned in the previous section, two new methods for determining the initial values for the nonlinear parameter estimation were suggested. The first method is applicable for a two layered crossflow system where the layers are isotropic and the second method is applicable for an N-layered crossflow system. The second method works better if the system is commingled only in the wellbore. In this section, examples are shown for each method. The example for the first method would be very hypothetical and the examples for the second method would be more realistic.

4.3.1 First Method

Data needed in the first method are the entire history of the wellbore pressure and the one time measurement of the production rate from the bottom layer in the late time. Wellbore pressure was calculated for a two layered reservoir with parameters in Table 4.2 and listed in Appendix D. The number of data selected for the analysis was ten per log cycle with uniform interval in the logarithmic time scale.

Table 4.2: Reservoir Parameters for the Example of the Initial Estimation Using the First Method

Layer	k(md)	k_v(md)	s	h(ft)	ϕ
1	1000	1000	1	10	0.3
2	100	100	4	10	0.3
$q_t = 100$(bbl/day) $\mu = 50$ (cp) $c_t = 0.000006$(1/psi) $r_w = 0.301$(ft)					

The first step is to determine the total productivity of the system and the average skin. Since the crossflow system always behaves like a homogeneous system in the late time, it shows the clear semilog straight line (Fig. 4.6). Using the conventional method, we can determine $(kh)_t$ as 11000 md-ft and $\overline{s}$ as 1.167.

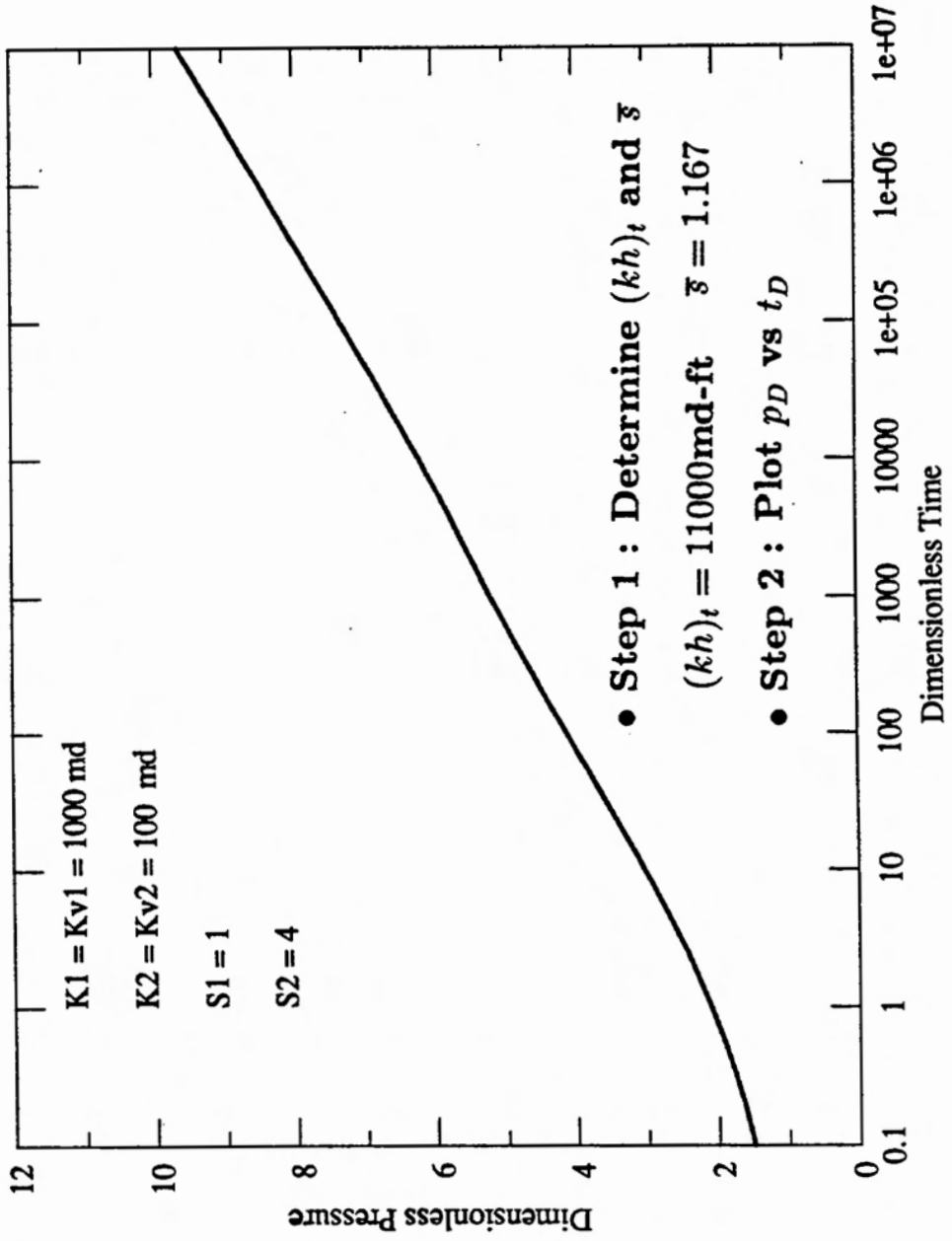

Figure 4.6: Wellbore Pressure Curve in the Example of the Parameter Estimation Using the First Method

The second step is to generate the plot of the derivative curve for the dimensionless pressure (Fig. 4.7). Non-dimensionalization is possible if we know the total productivity of the system:

$$p_D = \frac{(kh)_t}{141.25 q_t \mu}(p_i - p_{wf}) \tag{4.51}$$

$$t_D = \frac{0.0002637(kh)_t t}{(\phi h)_t \mu c_t r_w^2} \tag{4.52}$$

The third step is to match the location of t_D^*, the most diagnostic point of the transition phenomenon (Fig. 4.7). In most cases, the crossflow system shows the small concavity in the derivative of the dimensionless pressure curve. However, in some cases when the less permeable layer has very small skin factor, we may not have the small concavity. In these cases, we can still locate t_D^* in the dimensionless pressure curve, by noting that the commingled system and the equivalent homogeneous system cross each other just at the point t_D^*, as explained in Section 3.1. The location of t_D^* is a function of vertical permeability only. Since we assume isotropic layers, the location varies only with permeability ratio between the two layers. By generating several type curves of different (k_1/k_2), we can closely match the real permeability ratio between layers. With this ratio and the total productivity, we can determine the permeability of each layer, since we have two unknowns and two equations.

$$k_1 h_1 + k_2 h_2 = 11000(\text{md-ft}) \tag{4.53}$$

$$\frac{k_1}{k_2} = 10 \tag{4.54}$$

The thickness of each formation can be obtained using the production logging tool by noting the abrupt change in production profile at the intersection.

$$h_1 = h_2 = 10(\text{ft}) \tag{4.55}$$

Thus we can obtain the permeability of each layer as:

$$\begin{aligned} k_1 &= 1000(\text{ft}) \\ k_2 &= 100(\text{ft}) \end{aligned} \tag{4.56}$$

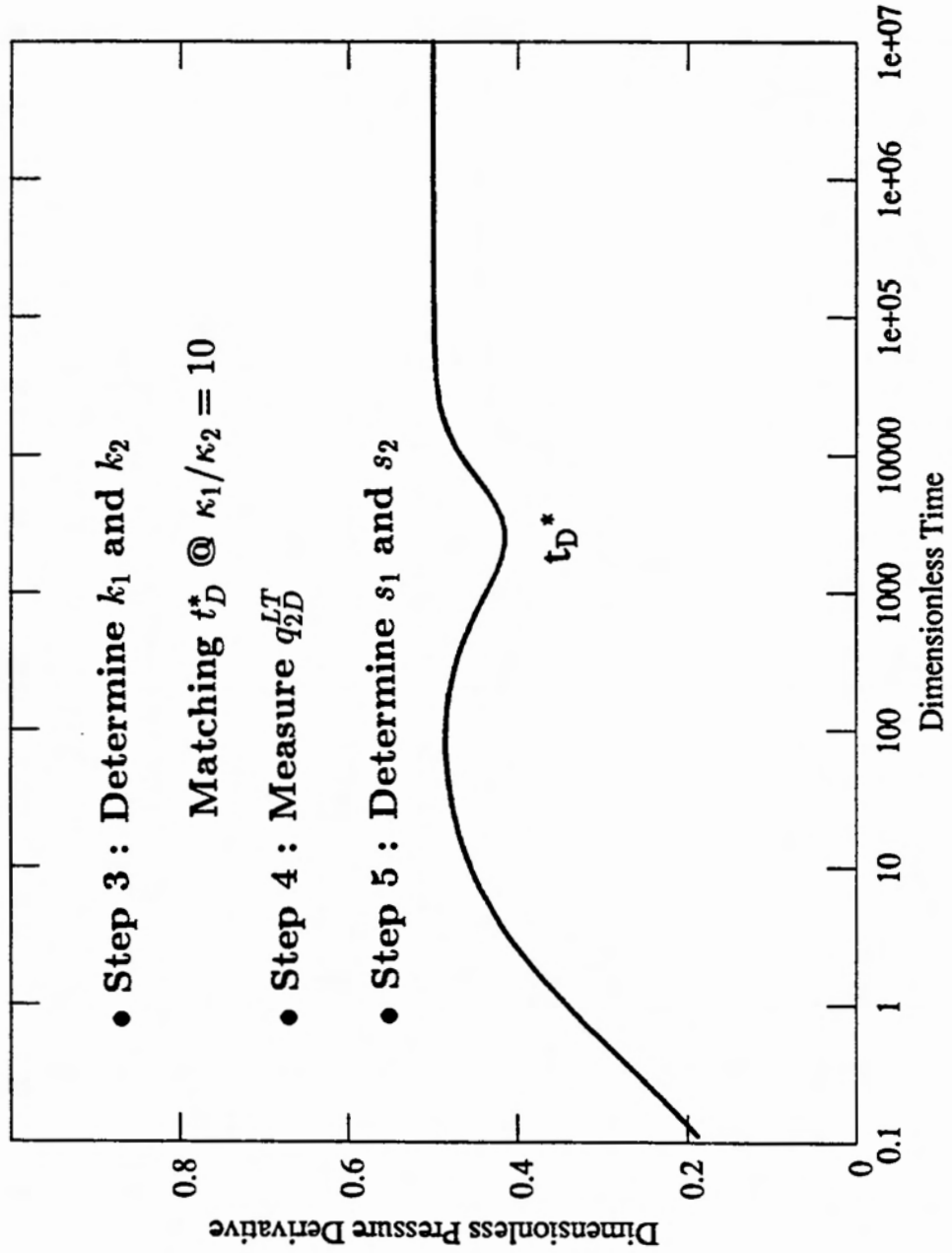

Figure 4.7: Wellbore Pressure Derivative Curve in the Example of the Parameter Estimation Using the First Method

The fourth step is to measure the production rate from the bottom layer at late time. Using the production logging tool, this can be easily done along with the measurement of the formation thickness:

$$q_2^{LT} = 5.55(\text{bbl/day}) \tag{4.57}$$

or in a dimensionless scale:

$$q_{2D}^{LT} = \frac{5.55}{q_t} = 0.0555 \tag{4.58}$$

The final step is to determine the skin factor of each layer. The equations developed in Section 3.9 will be used in this step.

$$q_{2D}^{LT} s_2 = \kappa_2 \overline{s} + (1 - q_{2D}^{LT} - \kappa_1) K_1^0(\sigma_1) \tag{4.59}$$

where:

$$K_1^0(\sigma_1) = \frac{K_0(\sigma_1)}{\sigma_1 K_1(\sigma_1)} \tag{4.60}$$

$$\sigma_1 = \sqrt{\frac{\lambda}{\kappa_1} + \frac{\lambda}{\kappa_2}} \tag{4.61}$$

By substituting all the known values into Eq. 4.59, we can determine s_1 as 1. And from the definition of the average of the skin factor of the total system:

$$q_{1D}^{LT} s_1 = \overline{s} - q_{2D}^{LT} s_2 \tag{4.62}$$

we can determine s_2 as 4.

$$\begin{aligned} s_1 &= 1 \\ s_2 &= 4 \end{aligned} \tag{4.63}$$

4.3.2 Second Method

In this subsection, three examples of the application of the second method will be demonstrated. The first example is for a four layered isotropic reservoir with positive skin factors, the second example is for a three layered reservoir with vertical permeabilities different from radial permeabilities, and the last example is for a three layered isotropic reservoir with negative skin factors.

Example 1

The first example is for a four layered reservoir where each layer is isotropic and has a positive skin factor, with parameters in Table 4.3. Data of wellbore pressure and layer production rates are listed in Appendix E. As in the example of the first method, the number of data for the analysis was ten per log cycle with uniform interval in the logarithmic time scale.

Table 4.3: Reservoir Parameters for Example 1 of Initial Estimation Using the Second Method

Layer	k(md)	k_v(md)	s	h(ft)	ϕ
1	900	900	2	10	0.3
2	300	300	1	10	0.3
3	700	700	5	10	0.3
4	100	100	2	10	0.3
q_t = 100 (bbl/day) μ = 50 (cp) c_t=0.000006(1/psi) r_w=0.301 (ft)					

The first step is to determine the total productivity and the average skin of the system using the conventional semilog method, as in the example of the first method.

$$\begin{aligned} (kh)_t &= 20000\text{md-ft} \\ \overline{s} &= 2.54 \end{aligned} \tag{4.64}$$

The second step is to plot the history of the production rate from each layer obtained by one of the three data acquisition methods described in Section 4.2.

The next step is the subjective part in the application of the second method. Using the data at early time and at intermediate time, approximate the production history for the commingled system with same reservoir parameters, from the early time to the late time (Fig. 4.8). If the vertical permeabilities of the layers are smaller, we will have longer portions of the early time and the intermediate time data, which will make the approximation more accurate. At this moment, we are not determining

the real values of the reservoir parameters, but are just trying to obtain reasonable values for the initial estimates which are needed for regression.

At very late time, the layer production rate of the commingled system is equivalent to the productivity ratio, κ_j, as mentioned in Section 4.2. Thus, we can use the long time limiting values of the production rate from each layer as the initial estimate of the layer productivities. In this example, the estimates for permeability, k_j^*, are shown in Table 4.4.

Table 4.4: Estimation Procedure for Example 1 Using the Second Method

Layer	$q_j^{LT,*}$(bbl/day)	κ^*	k^*(md)	$q_j^{ET,*}$(bbl/day)	s_j^*
1	50.0	0.50	1000	46	2.332
2	14.0	0.14	280	32	0.940
3	32.0	0.32	640	15	4.580
4	4.0	0.04	80	7	1.227
$*$ means the estimation					

At very early time, the layer production rate is determined by the permeability and skin factor. If some layers show no production at very early time, then we can tell that those layers have non-zero skin factors, while the others have zero skin factors. If every layer is producing, then the rate is determined by the ratio of the $\frac{\kappa_j}{s_j}$ to the summation of the ratios, as discussed in Section 3.8. With these early time production rates coupled with the late time production rates, we can determine the initial estimates for skin factors of each layer, as mentioned in Section 4.2. In this example, the early time limiting layer production rates are estimated as follows:

$$\begin{aligned} {q_1}^{ET,*} &= 46.0\text{bbl/day} \\ {q_2}^{ET,*} &= 32.0\text{bbl/day} \\ {q_3}^{ET,*} &= 15.0\text{bbl/day} \\ {q_4}^{ET,*} &= 7.0\text{bbl/day} \end{aligned} \tag{4.65}$$

Since every layer produces at very early time in this example, there is not a layer which has zero skin factor. Using Eq. 4.46, obtain an expression for the skin of any

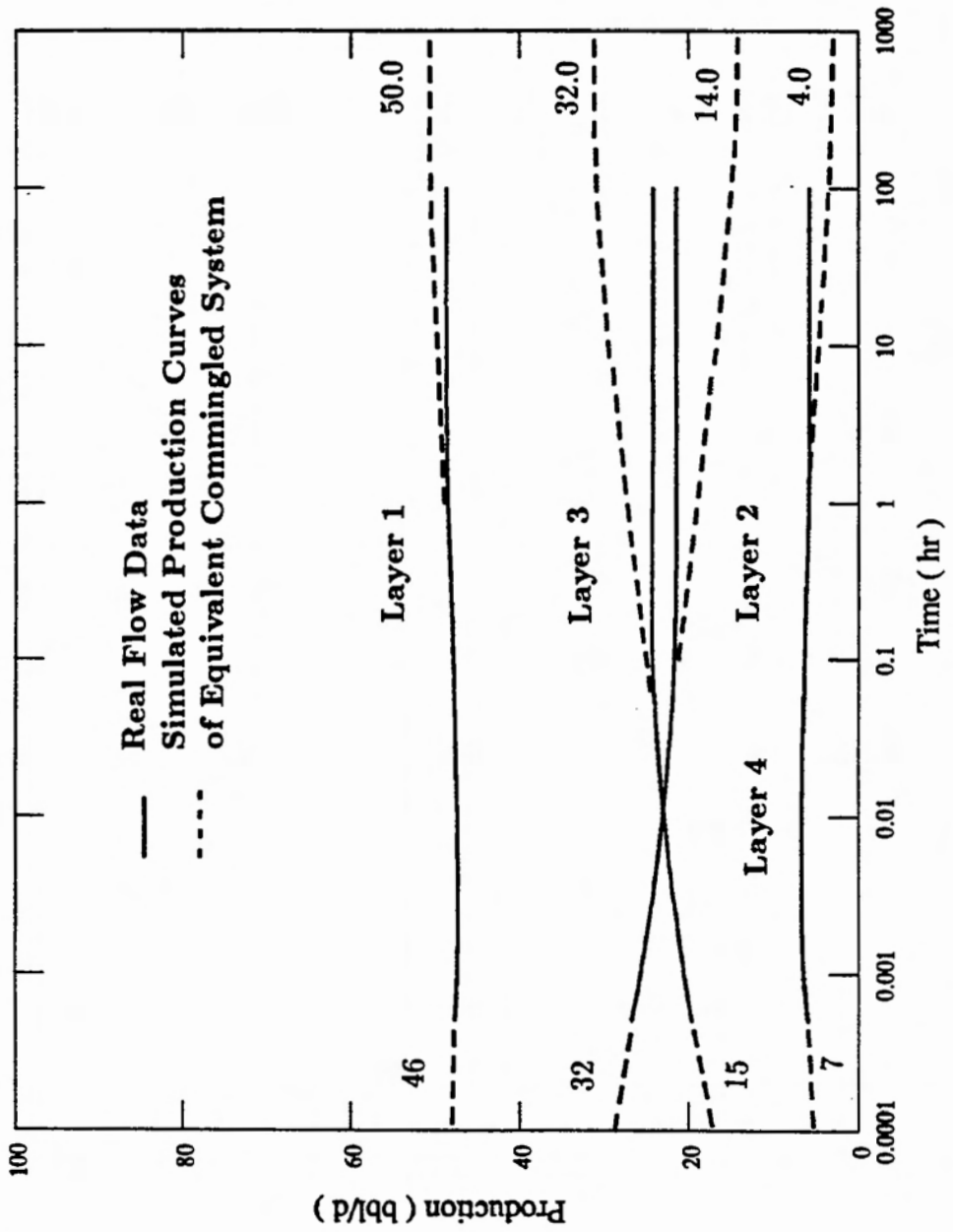

Figure 4.8: Production Rate from Each Layer and Simulated Production Curves for Example 1 of Parameter Estimation Using the Second Method

layer in terms of skin of layer 1.

$$s_j^* = \frac{q_{1D}^{ET,*}}{q_{jD}^{ET,*}} \frac{\kappa_j^*}{\kappa_1^*} s_1^* \tag{4.66}$$

For example, the skin factor of layer 2 is:

$$s_2^* = \frac{46.0}{32.0} \frac{0.14}{0.50} s_1^* = 0.4025\, s_1^* \tag{4.67}$$

Likewise:

$$\begin{aligned} s_3^* &= 1.9627 s_1^* \\ s_4^* &= 0.5257 s_1^* \end{aligned} \tag{4.68}$$

Using the definition of the average skin of the total system:

$$q_t^{LT} \overline{s} = q_1^{LT} s_1^* + \ldots + q_4^{LT} s_4^* \tag{4.69}$$

$$\begin{aligned} 100\text{x}2.54 &= 48.6 s_1^* + 20.8 s_2^* + 24.9 s_3^* + 5.7 s_4^* \\ &= (48.6 + 20.7\text{x}0.4025 + 24.9\text{x}1.9627 + 5.7\text{x}0.5257)\, s_1^* \end{aligned} \tag{4.70}$$

Solving for s_1^* and substituting the result into Eq. 4.66 yields:

$$\begin{aligned} s_1^* &= 2.332 \\ s_2^* &= 0.940 \\ s_3^* &= 4.580 \\ s_4^* &= 1.227 \end{aligned} \tag{4.71}$$

The initial values, k_j^* and s_j^*, obtained by the second method were named as "Initial Estimates A". Another set of initial estimates were made to see how sensitive the regression algorithm is to the poor estimation ("Initial Estimates B"). The estimation method for permeabilities are the same as before. However, at this time, skin factors of each layer were assumed to be the same as the average skin factor of the total system, obtained from the pressure analysis.

$$s_j^* = \overline{s} = 2.54 \tag{4.72}$$

The second method of initial estimation uses the limiting form of layer production rates at early time and at late time in obtaining the estimates of skin factors of each layer. Thus, if early time data are not so reliable, then we do not have many clues for skin factors. This is the reason for the choice of Eq. 4.72.

Some modification might be possible. The fractional production rates of each layer at late time can be taken as the productivity of the layer.

$$q_j^{ET,*} = \kappa_j^* \tag{4.73}$$

This is a reasonable assumption when the vertical communication between layers is negligible due to small vertical permeabilities.

From the productivity, κ_j^*, estimated by the second method and measured production data at late time, q_j^{LT}, we can modify the skin factors of each layer. If κ_j^* is greater than q_{jD}^{LT}, then s_j can be assumed smaller than $\overline{s}$, and if κ_j is smaller than q_{jD}^{LT}, then s_j can be assumed greater than $\overline{s}$, as might be guessed from Section 3.9. The magnitude of modification cannot be mathematically determined, but, in general, greater change is expected if the difference between κ_j and q_{jD}^{LT} is bigger. Actually, this type of initial estimation for skin factors was used in the third example, since the case does not show early time limiting production rates clearly.

In addition to the comparison of the results of Initial Estimates A and B, each set was tested for two cases; one case is to analyze wellbore pressure only and the other case is to analyze both wellbore pressure and layer production rate with proper weighting constants. That proper constants were taken so that production rates be the numbers of similar magnitude to the pressure data.

Using these initial estimates for the permeability and the skin of each layer, the optimization program in Appendix I is executed to determine the best fit reservoir parameters. As shown in Table 4.5, the regression method converged to the real answer after eight iterations. As can be seen from the results, the simultaneous analysis of pressure and production rates with proper weighting constants, always yielded quick convergence to the correct reservoir parameters.

Table 4.5: The Results of Parameter Estimation for Example 1

Original Parameter Values					
k_1	900.0	md	s_1	2.0	
k_2	300.0	md	s_2	1.0	
k_3	700.0	md	s_3	5.0	
k_4	100.0	md	s_4	2.0	
Initial Estimates A					
k_1	1000.0	md	s_1	2.358	
k_2	280.0	md	s_2	0.949	
k_3	640.0	md	s_3	4.629	
k_4	80.0	md	s_4	1.240	
With Weighting on Production Rates After 8_{th} Iteration					
k_1	900.8	(0.073)	s_1	2.005	(0.193)
k_2	300.1	(0.094)	s_2	1.002	(0.276)
k_3	701.1	(0.136)	s_3	5.013	(0.227)
k_4	100.0	(0.144)	s_4	2.002	(0.263)
Without Weighting on Production Rates After 8_{th} Iteration					
k_1	1001.9	(0.504)	s_1	2.523	(0.193)
k_2	238.8	(0.417)	s_2	0.859	(0.276)
k_3	637.4	(0.654)	s_3	4.167	(0.227)
k_4	77.9	(0.813)	s_4	1.407	(0.263)
Initial Estimates B					
k_1	1000.0	md	s_1	2.54	
k_2	280.0	md	s_2	2.54	
k_3	640.0	md	s_3	2.54	
k_4	80.0	md	s_4	2.54	
With Weighting on Production Rates After 8_{th} Iteration					
k_1	900.6	(0.342)	s_1	2.003	(0.888)
k_2	300.3	(0.406)	s_2	1.002	(1.189)
k_3	698.7	(0.521)	s_3	4.986	(0.867)
k_4	100.0	(0.683)	s_4	1.999	(1.327)
Without Weighting on Production Rates No Convergence					
(*) : Confidence Interval in %					

Example 2

The second example is for a three layered reservoir where each layer is anisotropic and has different porosity. Reservoir parameters for this example are listed in Table 4.6 and data for wellbore pressure and layer production rates are listed in Appendix F.

Table 4.6: Reservoir Parameters for the Example 2 of Initial Estimation Using the Second Method

Layer	k(md)	k_v(md)	s	h(ft)	ϕ
1	800	500	5	10	0.3
2	100	70	1	20	0.1
3	500	250	8	15	0.2
q_t = 100 (bbl/day) μ = 50 (cp) c_t=0.000006(1/psi) r_w=0.301 (ft)					

The total productivity and the average skin factor of the system were obtained using the conventional semilog method:

$$(kh)_t = 17500\text{md-ft} \tag{4.74}$$

$$\overline{s} = 10 \tag{4.75}$$

The production rates from each layer and the simulated production curves for the commingled system are plotted in Fig. 4.9. As in the first example, productivity ratio of each layer were obtained from the production curves of the commingled system at very late time.

The estimates for the productivity and the permeability of each layer are:

$$\begin{aligned} \kappa_1 &= 0.50 \\ \kappa_2 &= 0.15 \\ \kappa_3 &= 0.35 \\ k_1 &= 875 \text{ md} \end{aligned} \tag{4.76}$$

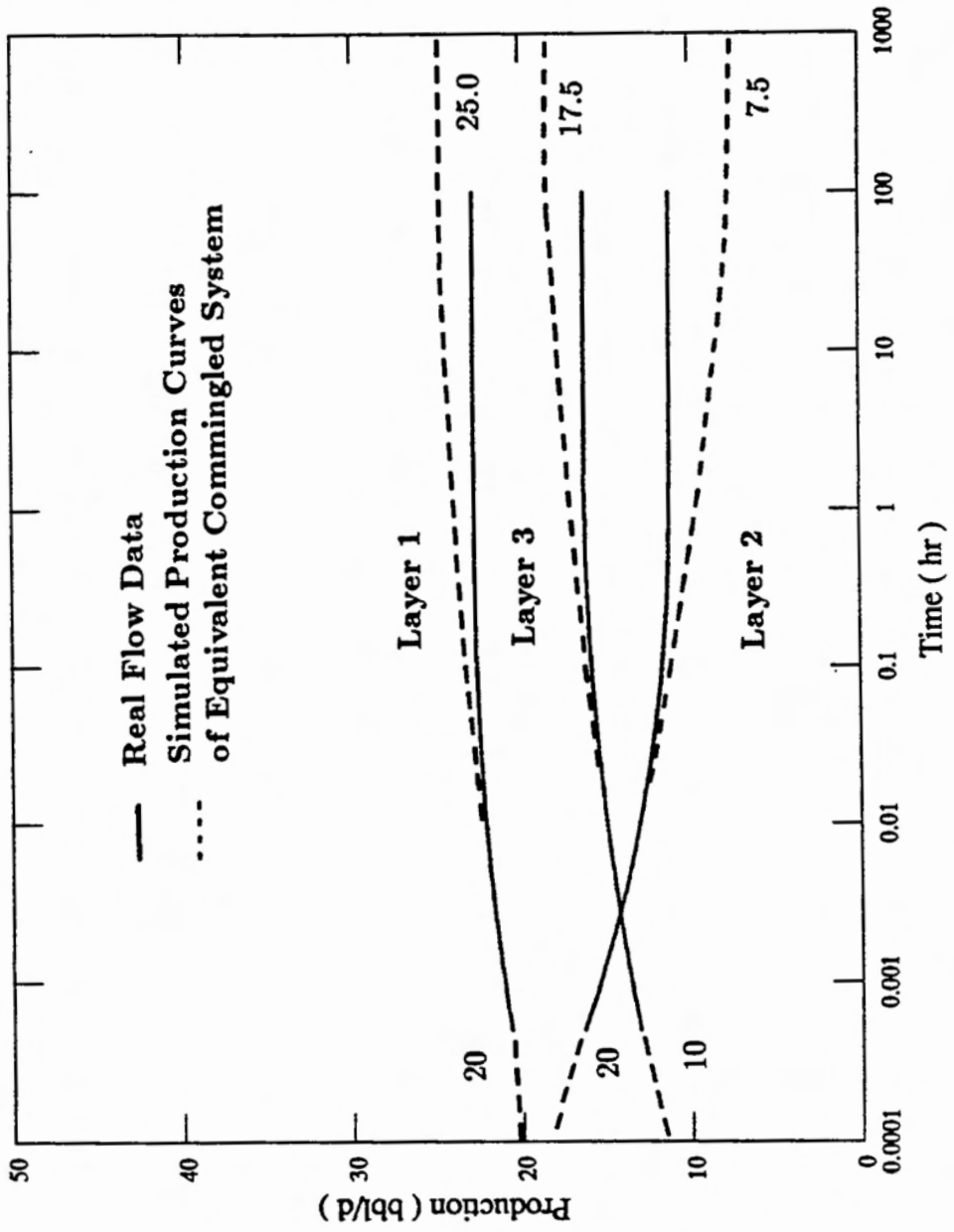

Figure 4.9: Production Rate from Each Layer and Simulated Production Curves for Example 2 of Parameter Estimation Using the Second Method

$$\begin{aligned} k_2 &= 132 \text{ md} \\ k_3 &= 408 \text{ md} \end{aligned}$$

The estimates for vertical permeability were taken as half of radial permeability of each layer.

Layer production rates at very early time were estimated as follows:

$$\begin{aligned} q_1^{ET,*} &= 20 \text{ bpd} \\ q_2^{ET,*} &= 20 \text{ bpd} \\ q_3^{ET,*} &= 10 \text{ bpd} \end{aligned} \tag{4.77}$$

Using Eq. 4.46, skin factors are estimated as follows:

$$s_2 = \frac{q_1^{ET,*}}{q_2^{ET,*}} \frac{\kappa_2^*}{\kappa_1^*} = 0.3 s_1 \tag{4.78}$$

$$s_3 = \frac{q_1^{ET,*}}{q_3^{ET,*}} \frac{\kappa_3^*}{\kappa_1^*} = 1.4 s_1$$

Since we can determine s_1 from the expression of the average skin factor, skin factors of each layer were determined as:

$$\begin{aligned} s_1 &= 5.14 \\ s_2 &= 1.54 \\ s_3 &= 7.12 \end{aligned} \tag{4.79}$$

As in the Example 1 of the second estimation method, these estimates for permeabilities, vertical permeabilities and skin factors were named as "Initial Estimates A". The procedure of determining the "Initial Estimates A" is summarized in Table 4.7.

For the purpose of comparison, another set of estimates was prepared where all skin factors were the same as the average skin value of the system. Also, each set was used twice in running the optimization program; one was run with proper weighting constants and the other was without weighting. The results were listed in Table 4.8.

After five iterations, Initial Estimates A with proper weighting constants converged to the correct permeabilities and skin factors. The converged value for vertical

Table 4.7: Estimation Procedure for Example 2 Using the Second Method

Layer	q_j^{LT} (bpd)	κ^*	k^*(md)	k_v^*(md)	$q_j^{ET,*}$ (bpd)	s_j^*
1	22.72	0.50	875.0	437.5	20.0	5.14
2	11.12	0.15	132.0	66.0	20.0	1.54
3	16.16	0.35	408.0	204.0	10.0	7.12
$*$ means the estimation						

Table 4.8: The Results of Parameter Estimation for Example 2

Original Parameter Values					
k_1	800.0	k_{v_1}	500.0	s_1	5.0
k_2	100.0	k_{v_2}	70.0	s_2	1.0
k_3	500.0	k_{v_3}	250.0	s_3	8.0
Initial Estimates A					
k_1	875.0	k_{v_1}	437.5	s_1	5.14
k_2	132.0	k_{v_2}	66.0	s_2	1.54
k_3	408.0	k_{v_3}	204.0	s_3	7.12
With Weighting on Production Rates After 5_{th} Iteration					
k_1	800.0	k_{v_1}	187.6	s_1	5.0
k_2	100.0	k_{v_2}	79.3	s_2	1.0
k_3	500.0	k_{v_3}	160.4	s_3	8.0
Without Weighting on Production Rates After 5_{th} Iteration					
k_1	843.4	k_{v_1}	441.3	s_1	6.612
k_2	143.4	k_{v_2}	45.2	s_2	1.171
k_3	413.6	k_{v_3}	141.0	s_3	6.886
Initial Estimates B					
k_1	875.0	k_{v_1}	437.5	s_1	5.08
k_2	132.0	k_{v_2}	66.0	s_2	5.08
k_3	408.0	k_{v_3}	204.0	s_3	5.08
With Weighting on Production Rates No Convergence					
Without Weighting on Production Rates No Convergence					

permeabilities might look incorrect. However, the multilayered system with crossflow cannot distinguish the vertical permeabilities of two layers as long as λ, a dimensionless term representing the formation crossflow between the layers, are the same. Actually, λ_j calculated using the original parameters are not different from λ_j calculated using the converged parameters. Thus, Initial Estimates B with weighting constants can be said to have converged to the correct parameters.

	Original Parameters	New Parameters
λ_1	0.934579E-04	0.934504E-04
λ_2	0.826446E-04	0.826506E-04

The analysis of the pressure data only with the same Initial Estimates A did not converge to the correct answer. This means that coupling wellbore pressure and layer production rate is useful not only for obtaining the initial estimates but also for the analysis of well test data.

However, Initial Estimates B did not converge at all for either the analysis of the pressure data only or the analysis of the pressure data and the production data at the same time. This means that good initial estimates are essential to obtain the correct reservoir parameters using the nonlinear regression technique.

Example 3

The last example is for a three layered reservoir with negative skin factors. Wellbore pressure and layer production rates were calculated from the reservoir parameters in Table 4.9 and listed in Appendix G.

From the pressure analysis, we can determine the total productivity and the average skin of the system as follows:

$$\begin{aligned} (kh)_t &= 4500\text{md-ft} \\ \overline{s} &= -1.72 \end{aligned} \tag{4.80}$$

As before, plot the production rates for each layer using the measured data and simulate the production curves of the commingled system with the same reservoir parameters (Fig. 4.10).

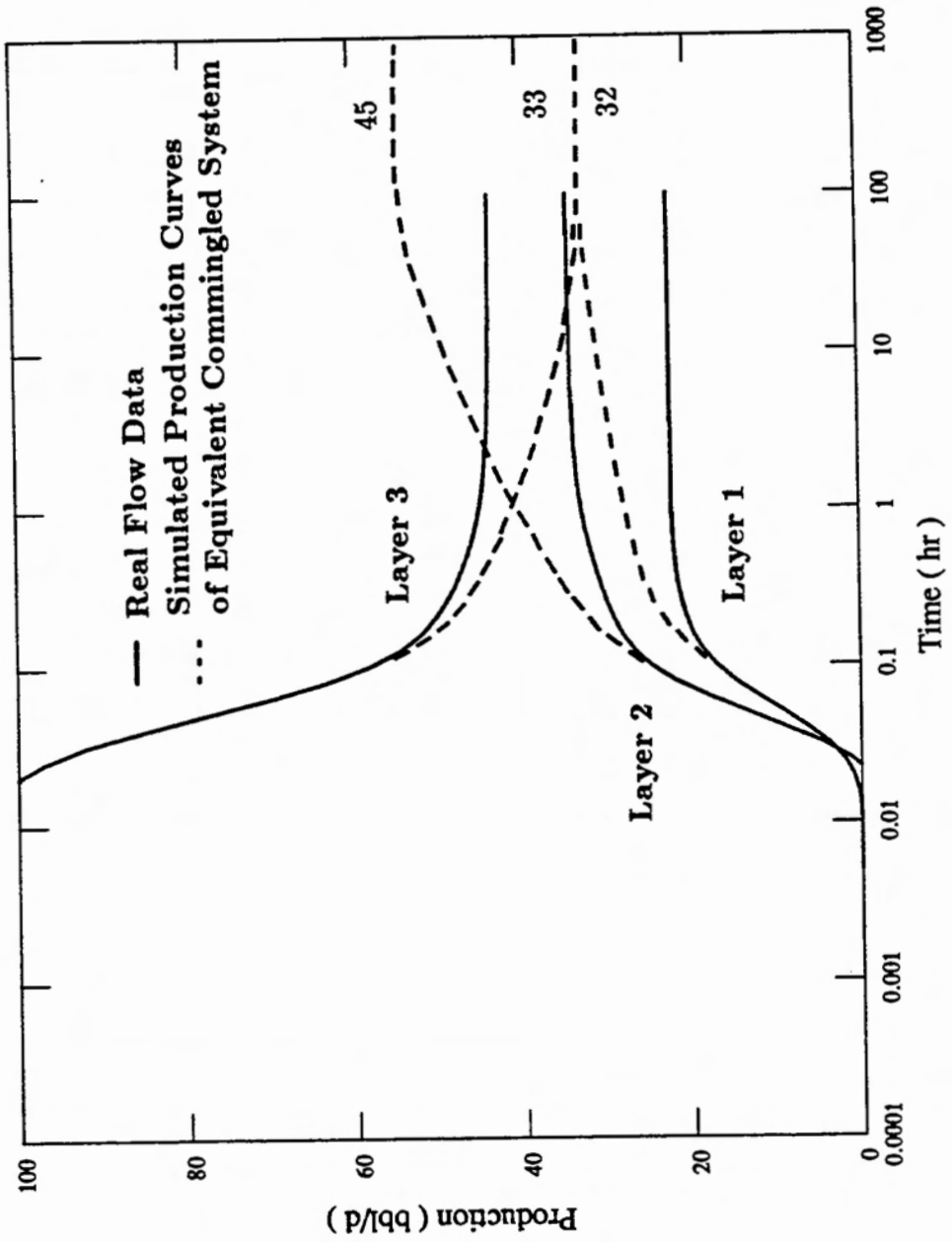

Figure 4.10: Production Rate from Each Layer and Simulated Production Curves for Example 3 of Parameter Estimation Using the Second Method

Table 4.9: Reservoir Parameters for Example 3 of Initial Estimation Using the Second Method

Layer	k(md)	k_v(md)	s	h(ft)	ϕ
1	180	180	-1	10	0.3
2	100	100	-2	20	0.1
3	70	70	-3	10	0.2
q_t = 100 (bbl/day) μ = 50 (cp) c_t=0.000006(1/psi) r_w=0.301 (ft)					

Table 4.10: Estimation Procedure for Example 3 Using the Second Method

Layer	q_j^{LT} (bpd)	κ^*	k^*(md)	s_j^*
1	22.21	0.32	144.0	-1.19
2	34.16	0.45	102.0	-1.27
3	43.63	0.33	99.0	-3.40
$*$ means the estimation				

The fractional production rate of the commingled system at very late time can be taken as the productivity ratio of the layer and the permeability of each layer can be determined by knowing the formation thickness. Using the late time production rate and the estimated productivity ratio of each layer, determine initial estimates for the skin factors. These estimates for permeability and skin were named as "Initial Estimates A" and summarized in Table 4.10.

Again, make "Initial Estimates B" for study of the effect of poor estimation. Each set was tested twice with and without analysis of the production rates together. The results for the test are shown in Table 4.11.

When the layer production rates were analyzed together with proper weighting constant, Initial Estimates A converged to the correct reservoir parameter values. However, the other cases did not approach to the correct parameters. This again emphasizes the importance of coupling the production data in the analysis of well

Table 4.11: The Results of Parameter Estimation for Example 3

Original Parameter Values					
k_1	180.0	(md)	s_1	-1.0	
k_2	100.0	(md)	s_2	-2.0	
k_3	70.0	(md)	s_3	-3.0	
Initial Estimates A					
k_1	144.0	(md)	s_1	-1.19	
k_2	102.0	(md)	s_2	-1.27	
k_3	99.0	(md)	s_3	-3.40	
With Weighting on Production Rates After 5_{th} Iteration					
k_1	179.5	(md)	s_1	-1.014	
k_2	99.9	(md)	s_2	-2.041	
k_3	70.0	(md)	s_3	-3.000	
Without Weighting on Production Rates No Convergence					
Initial Estimates B					
With Weighting on Production Rates No Convergence					
Without Weighting on Production Rates No Convergence					

test data of a multilayered reservoir.

Chapter 5

Conclusion

1. A multilayered system with formation crossflow responds to the production in three progressive stages. It behaves like a commingled system at early time and like an equivalent homogeneous system at late time (the semilog straight line in the pressure curve). Transition occurs in the intermediate stage.

2. Due to the transition phenomenon, a small concavity develops in the derivative of the pressure, the location of whose minimum point is identical to the inflection point of the pressure curve in the intermediate stage. It is also identical to the crossing point of the pressure curves of the commingled system and the homogeneous system in case the concavity does not develop because of the small skin factor of the less permeable layer.

3. The initiation and the termination of the transition is governed only by the vertical permeabilities. The transition occurs earlier when the vertical permeabilities of the system is larger and advances inversely proportional to the magnitude of the vertical permeability in logarithmic time scale.

4. The direction of the crossflow is governed first by the permeabilities and next by the skin factors. The crossflow starts from the less permeable layer to the more permeable layer in the beginning and from the layer with greater skin to the layer with smaller skin later.

5. Outer boundary conditions do not affect the production response of each layer as long as the transition terminates before the system feels the boundary. If the system feels the outer boundary before the transition is over, the production rate of a layer changes depending on the outer boundary condition. Under constant pressure conditions, the production rates are identical to the production rates of the system of infinite reservoir size, but reach earlier to the value. Under no flow conditions, the production rates are different from those of the infinite system.

6. By comparison of the sand face rate of a layer with the total sand face rate, we can eliminate the wellbore storage effect in the rate response of the multilayered crossflow system. By comparing the original production of the layer with the production rate with eliminated wellbore storage effect, we can determine the storage coefficient. And by knowing the storage coefficient, we can construct the pressure curve with no wellbore storage effect.

7. The order of layer changes the wellbore response in the intermediate and at late time by affecting λ, the parameter representing the crossflow, between two adjacent layers. However, the difference is negligible unless the heterogeneity of the system is very large.

8. At early time, the layer production rate becomes constant and is determined by the fraction of the ratio $\frac{\kappa_j}{s_j}$ over the summation of the ratios for all the layers, when all layers have non-zero skin. If all layers have zero skin, the production rate is determined by the fraction of the ratio $\sqrt{\omega_j \kappa_j}$ over the summation of the ratios for all the layers. As a general case when some of the layers have non-zero skin and the others have zero skin, the layers of non-zero skin produce nothing at very early time and the other layers produce according to the fraction of the ratio $\sqrt{\omega_j \kappa_j}$ over the summation of the ratios of the layers with zero skin.

9. At late time, all layers produce at constant rates determined by the radial permeabilities, the vertical permeabilities and skin factors. In particular, when all the layers have skin factors of the same magnitude, then the ratio is exactly

the same as the productivity ratio. In the two layer case, the layer with smaller skin produces more than the productivity ratio and vice versa. Thus, the production curve is an S-shaped curve whose early time limit and late time limit are constant.

10. At late time, the pressure response is the same as that of the equivalent homogeneous system (the semilog straight line part). Besides, the vertical pressure difference between layers becomes constant. Especially, in two layer systems, the pressure difference between layer 1 and layer 2, ($\Delta p_D = p_{D1} - p_{D2}$), becomes positively constant when layer 1 has smaller skin and negatively constant when layer 1 has bigger skin than the average skin of the system. When the skins of the two layers are of the same magnitude, then there is no vertical pressure difference and no crossflow between layers.

11. Two new methods for the initial estimation for the unknown reservoir parameters were suggested and tested for the multilayered crossflow system. This part may be significant since there is little study in the junction of the qualitative description of the multilayered system and the quantitative analysis of the automated well test without explaining the reason for the initial estimates for the unknown reservoir parameters.

12. The first method works for the isotropic two layered crossflow system, where the required data are the production history of the wellbore pressure and one time measurement of the production rate from any layer at late time.

13. The second method requires the pressure and the layer production data for the entire time range. Three possible methods for the data acquisition were described. This method works best in multilayered system with no formation crossflow, although the example was for the crossflow system. It works better if the vertical permeabilities of the layers are smaller, where we can obtain a longer portion of the data at early time and at intermediate time, needed in the constructing the production history of each layer.

Chapter 6

Nomenclature

$\underline{\underline{A}}$	Coefficient Matrix of Governing Equations	
$\underline{\underline{B}}$	Coefficient Matrix of Eigen-System	
$\underline{\underline{B'}}$	Modified Coefficient Matrix of Eigen-System	
$\underline{\underline{C}}$	Coefficient Matrix For	
	Functional Relationship Between A_j^k	
a, b	Proper Weighting Coefficient	
C	Storage Coefficient	psi/ft
c_t	Total Compressibility	psi^{-1}
$\overline{k}$	Average Permeability	md
k	Radial Permeability	md
k_v	Vertical Permeability	md
K, I	Modified Bessel Function	
h	Formation Thickness	ft
N_d	Number of Data	
N_l	Number of Layers	
N_p	Number of Parameters	
p_j	Pressure of Layer j	psi
p_{wf}	Wellbore Pressure	psi
Δp_D	Dimensionless Vertical Pressure Difference	

q_j	Production Rate from Layer j	bbl/day
q_t	Total Production Rate at the Wellhead	bbl/day
r	Radial Distance	ft
r_e	Outer Boundary Radius	ft
r_w	Wellbore Radius	ft
SSR	Objective Function	Sum of Square of Residuals
$\overline{s}$	Average Skin Factor	
s	Skin Factor	
t	Time	hr
t_D^*	The Most Diagnostic Point of the Transitional Phenomenon	
z	Vertical Distance or Laplacian Argument	ft
γ	Euler Constant	0.57722
κ	Dimensionless Productivity	
λ	Dimensionless Vertical Permeability	
μ	Viscosity	cp
ω	Dimensionless Storativity	
ϕ	Porosity	
σ^2	Eigenvalue of Matrix $\underline{\underline{B'}}$	
$\vec{\theta}$	A Set of Unknown Parameters	

	Subscripts		**Superscripts**
m	Measured	i	Initial
c	Calculated	LT	Late Time Limiting
j	Layer j	ET	Early Time Limiting
D	Dimensionless	$*$	Estimated

Bibliography

[1] Abramowitz, M., and Stegun, I. A.:"*Handbook of Mathematical Functions*," Dover Publications, Inc., New York (1970).

[2] Atkinson, K. E.:"*An Introduction to Numerical Analysis*," John Wiley and Sons, New York (1978).

[3] Bard, Y.:"*Nonlinear Parameter Estimation*," Academic Press, Inc. Ltd., New York, (1974).

[4] Barua, J., Horne, R. N., Greenstadt, J. L., and Lopez, L.:"Improved Estimation Algorithm for Automated Type-Curve Analysis of Well Tests," *SPE FE*, March (1988), 186-196.

[5] Bennett, C. O., Reynolds, A. C., and Raghavan, R.:"Analysis of Finite Conductivity Fractures Intercepting Multilayer Reservoir," *SPE FE*, June (1986), 259-274.

[6] Bourdet, D.:"Pressure Behavior of Layered Reservoirs with Crossflow,"SPE paper No. 13628, presented at the 55th Annual California Regional Meeting in Bakersfield, CA., Mar. 27-29, (1985).

[7] Bremer, R. E., Winston, H., and Vela, S.:"Analytical Model for Vertical Interference Tests Across Low-Permeability Zones," *Soc. Pet. Eng. J.*, (June 1985), 407-418.

[8] Camacho-V., R. G., Raghavan, R., Reynolds, A. C.:"Response of Wells Producing Layered Reservoirs: Unequal Fracture Length," SPE paper No. 12844 presented at the SPE/DOE/GRI Unconventional Gas Recovery Symposium, Pittsburgh, May 13-15, (1984).

[9] Chen, T.:"Pressure Drawdown in a Layered Reservoir with Linear Boundaries," SPE paper No. 16767, presented at the 62nd Annual Technical Conference and Exhibition in Dallas, TX., Sept. 27-30, (1987).

[10] Chu, W. C., and Raghavan, R.:"The Effect of Noncommunicating Layers on Interference Test Data," *J. Pet. Tech.*, Feb. (1981), 370-382.

[11] Coats, K. H., Dempsey, J. R., and Henderson, J. H.:"A New Technique for Determining Reservoir Description From Field Performance Data," *Soc. Pet. Eng. J.*, March (1970), 66-74, *Trans.*, AIME, **249**.

[12] Cobb, W. M., Ramey, H. J. Jr., and Miller, F. G.:"Well Test Analysis for Wells Producing Commingled Zones," *J. Pet. Tech.*, Jan. (1972), 27-37.

[13] Deans, H. A., and Gao, C-T.:"Pressure Transients and Crossflow in a Multilayer Reservoir: Single-Phase Flow," SPE paper No. 11966, presented at the 58th Annual Conference and Exhibition in San Francisco, CA., Oct. 5-8, (1983).

[14] Earlougher, R. C., Kersch, K. M., and Kunzman, W. J.:"Some Characteristics of Pressure Buildup Behavior in Bounded Multiple-Layered Reservoirs Without Crossflow," *J. Pet. Tech* Oct. (1974), 1178-1186.

[15] Ehlig-Economides, C. A., and Ayoub, J.:"Vertical Interference Testing Across a Low Permeability Zone," SPE paper No. 13251, presented at the 59th Annual Technical Conference and Exhibition in Houston, TX., Sep. 16-19 (1984).

[16] Ehlig-Economides, C. A., and Joseph, J. A.:"A New Test for Determination of Individual Layer Properties in a Multilayered Reservoir," SPE paper No. 14167, presented at 60th SPE Annual Technical Conference and Exhibition, Las Vegas, NV., Sept. 22-25 (1985).

[17] Gao, C-T.:"Single-Phase Fluid Flow in a Stratified Porous Medium with Crossflow," *Soc. Pet. Eng. J.*, Feb. (1984), 97-106.

[18] Gao, C-T.:"Crossflow Behavior in a Partially Perforated Two Layer Reservoir: the Evaluation of Reservoir Parameters by Transient Well Tests," SPE paper No. 11875, (1983 a).

[19] Gao, C-T.:" The Crossflow Behavior and the Determination of Reservoir Parameters by Drawdown Tests in Multilayer Reservoirs," SPE paper No. 12580, (1983 b).

[20] Gao, C-T., and Deans, H. A.:"Single-Phase Flow in a Two-Layer Reservoir with Significant Crossflow - Pressure Drawdown and Buildup Behavior When Both Layers are Completed at a Single Well," SPE paper No. 11874, (1983).

[21] Householder, A. S.:"*Principles of Numerical Analysis*," McGraw-Hill Book Co. Inc., New York (1953).

[22] Jacquard, P. and Jain, C.:"Permeability Distribution From Field Pressure Data," *Soc. Pet. Eng. J.*, Dec. (1965), 281-294.

[23] Jahns, H. O.:"A Rapid Method for Obtaining a Two-Dimensional Reservoir Description From Well Pressure Response Data," *Soc. Pet. Eng. J.*, Dec. (1966), 315-327, *Trans.*, AIME, **237**.

[24] Katz, M. L., and Tek, M. R.:" A Theoretical Study of Pressure Distribution and Fluid Flux in Bounded Stratified Porous Systems with Crossflow," *Soc. Pet. Eng. J.*, Mar. (1962), 68-82.

[25] Kazemi, H.:"Pressure Buildup in Reservoir Limit Testing of Stratified Systems." *J. Pet. Tech.*, Apr. (1970), 503-511.

[26] Kazemi, H., and Seth, M. S.:"Effect of Anisotropy and Stratification on Pressure Transient Analysis of Wells with Restricted Flow Entry," *J. Pet. Tech.* (May 1969), 639-647.

[27] Kucuk, F., Karakas, M., and Ayestaran, L.:"Well Test Analysis of Commingled Zones Without Crossflow," SPE paper No. 13081 presented at the 59th Annual Technical Conference and Exhibition in Houston, TX., Sep. 16-19 (1984).

[28] Kucuk, F., and Ayestaran, L.:"Analysis of Simultaneously Measured Pressure and Sandface Flow Rate in Transient Well Testing," *J. Pet. Tech.*, Feb. (1985), 323-334.

[29] Kucuk, F., Karakas, M., and Ayestaran, L.:"Well Testing and Analysis Techniques for Layered Reservoirs, " *SPE FE*, Aug. (1986), 342-354.

[30] Larsen, L.:"Wells Producing Commingled Zones with Unequal Initial Pressures and Reservoir Properties," SPE paper No. 10325, presented at the 56th Annual Technical Conference and Exhibition in San Antonio, TX., Oct 5-7 (1981).

[31] Larsen, L.:" Determination of Skin Factors and Flow Capacities of Individual Layers in Two-Layered Reservoirs," SPE paper No. 11138, presented at the 57th Annual Technical Conference and Exhibition in New Orleans, LA., Sep. 26-29 (1982).

[32] Lee, S. T., Chien, M. C. H., and Culham, W. E.:"Vertical Single-Well Testing of a Three-Layer Stratified Reservoir,"SPE paper No. 13249, presented at the 59th Annual Technical Conference and Exhibition in Houston, TX., Sep. 16-19 (1984).

[33] Lefkovits, H. C., Hazebroek, P., Allen, E. E., and Matthew, C. S.:"A Study of the Behavior of Bounded Reservoirs Composed of Stratified Layers," *Soc. Pet. Eng. J.* Mar. (1961), 43-58.

[34] Marquardt, D. W.: "An Algorithm for Least-Squares Estimation of Nonlinear Parameters," *J. Soc. Indust. Appl. Math.* vol. 11, No. 2, June (1963), 431-441.

[35] Meunier, D., Wittmann, M. J., and Stewart, G.:" Interpretation of Pressure Buildup Test Using In-Situ Measurement of Afterflow," *J. Pet. Tech.*, Jan. (1985), 143-152.

[36] Niko, H.:"Well Test Interpretation in Heterogeneous Reservoirs with Skin and Afterflow: Some New Theoretical Solutions and General Field Experience," SPE paper No. 11964, presented at the 58th Annual Conference and Exhibition in San Francisco, CA., Oct. 5-8 (1983).

[37] Pendergrass, J. D., and Berry, V. J.:"Pressure Transient Performance of a Multilayered Reservoir with Crossflow," *Soc. Pet. Eng. J.* , Dec. (1962), 347-354.

[38] Prats, M.:"Interpretation of Pulse Tests in Reservoirs with Crossflow Between Contiguous Layers," SPE paper No. 11963, presented at the 58th Annual Conference and Exhibition in San Francisco, CA., Oct. 5-8 (1983).

[39] Raghavan, R., Prijambodo, R., and Reynolds, A. C.:"Well Test Analysis for Wells Producing Layered Reservoirs with Crossflow,"*Soc. Pet. Eng. J.* June (1985), 407-418.

[40] Raghavan, R., Topaloglu, H. N., Cobb, W. M., and Ramey, H. J. Jr.:"Well-Test Analysis for Wells Producing From Two Commingled Zones of Unequal Thicknesss," *J. Pet. Tech.*, Sep. (1974), 1035-1043.

[41] Raghavan, R.:"Behavior of Wells Completed in Multiple Producing Zones," SPE paper No. 14111, presented at the SPE International Meeting, Beijing, March 17-20 (1986).

[42] Rosa, A. J., and Horne, R. N.:"Automated Type-Curve Matching in Well Test Analysis Using Laplace Space Determination of Parameters," SPE paper No. 12131, presented at the 58th Annual Technical Conference and Exhibition, San Francisco, CA., Oct. 5-8, (1983).

[43] Russell, D. G., and Prats, M.,:"Performance of Layered Reservoirs with Crossflow - Single-Compressible-Fluid Case," *Soc. Pet. Eng. J.*., Mar. (1962 a), 53-67.

[44] Russell, D. G., and Prats, M.:"The Practical Aspects of Interlayer Crossflow," *J. Pet. Tech.*, June (1962 b), 589-594.

[45] Shah, P. C., Karakas, M., Kucuk, F., and Ayestaran, L.:"Estimation of the Permeabilities and Skin Factors in Layered Reservoirs Using Downhole Rate and Pressure Data," SPE paper No. 14131, presented at the SPE International Meeting, Beijing, March 17-20 (1986).

[46] Stehfest, H.:"Algorithm 368, Numerical Inversion of Laplace Transforms," D-5 Communications of the ACM , vol. 13, No. 1 , Jan. (1970), 47-49.

[47] Streltsova, T.:"Buildup Analysis for Interference Tests in Stratified Formations," *J. Pet. Tech.*, Feb. (1984), 301-310

[48] Tempelaar-Leitz, W.:"Effect of Oil Production Rate on Performance of Wells Producing from More Than One Horizon," *Soc. Pet. Eng. J.*, Mar. (1961), 26-31.

[49] Tariq, S. M., and Ramey, H. J. Jr.:"Drawdown Behavior of a Well With Storage and Skin Effect Communicating With Layers of Different Radii and Other Characteristics," SPE paper No. 7453, presented at the 53rd Annual Technical Conference and Exhibition in Houston, TX., Oct 1-3 (1978)

[50] Woods, E. G.:"Pulse Test Response of a Two-Zone Reservoir," *Soc. Pet. Eng. J.*, Sep. (1970), 245-256.

Appendix A

N-Layered Crossflow System

The solutions for wellbore pressure and layer flow rate in a multilayered crossflow system are firstly developed for a two layered case by Bourdet (1985) and generalized for an N-layered case by Ehlig-Economides and Joseph (1985). The governing equation and all the conditions are transformed into Laplace space, and the solutions are sought and inversely transformed back to real space by the Stehfest (1970) algorithm.

Dimensionless variables and parameters are defined as follows:

$$p_{jD}(r_D, t_D) = \frac{2\pi(kh)_t}{q_t\mu}(p_i - p_j) \tag{A.1}$$

$$q_{jD}(t_D) = \frac{q_j}{q_t} = -\kappa_j \frac{\partial p_{jD}}{\partial r_D} \tag{A.2}$$

$$t_D = \frac{(kh)_t t}{(\phi h)_t \mu c_t r_w^2} \tag{A.3}$$

$$r_D = \frac{r}{r_w} \tag{A.4}$$

$$r_{eD} = \frac{r_e}{r_w} \tag{A.5}$$

$$\kappa_j = \frac{(kh)_j}{(kh)_t} \tag{A.6}$$

$$\omega_j = \frac{(\phi h)_j}{(\phi h)_t} \tag{A.7}$$

$$\lambda_{j+\frac{1}{2}} = \frac{r_w^2}{(kh)_t}\left(\frac{k_v}{h}\right)_{j+\frac{1}{2}} \tag{A.8}$$

$$C_D = \frac{C}{2\pi(\phi h)_t c_t r_w^2} \tag{A.9}$$

where:

$$(kh)_t = \sum_{j=1}^{n} k_j h_j \tag{A.10}$$

$$(\phi h)_t = \sum_{j=1}^{n} \phi_j h_j \tag{A.11}$$

The governing equations and the conditions in Chapter 2 are nondimensionalized as follows.

Governing equation:

$$\kappa_j \nabla^2 p_{jD} + \lambda_{j+\frac{1}{2}}(p_{j+1D} - p_{jD}) + \lambda_{j-\frac{1}{2}}(p_{j-1D} - p_{jD}) = \omega_j \frac{\partial p_{jD}}{\partial t_D} \tag{A.12}$$

Inner boundary condition for wellbore pressure:

$$p_{wD} = \left(p_{jD} - s_j \frac{\partial p_{jD}}{\partial r_D} \right) |_{r_D=1} \qquad (j = 1, \ldots, n) \tag{A.13}$$

Inner boundary condition for constant production rate at the wellhead:

$$1 = C_D \frac{dp_{wD}}{dt_D} - \sum_{j=1}^{n} \kappa_j \frac{\partial p_{jD}}{\partial r_D} |_{r_D=1} \tag{A.14}$$

Initial condition:

$$p_{jD}(r_D, 0) = 0 \tag{A.15}$$

Outer boundary conditions:

$$\lim_{r_D \to \infty} p_{jD}(r_D, t_D) = 0 \qquad \text{for infinite reservoir} \tag{A.16}$$

$$\frac{\partial p_{jD}}{\partial r_D}(r_{eD}, t_D) = 0 \qquad \text{for closed boundary} \tag{A.17}$$

$$p_{jD}(r_{eD}, t_D) = 0 \quad \text{for constant pressure outer boundary} \tag{A.18}$$

These nondimensionalized equations and the conditions are transformed into Laplace space as follows.

Governing equation:

$$\kappa_j \nabla^2 \overline{p_{jD}} + \lambda_{j+\frac{1}{2}}(\overline{p_{j+1D}} - \overline{p_{jD}}) + \lambda_{j-\frac{1}{2}}(\overline{p_{j-1D}} - \overline{p_{jD}}) = \omega_j z \overline{p_{jD}} \tag{A.19}$$

Inner boundary condition for wellbore pressure:

$$\overline{p_{wD}} = \left(\overline{p_{jD}} - s_j \frac{\partial \overline{p_{jD}}}{\partial r_D} \right) |_{r_D=1} \qquad (j = 1, \ldots, n) \tag{A.20}$$

Inner boundary condition for constant production rate at the wellhead:

$$\frac{1}{z} = C_D z \overline{p_{wD}} - \sum_{j=1}^{n} \kappa_j \frac{\partial \overline{p_{jD}}}{\partial r_D} |_{r_D=1} \tag{A.21}$$

Outer boundary conditions:

$$\lim_{r_D \to \infty} \overline{p_{jD}}(r_D, z) = 0 \qquad \text{for infinite reservoir} \tag{A.22}$$

$$\frac{\partial \overline{p_{jD}}}{\partial r_D}(r_{eD}, z) = 0 \qquad \text{for closed boundary} \tag{A.23}$$

$$\overline{p_{jD}}(r_{eD}, z) = 0 \quad \text{for constant pressure outer boundary} \tag{A.24}$$

As Bourdet (1985) mentioned, the solutions for this system are the modified Bessel function $I_0(\sigma r_D)$ and $K_0(\sigma r_D)$. Thus the dimensionless wellbore pressure and dimensionless production rate from layer j in Laplace space may be sought in the form of:

$$\overline{p_{jD}}(r_D, z) = A_j K_0(\sigma r_D) + B_j K_0(\sigma r_D) \tag{A.25}$$

$$\begin{aligned} \overline{q_{jD}} &= -\kappa_j \frac{\partial \overline{p_{jD}}}{\partial r_D} |_{r_D=1} \\ &= A_j \kappa_j \sigma K_1(\sigma) + B_j \kappa_j \sigma K_1(\sigma) \end{aligned} \tag{A.26}$$

Substitution of Eq. A.25 into Eq. A.19 results:

$$\begin{aligned} K_0(\sigma r_D) \left[\lambda_{j-\frac{1}{2}} A_{j-1} + (\kappa_j \sigma^2 - \omega_j z - \lambda_{j-\frac{1}{2}} - \lambda_{j+\frac{1}{2}}) A_j + \lambda_{j+\frac{1}{2}} A_{j+1} \right] \\ + I_0(\sigma r_D) \left[\lambda_{j+\frac{1}{2}} B_{j-1} + (\kappa_j \sigma^2 - \omega_j z - \lambda_{j+\frac{1}{2}} - \lambda_{j+\frac{1}{2}}) B_j + \lambda_{j+\frac{1}{2}} B_{j+1} \right] = 0 \\ (j = 1, \ldots, n) \end{aligned} \tag{A.27}$$

These N homogeneous equations can be expressed in the matrix form as follows:

$$\underline{\underline{A}} . \vec{X} = 0 \tag{A.28}$$

where $\underline{\underline{A}}$ is a symmetric tridiagonal matrix:

$$\underline{\underline{A}} \equiv \begin{bmatrix} a_{11} & a_{12} & \dots & \dots & a_{1n} \\ a_{11} & a_{22} & a_{23} & \dots & a_{2n} \\ \vdots & \vdots & \vdots & \vdots & \vdots \\ a_{n-1,1} & \dots & a_{n-1,n-2} & a_{n-1,n-1} & a_{n-1,n} \\ a_{n,1} & \dots & \dots & a_{n,n-1} & a_{n,n} \end{bmatrix} \tag{A.29}$$

and each element a_{jk} in matrix $\underline{\underline{A}}$ is:

$$a_{jk} = \begin{bmatrix} \lambda_{j-\frac{1}{2}} & \text{for } k = j-1 (j > 1) \\ \kappa_j \sigma_2 - \omega_j z - \lambda_{j-\frac{1}{2}} + \lambda_{j+\frac{1}{2}} & \text{for } k = j \\ \lambda_{j+\frac{1}{2}} & \text{for } k = j+1 (j < n) \\ 0 & \text{for other elements} \end{bmatrix} \tag{A.30}$$

and $\vec{X}$ is a vector defined as:

$$\vec{X} = \begin{bmatrix} A_1 K_0(\sigma r_D) + B_1 I_0(\sigma r_D) \\ \vdots \\ A_j K_0(\sigma r_D) + B_j I_0(\sigma r_D) \\ \vdots \\ A_n K_0(\sigma r_D) + B_n I_0(\sigma r_D) \end{bmatrix} \tag{A.31}$$

For the system to have a nontrivial solutions, the determination of matrix $\underline{\underline{A}}$ must be zero:

$$\det \underline{\underline{A}}(\sigma) = 0 \tag{A.32}$$

To find σ in $\underline{\underline{A}}$ that satisfies Eq. A.32 is equivalent to find eigenvalues in N by N matrix $\underline{\underline{B'}}$, whose elements may be defined as:

$$b'_{jk} = \begin{bmatrix} -\frac{\lambda_{j-\frac{1}{2}}}{\kappa_j} & k = j-1 (j > 1) \\ \frac{\omega_j z + \lambda_{j+\frac{1}{2}}}{\kappa_j} & k = j \\ -\frac{\lambda_{j+\frac{1}{2}}}{\kappa_j} & k = j+1 (j < n) \\ 0 & \text{for other elements} \end{bmatrix} \tag{A.33}$$

The matrix $\underline{\underline{B'}}$ is asymmetric matrix, and jeopardizes the necessity for the system to have N real eigenvalues. Fortunately, the determinant of asymmetric tridiagonal matrix $\underline{\underline{B'}}$ is identical to the determinant of the N by N symmetric matrix $\underline{\underline{B}}$, whose elements are defined as:

$$b_{jk} = \begin{bmatrix} -\frac{\lambda_{j-\frac{1}{2}}}{\sqrt{\kappa_{j-1}\kappa_j}} & k = j-1 (j > 1) \\ \frac{\omega_j z + \lambda_{j+\frac{1}{2}}}{\kappa_j} & k = j \\ -\frac{\lambda_{j+\frac{1}{2}}}{\sqrt{\kappa_j \kappa_{j+1}}} & k = j+1 (j < n) \\ 0 & \text{for other elements} \end{bmatrix} \tag{A.34}$$

Above argument can be proved by the fact that the determinant of a tridiagonal matrix can be expressed in the recursive form as follow:

$$\gamma_n = b_{n,n}\gamma_{n-1} - b_{n,n-1}b_{n-1,n}\gamma_{n-2} \tag{A.35}$$

where γ_n is the determinant of a tridiagonal matrix of order n, with $\gamma_0 = 1$ and $\gamma_1 = b_{1,1}$.

In Eq. A.35, the coefficient of the second term in the right hand side can be modified as:

$$\begin{aligned} b_{j,j-1}b_{j-1,j} &= \frac{\lambda_{j-\frac{1}{2}}}{\sqrt{\kappa_j\kappa_{j-1}}}\frac{\lambda_{j-\frac{1}{2}}}{\sqrt{\kappa_j\kappa_{j-1}}} \\ &= \frac{\lambda_{j-\frac{1}{2}}}{\kappa_j}\frac{\lambda_{j-\frac{1}{2}}}{\kappa_{j-1}} \\ &= b'_{j,j-1}b'_{j-1,j} \end{aligned} \tag{A.36}$$

Since the diagonal elements of the two matrices $\underline{\underline{B}}$ and $\underline{\underline{B'}}$ are the same, the eigenvalues for the matrices are also the same. Because the matrix $\underline{\underline{B}}$ is symmetric, the eigenvalues are all real, which is what we want.

Even if the system has such a simplicity as the tridiagonal symmetric matrix like $\underline{\underline{B}}$, there is no general solution in a closed form for the eigenvalues. However, the eigenproblem may be solved numerically. In this study, the subroutine SYMEIG.F is used to solve for the eigenvalues for the N by N tridiagonal symmetric matrix.

Once all the eigenvalues are found, then the general solution for the dimensionless pressure in layer j can be expressed as:

$$\overline{p_{jD}} = \left[\sum_{k=1}^{n} A_j^k K_0(\sigma_k r_D) + B_j^k I_0(\sigma_k r_D)\right] \tag{A.37}$$

The total numbers of coefficients, A_j^k and B_j^k, are $2n^2$ whereas we have only $2n$ inner and outer boundary conditions. As Ehlig-Economides and Joseph (1985) showed, the functional relationship between coefficients must be exploited. The outer boundary condition reduces the number of unknowns by half, since there is a relationship between A_j^k and B_j^k for each eigenvalues for each layer:

$$B_j^k = b^k A_j^k \tag{A.38}$$

where:

$$b_k = \left\{ \begin{array}{ll} 0 & \text{for the infinity outer boundary condition} \\ \frac{K_1(\sigma_k r_{eD})}{I_1(\sigma_k r_{eD})} & \text{for no flow outer boundary condition} \\ -\frac{K_0(\sigma_k r_{eD})}{I_0(\sigma_k r_{eD})} & \text{for constant pressure outer boundary condition} \end{array} \right\} \tag{A.39}$$

Thus the dimensionless pressure in layer j may be simplified as:

$$\overline{p_{jD}} = \sum_{k=1}^{n} A_j^k \left[K_0(\sigma_k r_D) + b^k I_0(\sigma_k r_D)\right] \tag{A.40}$$

For each eigenvalue σ_k, we have $(N-1)$ functional relationships:

$$0 = \underline{\underline{A}}(\sigma_k).\left[\begin{array}{c} A_1^k \left\{K_0(\sigma_k r_D) + b^k I_0(\sigma_k r_D)\right\} \\ A_2^k \left\{K_0(\sigma_k r_D) + b^k I_0(\sigma_k r_D)\right\} \\ \vdots \\ A_n^k \left\{K_0(\sigma_k r_D) + b^k I_0(\sigma_k r_D)\right\} \end{array}\right] \tag{A.41}$$

Thus the A_j^k can be expressed in terms of A_1:

$$\begin{array}{rcccl} A_2^k & = & -\frac{a_{11}}{a_{12}} A_1^k & = & \alpha_2^k A_1^k \\ A_3^k & = & -\frac{1}{a_{23}}(a_{21} A_1^k + a_{22} A_2^k) & = & \alpha_3^k A_1^k \\ & & \vdots & & \\ A_n^k & = & -\frac{1}{a_{n,n}}(a_{n,n-1} A_{n-1}^k) & = & \alpha_n^k A_1^k \end{array} \tag{A.42}$$

After solving for each eigenvalue, we have only N unknown coefficients, A_1^k for $k = 1, \ldots, n$, which can be solved using N inner boundary conditions.

The equation for the dimensionless pressure is now:

$$\overline{p_{jD}} = \sum_{k=1}^{n} \alpha_j^k A_1^k \left\{ K_0(\sigma_k r_D) + b^k I_0(\sigma_k r_D) \right\} \tag{A.43}$$

Inner boundary conditions are applied to solve the last N unknown coefficients, $A_1^k (k = 1, \ldots, n)$, using the following N equations.

$$\overline{p_{jD}} - s_j \frac{\partial \overline{p_{jD}}}{\partial r_D}|_{r_D=1} = \overline{p_{j+1D}} - s_{j+1} \frac{\partial \overline{p_{j+1D}}}{\partial r_D}|_{r_D=1} \tag{A.44}$$

$$\frac{1}{z} = C_D z \overline{p_{wD}} - \sum_{j=1}^{n} \kappa_j \frac{\partial \overline{p_{jD}}}{\partial r_D}|_{r_D=1} \tag{A.45}$$

Once we solve for the N coefficients of A_1^k, then we can also solve for A_j^k using Eq. A.42. Combining with the eigenvalues sought from the subroutine SYMEIG.F, we have the expression for the pressure and the sand face production rate for each layer as in Eq. A.25 and Eq. A.26:

$$\overline{p_{jD}}(r_D, z) = A_j K_0(\sigma r_D) + B_j K_0(\sigma r_D) \tag{A.46}$$

$$\begin{aligned} \overline{q_{jD}} &= -\kappa_j \frac{\partial \overline{p_{jD}}}{\partial r_D}|_{r_D=1} \\ &= A_j \kappa_j \sigma K_1(\sigma) + B_j \kappa_j \sigma K_1(\sigma) \end{aligned} \tag{A.47}$$

Wellbore pressure is determined using A.20.

$$\overline{p_{wD}} = \left(\overline{p_{jD}} - s_j \frac{\partial \overline{p_{jD}}}{\partial r_D} \right) |_{r_D=1} \qquad (j = 1, \ldots, n) \tag{A.48}$$

These solutions sought in Laplace domain are inversely transformed into real domain numerically using the Stehfest algorithm.

Appendix B

Infinite Commingled System

This part shows the derivation of the analytical solution for the pressure and the prodution rate from each layer for the infinitely large N-layered commingled system. The solution is a simplified form of the solution of Lefkovits, *et al.* (1961) as it is derived in terms of dimensionless variables and parameters, especially for the infinite system. For the definition of the dimensionless terms, refer to Appendix A.

The governing equation is the same as that in Appendix A, except that all λ's , which represent the crossflow effect between layers, are zero:

$$\kappa_j \nabla^2 p_{jD} = \omega_j \frac{\partial p_{jD}}{\partial t_D} \tag{B.1}$$

Inner boundary conditions are:

$$p_{wD} = p_{jD} - s_j \frac{\partial p_{jD}}{\partial r_D}|_{r_D=1} \tag{B.2}$$

$$1 = C_D \frac{dp_{wD}}{dt_D} - \sum_{j=1}^{n} \kappa_j \frac{\partial p_{jD}}{\partial r_D} \tag{B.3}$$

Outer boundary condition is:

$$\lim_{r_D \to \infty} p_{jD}(r_D, t_D) = 0 \tag{B.4}$$

These nondimensionalized equations are transformed into Laplace domain first. The governing equation is then:

$$\kappa_j \nabla^2 \overline{p_{jD}} = \omega_j z \overline{p_{jD}} \tag{B.5}$$

Inner boundary conditions become:

$$\overline{p_{wD}} = \overline{p_{jD}} - s_j \frac{\partial \overline{p_{jD}}}{\partial r_D}|_{r_D=1} \qquad (j = 1, \ldots, n) \tag{B.6}$$

$$\frac{1}{z} = C_D z p_{wD} - \sum_{j=1}^{n} \kappa_j \frac{\partial \overline{p_{jD}}}{\partial r_D} \tag{B.7}$$

Outer boundary condition is:

$$\lim_{r_D \to \infty} \overline{p_{jD}}(r_D, t_D) = 0 \tag{B.8}$$

The suggested solutions for these n equations are the combination of the modified Bessel functions (K_0 and I_0):

$$\overline{p_{jD}} = A_j K_0(\sigma_j r_D) + B_j I_0(\sigma_j r_D) \tag{B.9}$$

To satisfy the outer boundary condition, the coefficient B_j must be zero. Thus the solution for the pressure in layer j becomes:

$$\overline{p_{jD}} = A_j K_0(\sigma_j r_D) \tag{B.10}$$

Substitution of Eq. B.10 into Eq. B.5 results:

$$\kappa_j \sigma_j^2 K_0(\sigma_j r_D) = \omega_j K_0(\sigma_j r_D) \tag{B.11}$$

Solve for σ_j:

$$\sigma_j = \sqrt{\frac{\omega_j z}{\kappa_j}} \tag{B.12}$$

Then the solution for the production rate from layer j becomes:

$$\begin{aligned} \overline{q_{jD}} &= -\kappa_j \frac{\partial \overline{p_{jD}}}{\partial r_D}|_{r_D=1} \\ &= A_j \kappa_j \sigma_j K_1(\sigma_j) \end{aligned} \tag{B.13}$$

and wellbore pressure becomes:

$$\begin{aligned} \overline{p_{wD}} &= \overline{p_{jD}} - s_j \frac{\partial \overline{p_{jD}}}{\partial r_D}|_{r_D=1} \qquad (j = 1, \ldots, n) \\ &= A_j \left[K_0(\sigma_j) + s_j \sigma_j K_1(\sigma_j) \right] \end{aligned} \tag{B.14}$$

We can decide A_j from Eq. B.14:

$$A_j = \frac{\overline{p_{wD}}}{K_0(\sigma_j) + s_j \sigma_j K_1(\sigma_j)} \tag{B.15}$$

Substitute Eq. B.15 into Eq. B.7, the other inner boundary condition for the constant total production rate at the wellhead:

$$\begin{aligned} \frac{1}{z} &= C_D z \overline{p_{wD}} + \sum_{j=1}^{n} A_j \kappa_j \sigma_j K_1(\sigma_j) \\ &= C_D z \overline{p_{wD}} + \sum_{j=1}^{n} \frac{\kappa_j \sigma_j K_1(\sigma_j) \overline{p_{wD}}}{K_0(\sigma_j) + s_j \sigma_j K_1(\sigma_j)} \end{aligned} \tag{B.16}$$

Finally, the desired solution of wellbore pressure in an infinitely large commingled system becomes:

$$\overline{p_{wD}} = \frac{1}{z \left[C_D z + \sum_{j=1}^{n} \frac{\kappa_j \sigma_j K_1(\sigma_j)}{K_0(\sigma_j) + s_j \sigma_j K_1(\sigma_j)} \right]} \tag{B.17}$$

and the solution for the production rate from layer j becomes:

$$\begin{aligned} \overline{q_{jD}} &= -\kappa_j A_j \sigma_j K_1(\sigma_j) \\ &= \frac{\kappa_j \sigma_j K_1(\sigma_j) \overline{p_{wD}}}{K_0(\sigma_j) + s_j \sigma_j K_1(\sigma_j)} \end{aligned} \tag{B.18}$$

Appendix C

Two Layered Crossflow System

This part is the derivation of the solutions for wellbore pressure and the production rate from each layer for a two layered crossflow system, done by Bourdet (1985). The solutions are first sought in Laplace domain in terms of dimensionless variables and parameters, and numerically inverse transformed into real space. For the definition of the dimensionless terms, refer to Appendix A.

The governing equations are:

$$\kappa_1 \nabla^2 p_{1D} + \lambda(p_{2D} - p_{1D}) = \omega_1 \frac{\partial p_{1D}}{\partial t_D} \tag{C.1}$$

$$\kappa_2 \nabla^2 p_{2D} - \lambda(p_{2D} - p_{1D}) = \omega_2 \frac{\partial p_{2D}}{\partial t_D} \tag{C.2}$$

Inner boundary conditions are:

$$\begin{aligned} p_{wD} &= p_{1D} - s_1 \frac{\partial p_{1D}}{\partial r_D} \\ &= p_{2D} - s_2 \frac{\partial p_{2D}}{\partial r_D} \end{aligned} \tag{C.3}$$

$$1 = C_D \frac{dp_{wD}}{dt_D} - \kappa_1 \frac{\partial p_{1D}}{\partial r_D}|_{r_D=1} - \kappa_2 \frac{\partial p_{2D}}{\partial r_D}|_{r_D=1} \tag{C.4}$$

Outer boundary conditions are:

$$\lim_{r_D \to \infty} p_{jD} = 0 \qquad \text{infinite reservoir} \tag{C.5}$$

$$\frac{\partial p_{jD}}{\partial r_D}|_{r_D=r_{eD}} = 0 \qquad \text{no flow boundary} \tag{C.6}$$

$$p_{jD}(r_{eD}, t_D) = 0 \quad \text{constant pressure boundary} \tag{C.7}$$

Initial condition is:

$$p_{jD}(r_D, 0) = 0 \tag{C.8}$$

Laplace transformation of the above equations yields the following.

Governing equations are:

$$\kappa_1 \nabla^2 \overline{p_{1D}} + \lambda(\overline{p_{2D}} - \overline{p_{1D}}) = \omega_1 z \overline{p_{1D}} \tag{C.9}$$

$$\kappa_2 \nabla^2 \overline{p_{2D}} - \lambda(\overline{p_{2D}} - \overline{p_{1D}}) = \omega_2 z \overline{p_{2D}} \tag{C.10}$$

Inner boundary conditions are:

$$\begin{aligned} \overline{p_{wD}} &= \overline{p_{1D}} - s_1 \frac{\partial \overline{p_{1D}}}{\partial r_D} \\ &= \overline{p_{2D}} - s_2 \frac{\partial \overline{p_{2D}}}{\partial r_D} \end{aligned} \tag{C.11}$$

$$\frac{1}{z} = C_D z \overline{p_{wD}} - \kappa_1 \frac{\partial \overline{p_{1D}}}{\partial r_D}|_{r_D=1} - \kappa_2 \frac{\partial \overline{p_{2D}}}{\partial r_D}|_{r_D=1} \tag{C.12}$$

Outer boundary conditions are:

$$\lim_{r_D \to \infty} \overline{p_{jD}} = 0 \qquad \text{infinite reservoir} \tag{C.13}$$

$$\frac{\partial \overline{p_{jD}}}{\partial r_D}|_{r_D=r_{eD}} = 0 \qquad \text{no flow boundary} \tag{C.14}$$

$$\overline{p_{jD}}(r_{eD}, z) = 0 \quad \text{constant pressure boundary} \tag{C.15}$$

The suggested form for the pressure is:

$$\overline{p_{1D}} = A_j K_0(\sigma r_D) + B_j I_0(\sigma r_D) \tag{C.16}$$

Substitution of Eq. C.16 into Eq. C.9 and Eq. C.10 yields

$$\kappa_1 \sigma^2 \overline{p_{1D}} = \omega_1 z \overline{p_{1D}} - \lambda(\overline{p_{2D}} - \overline{p_{1D}}) \tag{C.17}$$

$$\kappa_2 \sigma^2 \overline{p_{2D}} = \omega_2 z \overline{p_{2D}} + \lambda(\overline{p_{2D}} - \overline{p_{1D}}) \tag{C.18}$$

By rearrangement:

$$\left(\kappa_1 \sigma^2 - \omega_1 z - \lambda\right) \overline{p_{1D}} + \lambda \overline{p_{2D}} = 0 \tag{C.19}$$

$$\lambda \overline{p_{1D}} + \left(\kappa_2 \sigma^2 - \omega_2 z - \lambda\right) \overline{p_{2D}} = 0 \tag{C.20}$$

For Eq. C.19 and Eq. C.20 to have non-trivial solution:

$$\det \begin{vmatrix} (\kappa_1\sigma^2 - \omega_1 z - \lambda) & \lambda \\ \lambda & (\kappa_2\sigma^2 - \omega_2 z - \lambda) \end{vmatrix} = 0 \tag{C.21}$$

Solving for σ^2 that satisfies Eq. C.21:

$$(\kappa_1\sigma^2 - \omega_1 z - \lambda)(\kappa_2\sigma^2 - \omega_2 z - \lambda) - \lambda^2 = 0 \tag{C.22}$$

$$\kappa_1\kappa_2\sigma^4 - [\kappa_1(\omega_2 z + \lambda) + \kappa_2(\omega_1 z + \lambda)]\sigma^2 + (\omega_1 z + \lambda)(\omega_2 z + \lambda) - \lambda^2 = 0 \tag{C.23}$$

$$\sigma^4 - \left(\frac{\omega_1 z + \lambda}{\kappa_1} + \frac{\omega_2 z + \lambda}{\kappa_2}\right)\sigma^2 + \frac{(\omega_1 z + \lambda)(\omega_2 z + \lambda) - \lambda^2}{\kappa_1\kappa_2} = 0 \tag{C.24}$$

Then, we will have two different values for σ^2:

$$\sigma_1^2 = \frac{1}{2}\left[\frac{\omega_1 z + \lambda}{\kappa_1} + \frac{\omega_2 z + \lambda}{\kappa_2} - \Delta\right] \tag{C.25}$$

$$\sigma_2^2 = \frac{1}{2}\left[\frac{\omega_1 z + \lambda}{\kappa_1} + \frac{\omega_2 z + \lambda}{\kappa_2} + \Delta\right] \tag{C.26}$$

where Δ is:

$$\begin{aligned} \Delta &= \sqrt{\left[\frac{\omega_1 z + \lambda}{\kappa_1} + \frac{\omega_2 z + \lambda}{\kappa_2}\right]^2 - 4\frac{(\omega_1 z + \lambda)(\omega_2 z + \lambda) - \lambda^2}{\kappa_1\kappa_2}} \\ &= \sqrt{\left[\frac{\omega_1 z + \lambda}{\kappa_1} - \frac{\omega_2 z + \lambda}{\kappa_2}\right]^2 + \frac{4\lambda^2}{\kappa_1\kappa_2}} > 0 \end{aligned} \tag{C.27}$$

By superposition, the equations for the pressure in the layers become:

$$\overline{p_{1D}} = A_1^1 K_0(\sigma_1 r_D) + A_1^2 K_0(\sigma_2 r_D) + B_1^1 I_0(\sigma_1 r_D) + B_1^2 I_0(\sigma_2 r_D) \tag{C.28}$$

$$\overline{p_{2D}} = A_2^1 K_0(\sigma_1 r_D) + A_2^2 K_0(\sigma_2 r_D) + B_2^1 I_0(\sigma_1 r_D) + B_2^2 I_0(\sigma_2 r_D) \tag{C.29}$$

The coefficients A and B have the following relations.

$$\begin{aligned} A_2^1 &= a_1 A_1^1 \\ A_2^2 &= a_2 A_1^2 \\ B_2^1 &= a_1 B_1^1 \\ B_2^2 &= a_2 B_1^2 \end{aligned} \tag{C.30}$$

where:

$$\begin{aligned} a_1 &= -\frac{\kappa_1\sigma_1^2 - \omega_1 z - \lambda}{\lambda} \\ &= 1 + \frac{1}{\lambda}(\omega_1 z - \kappa_1\sigma_1^2) \end{aligned} \tag{C.31}$$

$$\begin{aligned} a_2 &= -\frac{\kappa_1\sigma_2^2 - \omega_1 z - \lambda}{\lambda} \\ &= 1 + \frac{1}{\lambda}(\omega_1 z - \kappa_1\sigma_2^2) \end{aligned} \tag{C.32}$$

From the outer boundary conditions, A_j^k have following relations with B_j^k:

$$B_j^k = b^k A_j^k \tag{C.33}$$

where:

$$b^k = 0 \qquad \text{infinite reservoir} \tag{C.34}$$

$$b^k = \frac{K_1(\sigma_k r_{eD})}{I_1(\sigma_k r_{eD})} \qquad \text{no flow boundary} \tag{C.35}$$

$$b^k = -\frac{K_0(\sigma_k r_{eD})}{I_0(\sigma_k r_{eD})} \qquad \text{constant pressure boundary} \tag{C.36}$$

Now, the equations for the layer pressure can be written as:

$$\overline{p_{1D}} = A_1^1[K_0(\sigma_1 r_D) + b^1 I_0(\sigma_1 r_D)] + A_1^2[K_0(\sigma_2 r_D) + b^2 I_0(\sigma_2 r_D)] \tag{C.37}$$

$$\overline{p_{2D}} = a_1 A_1^1[K_0(\sigma_1 r_D) + b^1 I_0(\sigma_1 r_D)] + a_2 A_1^2[K_0(\sigma_2 r_D) + b^2 I_0(\sigma_2 r_D)] \tag{C.38}$$

At this stage, we have two unknowns, A_1^1 and A_1^2, and two inner boundary conditions. Define X and Y as:

$$\begin{aligned} X_1 &= K_0(\sigma_1 r_D) + b^1 I_0(\sigma_1 r_D) \\ X_2 &= K_0(\sigma_2 r_D) + b^2 I_0(\sigma_2 r_D) \\ Y_1 &= \sigma_1[K_1(\sigma_1 r_D) - b^1 I_1(\sigma_1 r_D)] \\ Y_2 &= \sigma_2[K_1(\sigma_2 r_D) - b^2 I_1(\sigma_2 r_D)] \end{aligned} \tag{C.39}$$

Then:

$$\begin{aligned} \overline{p_{1D}} &= A_1^1 X_1 + A_1^2 X_2 \\ \overline{p_{2D}} &= a_1 A_1^1 X_1 + a_2 A_1^2 X_2 \end{aligned} \tag{C.40}$$

Substitute Eq. C.40 into the first inner boundary condition for wellbore pressure.

$$\overline{p_{1D}} - s_1 \frac{\partial p_{1D}}{\partial r_D}|_{r_D=1} = \overline{p_{2D}} - s_2 \frac{\partial p_{2D}}{\partial r_D}|_{r_D=1} \tag{C.41}$$

Then we have:

$$\begin{aligned} & A_1^1 \left([K_0(\sigma_1) + b^1 I_0(\sigma_1)] + s_1 \sigma_1 [K_1(\sigma_1) - b^1 I_1(\sigma_1)] \right) \\ + \; & A_1^2 \left([K_0(\sigma_2) + b^2 I_0(\sigma_2)] + s_1 \sigma_2 [K_1(\sigma_2) - b^2 I_1(\sigma_2)] \right) \\ = \; & a_1 A_1^1 \left([K_0(\sigma_1) + b^1 I_0(\sigma_1)] + s_2 \sigma_1 [K_1(\sigma_1) - b^1 I_1(\sigma_1)] \right) \\ + \; & a_2 A_1^2 \left([K_0(\sigma_2) + b^2 I_0(\sigma_2)] + s_2 \sigma_2 [K_1(\sigma_2) - b^2 I_1(\sigma_2)] \right) \end{aligned} \tag{C.42}$$

or using the definitions for X and Y:

$$\begin{aligned} & A_1^1 [X_1 + s_1 Y_1] + A_1^2 [X_2 + s_1 Y_2] \\ = \; & a_1 A_1^1 [X_1 + s_2 Y_1] + a_2 A_1^2 [X_2 + s_2 Y_2] \end{aligned} \tag{C.43}$$

By rearrangement:

$$0 = A_1^1 \left[(a_1 - 1) X_1 + (a_1 s_2 - s_1) Y_1 \right] + A_1^2 \left[(a_2 - 1) X_2 + (a_2 s_2 - s_1) Y_2 \right] \tag{C.44}$$

Solve for A_1^1:

$$A_1^1 = -A_1^2 \frac{(a_2 - 1) X_2 + (a_2 s_2 - s_1) Y_2}{(a_1 - 1) X_1 + (a_1 s_2 - s_1) Y_1} \tag{C.45}$$

Let us define E as:

$$E = -\frac{(a_1 - 1) X_1 + (a_1 s_2 - s_1) Y_1}{(a_2 - 1) X_2 + (a_2 s_2 - s_1) Y_2} \tag{C.46}$$

Then:

$$A_1^2 = E A_1^1 \tag{C.47}$$

Apply the second inner boundary condition for the constant total production rate at the well head with no wellbore storage effect for the moment.

$$\frac{1}{z} = -\kappa_1 \frac{\partial \overline{p_{1D}}}{\partial r_D}|_{r_D=1} - \kappa_2 \frac{\partial \overline{p_{2D}}}{\partial r_D}|_{r_D=1} \tag{C.48}$$

Using Eq. C.40 and Eq. C.47, we can modify Eq. C.48 as:

$$\begin{aligned}\frac{1}{z} &= \kappa_1\left(A_1^1Y_1 + A_1^2Y_2\right) + \kappa_2\left(a_1A_1^1Y_1 + a_2A_1^2Y_2\right) \\ &= \kappa_1A_1^1\left(Y_1 + EY_2\right) + \kappa_2A_1^1\left(a_1Y_1 + a_2EY_2\right)\end{aligned} \tag{C.49}$$

The only unknown A_1^1 can be determined as:

$$\begin{aligned}A_1^1 &= \frac{1}{z\left[\kappa_1\left(Y_1 + EY_2\right) + \kappa_2\left(a_1Y_1 + a_2EY_2\right)\right]} \\ &= \frac{1}{z\left[\left(\kappa_1 + a_1\kappa_2\right)Y_1 + \left(\kappa_1 + a_2\kappa_2\right)EY_2\right]}\end{aligned} \tag{C.50}$$

By defining F as:

$$F = \left(\kappa_1 + a_1\kappa_2\right)Y_1 + \left(\kappa_1 + a_2\kappa_2\right)EY_2 \tag{C.51}$$

we can have the following equations:

$$A_1^1 = \frac{1}{zF} \tag{C.52}$$

$$A_1^2 = \frac{E}{zF} \tag{C.53}$$

$$\overline{p_{1D}} = \frac{1}{zF}\left[X_1 + EX_2\right] \tag{C.54}$$

$$\overline{p_{2D}} = \frac{1}{zF}\left[a_1X_1 + a_2EX_2\right] \tag{C.55}$$

Then, the wellbore pressure with no wellbore storage effect becomes:

$$\overline{p_{wD,C_D=0}} = \frac{1}{zF}\left[X_1 + s_1Y_1 + E(X_2 + s_1Y_2)\right] \tag{C.56}$$

Now considering wellbore storage effect, the inner boundary condition becomes:

$$\begin{aligned}\frac{1}{z} - C_Dz\overline{p_{wD}} &= -\kappa_1\frac{\partial\overline{p_{1D}}}{\partial r_D}|_{r_D=1} - \kappa_2\frac{\partial\overline{p_{2D}}}{\partial r_D}|_{r_D=1} \\ &= A_1^1F\end{aligned} \tag{C.57}$$

Solving Eq. C.57 for wellbore pressure:

$$A_1^1 = \frac{1}{zF}\left(1 - C_Dz^2\overline{p_{wD}}\right) \tag{C.58}$$

$$\overline{p_{wD}} = \frac{1}{zF}\left(1 - C_Dz^2\overline{p_{wD}}\right)\left[X_1 + s_1Y_1 + E\left(X_2 + s_1Y_2\right)\right] \tag{C.59}$$

Using Eq. C.56:

$$\overline{p_{wD}} = \left(1 - C_D z^2 \overline{p_{wD}}\right) \overline{p_{wD,C_D=0}} \tag{C.60}$$

Finally, the wellbore pressure with the consideration of wellbore storage effect becomes:

$$\overline{p_{wD}} = \frac{1}{C_D z^2 + \frac{1}{\overline{p_{wD,C_D=0}}}} \tag{C.61}$$

and the sandface production rate from each layer is determined as:

$$\overline{q_{1D}} = \frac{\kappa_1}{zF}\left(1 - C_D z^2 \overline{p_{wD}}\right)[Y_1 + EY_2] \tag{C.62}$$

$$\overline{q_{2D}} = \frac{\kappa_2}{zF}\left(1 - C_D z^2 \overline{p_{wD}}\right)[a_1 Y_1 + a_2 EY_2] \tag{C.63}$$

Appendix D

Data for the First Method

t(hr)	p_{wf} (psi)	q_1(b/d)	q_2(b/d)
0.50000E-05	0.9482E+02	0.9674E+02	0.3251E+01
0.62946E-05	0.9748E+02	0.9666E+02	0.3330E+01
0.79244E-05	0.1003E+03	0.9658E+02	0.3415E+01
0.99762E-05	0.1034E+03	0.9649E+02	0.3506E+01
0.12559E-04	0.1068E+03	0.9639E+02	0.3602E+01
0.15811E-04	0.1103E+03	0.9629E+02	0.3704E+01
0.19905E-04	0.1142E+03	0.9618E+02	0.3811E+01
0.25059E-04	0.1183E+03	0.9607E+02	0.3923E+01
0.31547E-04	0.1226E+03	0.9596E+02	0.4039E+01
0.39716E-04	0.1272E+03	0.9584E+02	0.4160E+01
0.49999E-04	0.1320E+03	0.9571E+02	0.4283E+01
0.62945E-04	0.1370E+03	0.9559E+02	0.4409E+01
0.79244E-04	0.1423E+03	0.9546E+02	0.4536E+01
0.99762E-04	0.1478E+03	0.9533E+02	0.4664E+01
0.12559E-03	0.1535E+03	0.9520E+02	0.4792E+01
0.15811E-03	0.1594E+03	0.9508E+02	0.4919E+01
0.19905E-03	0.1654E+03	0.9495E+02	0.5044E+01
0.25059E-03	0.1716E+03	0.9483E+02	0.5166E+01
0.31547E-03	0.1780E+03	0.9471E+02	0.5285E+01
0.39715E-03	0.1845E+03	0.9459E+02	0.5400E+01
0.49999E-03	0.1911E+03	0.9448E+02	0.5511E+01

Table Continued

t(hr)	p_{wf} (psi)	q_1(b/d)	q_2(b/d)
0.62945E-03	0.1979E+03	0.9438E+02	0.5616E+01
0.79243E-03	0.2047E+03	0.9428E+02	0.5716E+01
0.99761E-03	0.2116E+03	0.9418E+02	0.5810E+01
0.12559E-02	0.2186E+03	0.9410E+02	0.5899E+01
0.15811E-02	0.2256E+03	0.9401E+02	0.5982E+01
0.19905E-02	0.2327E+03	0.9394E+02	0.6059E+01
0.25058E-02	0.2398E+03	0.9387E+02	0.6130E+01
0.31547E-02	0.2469E+03	0.9380E+02	0.6195E+01
0.39715E-02	0.2541E+03	0.9374E+02	0.6255E+01
0.49998E-02	0.2613E+03	0.9369E+02	0.6309E+01
0.62944E-02	0.2684E+03	0.9364E+02	0.6357E+01
0.79242E-02	0.2756E+03	0.9360E+02	0.6398E+01
0.99760E-02	0.2827E+03	0.9356E+02	0.6434E+01
0.12559E-01	0.2898E+03	0.9353E+02	0.6462E+01
0.15811E-01	0.2968E+03	0.9351E+02	0.6482E+01
0.19904E-01	0.3038E+03	0.9350E+02	0.6495E+01
0.25058E-01	0.3107E+03	0.9350E+02	0.6498E+01
0.31547E-01	0.3175E+03	0.9350E+02	0.6492E+01
0.39715E-01	0.3243E+03	0.9352E+02	0.6475E+01
0.49998E-01	0.3308E+03	0.9355E+02	0.6446E+01
0.62944E-01	0.3373E+03	0.9359E+02	0.6406E+01
0.79242E-01	0.3437E+03	0.9364E+02	0.6354E+01
0.99760E-01	0.3499E+03	0.9370E+02	0.6291E+01
0.12559E+00	0.3561E+03	0.9378E+02	0.6218E+01
0.15810E+00	0.3622E+03	0.9386E+02	0.6139E+01
0.19904E+00	0.3683E+03	0.9394E+02	0.6056E+01
0.25058E+00	0.3746E+03	0.9402E+02	0.5975E+01
0.31546E+00	0.3810E+03	0.9410E+02	0.5899E+01
0.39715E+00	0.3875E+03	0.9416E+02	0.5830E+01
0.49998E+00	0.3943E+03	0.9422E+02	0.5772E+01
0.62943E+00	0.4012E+03	0.9427E+02	0.5724E+01
0.79241E+00	0.4082E+03	0.9431E+02	0.5686E+01
0.99759E+00	0.4154E+03	0.9434E+02	0.5656E+01
0.12558E+01	0.4227E+03	0.9436E+02	0.5633E+01
0.15810E+01	0.4299E+03	0.9438E+02	0.5616E+01

Table Continued

t(hr)	p_{wf} (psi)	q_1(b/d)	q_2(b/d)
0.19904E+01	0.4373E+03	0.9439E+02	0.5603E+01
0.25058E+01	0.4446E+03	0.9440E+02	0.5592E+01
0.31546E+01	0.4520E+03	0.9441E+02	0.5584E+01
0.39714E+01	0.4593E+03	0.9442E+02	0.5578E+01
0.49997E+01	0.4667E+03	0.9442E+02	0.5573E+01
0.62943E+01	0.4741E+03	0.9443E+02	0.5569E+01
0.79241E+01	0.4814E+03	0.9443E+02	0.5566E+01
0.99758E+01	0.4888E+03	0.9443E+02	0.5564E+01
0.12558E+02	0.4962E+03	0.9443E+02	0.5562E+01
0.15810E+02	0.5036E+03	0.9443E+02	0.5561E+01
0.19904E+02	0.5110E+03	0.9444E+02	0.5559E+01
0.25058E+02	0.5184E+03	0.9444E+02	0.5558E+01
0.31546E+02	0.5258E+03	0.9444E+02	0.5558E+01
0.39714E+02	0.5332E+03	0.9444E+02	0.5557E+01
0.49997E+02	0.5405E+03	0.9444E+02	0.5557E+01
0.62943E+02	0.5479E+03	0.9444E+02	0.5556E+01
0.79240E+02	0.5553E+03	0.9444E+02	0.5556E+01
0.99757E+02	0.5627E+03	0.9444E+02	0.5556E+01
0.12558E+03	0.5701E+03	0.9444E+02	0.5556E+01
0.15810E+03	0.5775E+03	0.9444E+02	0.5555E+01
0.19904E+03	0.5849E+03	0.9444E+02	0.5555E+01
0.25057E+03	0.5923E+03	0.9444E+02	0.5555E+01
0.31546E+03	0.5997E+03	0.9444E+02	0.5555E+01
0.39714E+03	0.6071E+03	0.9444E+02	0.5555E+01
0.49997E+03	0.6145E+03	0.9444E+02	0.5555E+01
0.62942E+03	0.6218E+03	0.9444E+02	0.5555E+01
0.79239E+03	0.6292E+03	0.9444E+02	0.5555E+01
0.99757E+03	0.6366E+03	0.9444E+02	0.5555E+01
0.12558E+04	0.6440E+03	0.9444E+02	0.5555E+01
0.15810E+04	0.6514E+03	0.9444E+02	0.5555E+01
0.19904E+04	0.6588E+03	0.9444E+02	0.5555E+01
0.25057E+04	0.6662E+03	0.9444E+02	0.5555E+01
0.31545E+04	0.6736E+03	0.9444E+02	0.5555E+01
0.39713E+04	0.6810E+03	0.9444E+02	0.5555E+01
0.49996E+04	0.6884E+03	0.9444E+02	0.5555E+01

Appendix E

Data for Example 1

0.5000E-03	0.129E+03	0.476E+02	0.267E+02	0.196E+02	0.594E+01
0.6294E-03	0.131E+03	0.475E+02	0.263E+02	0.199E+02	0.614E+01
0.7924E-03	0.134E+03	0.474E+02	0.260E+02	0.202E+02	0.629E+01
0.9976E-03	0.137E+03	0.473E+02	0.257E+02	0.205E+02	0.642E+01
0.1255E-02	0.141E+03	0.473E+02	0.253E+02	0.207E+02	0.651E+01
0.1581E-02	0.144E+03	0.472E+02	0.250E+02	0.210E+02	0.659E+01
0.1990E-02	0.148E+03	0.472E+02	0.247E+02	0.213E+02	0.664E+01
0.2505E-02	0.152E+03	0.472E+02	0.244E+02	0.215E+02	0.667E+01
0.3154E-02	0.156E+03	0.472E+02	0.242E+02	0.218E+02	0.669E+01
0.3971E-02	0.159E+03	0.472E+02	0.239E+02	0.220E+02	0.670E+01
0.5000E-02	0.163E+03	0.472E+02	0.237E+02	0.222E+02	0.670E+01
0.6294E-02	0.167E+03	0.473E+02	0.235E+02	0.224E+02	0.669E+01
0.7924E-02	0.172E+03	0.473E+02	0.232E+02	0.227E+02	0.667E+01
0.9976E-02	0.176E+03	0.473E+02	0.230E+02	0.229E+02	0.665E+01
0.1255E-01	0.180E+03	0.473E+02	0.228E+02	0.230E+02	0.663E+01
0.1581E-01	0.184E+03	0.474E+02	0.226E+02	0.232E+02	0.660E+01
0.1990E-01	0.188E+03	0.474E+02	0.225E+02	0.234E+02	0.657E+01
0.2505E-01	0.192E+03	0.474E+02	0.223E+02	0.236E+02	0.654E+01
0.3154E-01	0.196E+03	0.475E+02	0.222E+02	0.237E+02	0.651E+01
0.3971E-01	0.200E+03	0.475E+02	0.220E+02	0.238E+02	0.647E+01
0.5000E-01	0.205E+03	0.476E+02	0.219E+02	0.239E+02	0.643E+01
0.6294E-01	0.209E+03	0.476E+02	0.218E+02	0.240E+02	0.639E+01
0.7924E-01	0.213E+03	0.477E+02	0.217E+02	0.241E+02	0.635E+01

Table Continued

t(hr)	p_{wf}(psi)	q_1(b/d)	q_2(b/d)	q_3(b/d)	q_4(b/d)
0.9976E-01	0.217E+03	0.477E+02	0.216E+02	0.242E+02	0.630E+01
0.1255E+00	0.221E+03	0.478E+02	0.216E+02	0.242E+02	0.625E+01
0.1581E+00	0.225E+03	0.478E+02	0.215E+02	0.243E+02	0.620E+01
0.1990E+00	0.229E+03	0.479E+02	0.215E+02	0.243E+02	0.615E+01
0.2505E+00	0.232E+03	0.480E+02	0.215E+02	0.243E+02	0.609E+01
0.3154E+00	0.236E+03	0.480E+02	0.214E+02	0.243E+02	0.604E+01
0.3971E+00	0.240E+03	0.481E+02	0.214E+02	0.243E+02	0.599E+01
0.5000E+00	0.244E+03	0.482E+02	0.214E+02	0.243E+02	0.594E+01
0.6294E+00	0.248E+03	0.483E+02	0.214E+02	0.243E+02	0.589E+01
0.7924E+00	0.252E+03	0.483E+02	0.214E+02	0.242E+02	0.585E+01
0.9976E+00	0.256E+03	0.484E+02	0.214E+02	0.242E+02	0.582E+01
0.1255E+01	0.260E+03	0.484E+02	0.214E+02	0.242E+02	0.580E+01
0.1581E+01	0.264E+03	0.485E+02	0.214E+02	0.242E+02	0.578E+01
0.1990E+01	0.268E+03	0.485E+02	0.214E+02	0.242E+02	0.576E+01
0.2505E+01	0.272E+03	0.485E+02	0.214E+02	0.242E+02	0.575E+01
0.3154E+01	0.276E+03	0.485E+02	0.214E+02	0.242E+02	0.574E+01
0.3971E+01	0.280E+03	0.486E+02	0.214E+02	0.242E+02	0.573E+01
0.5000E+01	0.284E+03	0.486E+02	0.214E+02	0.242E+02	0.573E+01
0.6294E+01	0.288E+03	0.486E+02	0.214E+02	0.242E+02	0.572E+01
0.7924E+01	0.292E+03	0.486E+02	0.214E+02	0.242E+02	0.572E+01
0.9976E+01	0.296E+03	0.486E+02	0.214E+02	0.241E+02	0.572E+01
0.1255E+02	0.300E+03	0.486E+02	0.214E+02	0.241E+02	0.572E+01
0.1581E+02	0.304E+03	0.486E+02	0.214E+02	0.241E+02	0.571E+01
0.1990E+02	0.308E+03	0.486E+02	0.214E+02	0.241E+02	0.571E+01
0.2505E+02	0.312E+03	0.486E+02	0.214E+02	0.241E+02	0.571E+01
0.3154E+02	0.316E+03	0.486E+02	0.214E+02	0.241E+02	0.571E+01
0.3971E+02	0.321E+03	0.486E+02	0.214E+02	0.241E+02	0.571E+01
0.5000E+02	0.325E+03	0.486E+02	0.214E+02	0.241E+02	0.571E+01
0.6294E+02	0.329E+03	0.486E+02	0.214E+02	0.241E+02	0.571E+01
0.7924E+02	0.333E+03	0.486E+02	0.214E+02	0.241E+02	0.571E+01
0.9976E+02	0.337E+03	0.486E+02	0.214E+02	0.241E+02	0.571E+01
0.1000E+03	0.337E+03	0.486E+02	0.214E+02	0.241E+02	0.571E+01

Appendix F

Data for Example 2

t(hr)	p_{wf}(psi)	q_1(b/d)	q_2(b/d)	q_3(b/d)
0.5000E-03	0.118E+03	0.206E+02	0.163E+02	0.130E+02
0.6294E-03	0.120E+03	0.207E+02	0.160E+02	0.132E+02
0.7924E-03	0.122E+03	0.209E+02	0.157E+02	0.133E+02
0.9976E-03	0.124E+03	0.210E+02	0.154E+02	0.135E+02
0.1255E-02	0.127E+03	0.211E+02	0.151E+02	0.137E+02
0.1581E-02	0.129E+03	0.213E+02	0.148E+02	0.138E+02
0.1990E-02	0.131E+03	0.214E+02	0.145E+02	0.140E+02
0.2505E-02	0.134E+03	0.215E+02	0.143E+02	0.141E+02
0.3154E-02	0.136E+03	0.216E+02	0.140E+02	0.143E+02
0.3971E-02	0.139E+03	0.217E+02	0.138E+02	0.144E+02
0.5000E-02	0.141E+03	0.218E+02	0.136E+02	0.145E+02
0.6294E-02	0.144E+03	0.219E+02	0.133E+02	0.146E+02
0.7924E-02	0.147E+03	0.219E+02	0.131E+02	0.148E+02
0.9976E-02	0.149E+03	0.220E+02	0.129E+02	0.149E+02
0.1255E-01	0.152E+03	0.221E+02	0.128E+02	0.150E+02
0.1581E-01	0.155E+03	0.222E+02	0.126E+02	0.151E+02
0.1990E-01	0.157E+03	0.222E+02	0.124E+02	0.152E+02
0.2505E-01	0.160E+03	0.223E+02	0.123E+02	0.153E+02
0.3154E-01	0.163E+03	0.223E+02	0.121E+02	0.154E+02
0.3971E-01	0.165E+03	0.224E+02	0.120E+02	0.155E+02
0.5000E-01	0.168E+03	0.224E+02	0.119E+02	0.155E+02
0.6294E-01	0.170E+03	0.225E+02	0.118E+02	0.156E+02
0.7924E-01	0.173E+03	0.225E+02	0.117E+02	0.157E+02

Table Continued

t(hr)	p_{wf}(psi)	q_1(b/d)	q_2(b/d)	q_3(b/d)
0.9976E-01	0.176E+03	0.225E+02	0.116E+02	0.158E+02
0.1255E+00	0.178E+03	0.225E+02	0.115E+02	0.158E+02
0.1581E+00	0.181E+03	0.226E+02	0.114E+02	0.159E+02
0.1990E+00	0.183E+03	0.226E+02	0.114E+02	0.159E+02
0.2505E+00	0.186E+03	0.226E+02	0.113E+02	0.160E+02
0.3154E+00	0.188E+03	0.226E+02	0.113E+02	0.160E+02
0.3971E+00	0.191E+03	0.226E+02	0.112E+02	0.160E+02
0.5000E+00	0.193E+03	0.226E+02	0.112E+02	0.160E+02
0.6294E+00	0.195E+03	0.226E+02	0.112E+02	0.161E+02
0.7924E+00	0.198E+03	0.226E+02	0.111E+02	0.161E+02
0.9976E+00	0.200E+03	0.226E+02	0.111E+02	0.161E+02
0.1255E+01	0.203E+03	0.226E+02	0.111E+02	0.161E+02
0.1581E+01	0.205E+03	0.226E+02	0.111E+02	0.161E+02
0.1990E+01	0.207E+03	0.227E+02	0.111E+02	0.161E+02
0.2505E+01	0.210E+03	0.227E+02	0.111E+02	0.161E+02
0.3154E+01	0.212E+03	0.227E+02	0.111E+02	0.161E+02
0.3971E+01	0.214E+03	0.227E+02	0.111E+02	0.161E+02
0.5000E+01	0.217E+03	0.227E+02	0.111E+02	0.161E+02
0.6294E+01	0.219E+03	0.227E+02	0.111E+02	0.161E+02
0.7924E+01	0.221E+03	0.227E+02	0.111E+02	0.161E+02
0.9976E+01	0.224E+03	0.227E+02	0.111E+02	0.161E+02
0.1255E+02	0.226E+03	0.227E+02	0.111E+02	0.161E+02
0.1581E+02	0.228E+03	0.227E+02	0.111E+02	0.161E+02
0.1990E+02	0.231E+03	0.227E+02	0.111E+02	0.161E+02
0.2505E+02	0.233E+03	0.227E+02	0.111E+02	0.161E+02
0.3154E+02	0.235E+03	0.227E+02	0.111E+02	0.161E+02
0.3971E+02	0.238E+03	0.227E+02	0.111E+02	0.161E+02
0.5000E+02	0.240E+03	0.227E+02	0.111E+02	0.161E+02
0.6294E+02	0.242E+03	0.227E+02	0.111E+02	0.161E+02
0.7924E+02	0.245E+03	0.227E+02	0.111E+02	0.161E+02
0.9976E+02	0.247E+03	0.227E+02	0.111E+02	0.161E+02
0.1000E+03	0.247E+03	0.227E+02	0.111E+02	0.161E+02

Appendix G

Data for Example 3

t(hr)	p_{wf}(psi)	q_1(b/d)	q_2(b/d)	q_3(b/d)
0.5000E-02	0.263E-01	0.124E-01	-0.161E+01	0.101E+03
0.6294E-02	0.547E-01	0.129E-01	-0.196E+01	0.101E+03
0.7924E-02	0.690E-01	0.725E-02	-0.233E+01	0.102E+03
0.9976E-02	0.473E-01	0.112E-01	-0.265E+01	0.102E+03
0.1255E-01	0.414E-01	0.787E-01	-0.272E+01	0.102E+03
0.1581E-01	0.314E+00	0.317E+00	-0.230E+01	0.101E+03
0.1990E-01	0.150E+01	0.888E+00	-0.112E+01	0.100E+03
0.2505E-01	0.473E+01	0.197E+01	0.107E+01	0.969E+02
0.3154E-01	0.114E+02	0.370E+01	0.437E+01	0.919E+02
0.3971E-01	0.232E+02	0.609E+01	0.860E+01	0.852E+02
0.5000E-01	0.405E+02	0.897E+01	0.133E+02	0.777E+02
0.6294E-01	0.630E+02	0.119E+02	0.179E+02	0.701E+02
0.7924E-01	0.888E+02	0.147E+02	0.218E+02	0.634E+02
0.9976E-01	0.115E+03	0.169E+02	0.247E+02	0.582E+02
0.1255E+00	0.141E+03	0.186E+02	0.267E+02	0.546E+02
0.1581E+00	0.166E+03	0.197E+02	0.280E+02	0.521E+02

Table Continued

t(hr)	p_{wf}(psi)	q_1(b/d)	q_2(b/d)	q_3(b/d)
0.1990E+00	0.189E+03	0.205E+02	0.290E+02	0.504E+02
0.2505E+00	0.210E+03	0.210E+02	0.298E+02	0.491E+02
0.3154E+00	0.231E+03	0.213E+02	0.304E+02	0.481E+02
0.3971E+00	0.251E+03	0.216E+02	0.311E+02	0.472E+02
0.5000E+00	0.271E+03	0.218E+02	0.316E+02	0.465E+02
0.6294E+00	0.290E+03	0.219E+02	0.321E+02	0.459E+02
0.7924E+00	0.309E+03	0.220E+02	0.325E+02	0.454E+02
0.9976E+00	0.328E+03	0.220E+02	0.328E+02	0.450E+02
0.1255E+01	0.347E+03	0.221E+02	0.331E+02	0.447E+02
0.1581E+01	0.365E+03	0.221E+02	0.333E+02	0.445E+02
0.1990E+01	0.384E+03	0.221E+02	0.334E+02	0.443E+02
0.2505E+01	0.402E+03	0.221E+02	0.336E+02	0.441E+02
0.3154E+01	0.420E+03	0.221E+02	0.337E+02	0.440E+02
0.3971E+01	0.439E+03	0.221E+02	0.338E+02	0.439E+02
0.5000E+01	0.457E+03	0.221E+02	0.339E+02	0.439E+02
0.6294E+01	0.475E+03	0.221E+02	0.339E+02	0.438E+02
0.7924E+01	0.494E+03	0.221E+02	0.340E+02	0.437E+02
0.9976E+01	0.512E+03	0.222E+02	0.340E+02	0.437E+02
0.1255E+02	0.530E+03	0.222E+02	0.340E+02	0.437E+02
0.1581E+02	0.548E+03	0.222E+02	0.340E+02	0.437E+02
0.1990E+02	0.566E+03	0.222E+02	0.341E+02	0.436E+02
0.2505E+02	0.584E+03	0.222E+02	0.341E+02	0.436E+02
0.3154E+02	0.602E+03	0.222E+02	0.341E+02	0.436E+02
0.3971E+02	0.620E+03	0.222E+02	0.341E+02	0.436E+02
0.5000E+02	0.639E+03	0.222E+02	0.341E+02	0.436E+02
0.6294E+02	0.657E+03	0.222E+02	0.341E+02	0.436E+02
0.7924E+02	0.675E+03	0.222E+02	0.341E+02	0.436E+02
0.9976E+02	0.693E+03	0.222E+02	0.341E+02	0.436E+02
0.1000E+03	0.693E+03	0.222E+02	0.341E+02	0.436E+02